

# The Messenger



No. 128 – June 2007

Czech Republic joins ESO  
Progress on ALMA  
CRIRES Science Verification  
Gender balance among ESO staff



## The Czech Republic Joins ESO

**Catherine Cesarsky**  
(ESO Director General)

I am delighted to welcome the Czech Republic as our 13th member state. From its size, the Czech Republic may not belong to the 'big' member states, but the accession nonetheless marks an important point in ESO's history and, I believe, in the history of Czech astronomy as well. The Czech Republic is the first of the Central and East European countries to join ESO. The membership underlines ESO's continuing evolution as the prime European organisation for astronomy, whilst at the same time it enables Czech astronomers to become fully integrated in the European astronomical community.

As always in such cases, joining an international organisation requires a process with a political underpinning and a set of formal steps. Not surprisingly, this process can take years. In the case of the Czech Republic the first informal contacts occurred at the time of the XXVth General Assembly of the IAU in Sydney, Australia.

Discussions continued in the Czech Republic leading to an invitation for me to visit Prague on 10 November 2005. During the visit, in which I was accompanied by Claus Madsen, we had very successful interactions with high-ranking Czech officials, including Prof. Václav Pačes, President of the Czech Academy of Sciences, and representatives of several ministries. We were also received by Dr. Martin Jahn, the then Deputy Prime Minister of the Czech Republic, who expressed strong support for the Czech bid to join ESO. The visit also included a major press conference and a live TV interview with Dr. Jan Palouš, of the Astronomical Institute of the Academy of Sciences, and myself.

It was clear that the process was gaining considerable momentum, and thus the formal request for membership arrived in the spring of 2006, leading to the establishment by the ESO Council of a negotiating team, chaired by Council Vice-President Dr. Monnik Desmeth.

The XXVIth IAU General Assembly, held in Prague in 2006, clearly provided a boost for the Czech efforts to join ESO, not the least in securing the necessary public and political support. Thus our Czech colleagues used the opportunity to publish a fine and very interesting popular book about Czech astronomy and ESO, which, together with the General Assembly, created considerable media interest.

On 20 September 2006, at a meeting at ESO Headquarters, the negotiating teams from ESO and the Czech Republic arrived at an agreement in principle, which was subsequently presented to the Committee of Council.

This Agreement was formally confirmed by the ESO Council at its meeting on 6 December and a few days thereafter by the Czech government, enabling a signing ceremony in Prague on 22 December (see photograph below). This was important because the Agreement foresaw accession by 1 January 2007. With the signatures in place, the agreement could be submitted to the Czech Parliament for ratification within an agreed 'grace period'. This formal procedure was concluded on 30 April 2007, when I was notified of the deposition of the instrument of ratification at the French Ministry of Foreign Affairs.

We look forward to an active Czech participation in ESO's programmes in time to come.

Photo: Academy of Sciences of the Czech Republic



Ms. Miroslava Kopicová, Minister of Education, Youth and Sports of the Czech Republic, and Tom Wilson, Associate Director of ESO, shake hands following the signing of the agreement for the entry of the Czech Republic into ESO which took place on 22 December 2006 in Prague. The formal accession took place, without ceremony, on 30 April 2007.

Dr. Jan Palouš of the Astronomical Institute of the Czech Academy of Sciences addressing delegates at the ESO Industry Day held in Prague on 8 June 2007.



Photo: L. Calçada, ESO

# Astronomy in the Czech Republic

Jan Palouš, Petr Hadrava  
(Astronomical Institute, Academy of Sciences of the Czech Republic)

A brief historical outline of the development of astronomy in the Czech lands is presented, followed by an overview of the current observational, research and educational facilities.

## Historical development

In the Czech lands, astronomy has rather deep roots, covering at least all the last millenium. A significant milestone for pursuing astronomy in Bohemia and surrounding countries was represented by the establishment of the University in Prague by the Emperor Charles IV in 1348. Astronomy, as one of the seven liberal arts, was greatly emphasised right from the beginning of the lectures, and Prague University soon began to support the creative development of astronomical knowledge brought especially from Paris, Oxford and other places in Europe. It reached a remarkable level, e.g. in widely spread treatises “On the construction and on the use of the astrolabe” by Cristannus de Prachaticz (1407) or in the design of the Prague Astronomical Clock (1410) by Johannes Schindel.

The most famous era of astronomy in Prague was probably the period of rule of the Emperor Rudolph II at the turn of the 16th and 17th century, when Tycho Brahe and Johannes Kepler dwelt and worked at the Emperor’s court. The fact that Brahe, and later also Kepler, came to Prague, as well as Kepler’s success achieved in this city, were not a result of some lucky coincidence or the Emperor’s generosity and eccentric nature. To a great degree, these were logical consequences of the gradual development of Prague’s cultural and scientific environment. It was mainly Tycho’s friend Thaddaeus Hagecius, who prepared the grounds for Tycho’s arrival. Hagecius was the Emperor’s physician, and at the same time one of a few European astronomers of that time, who, like Tycho Brahe, studied the skies with a critical scientific approach. It was in Prague where Kepler found, during his stay in the years 1600–1612, his first two laws of



Photo: P. Hadrava, Astronomical Institute, Academy of Sciences of the Czech Republic

Figure 1: The Astronomical Clock in the Old Town of Prague.

planetary motions, while evaluating the positions of Mars observed by Tycho Brahe. He published numerous treatises, among them “Astronomia nova” including the laws of planetary motions, texts on the “New Star” of 1604 in the constellation Ophiuchus, and he wrote his first version of “The Dream, or Posthumous Work on Lunar astronomy” on the astronomy viewed from the surface of the Moon.

After the Thirty Years War, education was predominantly provided and controlled by the Jesuit order. Astronomy, as well as other sciences, was pursued mainly in the Clementinum College in Prague. In 1722 the Astronomical Tower was built there. Thanks to the care of the first director of the Clementinum observatory, Josef Stepling, the Astronomical Tower was equipped with new instruments around 1750, becoming the first state-supported astronomical observatory in Czech lands.

The advance of astronomy went hand in hand with the development of other sciences. Among the important scientific personalities in the 19th century were the mathematician Bernard Bolzano and the biologist Jan Evangelista Purkyně, who studied, besides other things, the



Figure 2: New star of 1572 in the constellation of Cassiopeia from “Dialexis” by Thaddaeus Hagecius (Frankfurt am Main 1574).

physiology of the human eye. Of absolutely crucial importance for the future development of astronomy and other sciences was the idea of the influence of a binary star’s motion on the colour of their light, which Christian Doppler, the professor of the Prague Polytechnic, presented in his lecture held in the Carolinum in 1842. He published his result in a



Photo: I. Král, National Library, Prague

Figure 3: The allegory of sciences on the ceiling fresco in the New Mathematical Hall in Prague Clementinum. It shows the Clementinum Astronomical Tower along with the extrasolar planetary systems according to Giordano Bruno’s idea of the “multiplicity of worlds” (National Library of the Czech Republic).

local Bohemian journal, consequently his principle was later rediscovered by H. A. Fizeau. In the second half of the 19th century, Ernst Mach contributed enormously to the education of a whole generation of both German and Czech physicists and astronomers. He also helped in the general recognition of Christian Doppler's achievement.

In 1886, the Astronomical Institute of the Charles University in Prague was established by August Seydler, who served as its first director. He elaborated sophisticated methods for determination of orbits of minor planets and wrote textbooks on theoretical physics and many popular articles on astrophysics. In the last decade of the 19th century, Seydler's successor, Gustav Gruss, observed variable stars and carried out visual observations of stellar spectra.

Albert Einstein spent one and a half years (1911–1912) in Prague, being appointed professor at the German Prague University. During his Prague time he published eleven papers, including the first one on the deflection of light by the gravitational field of the Sun, containing the formulation of the first fundamentals of the theory of General Relativity.

There is an interesting connection between astronomy and literature: Jan Neruda (1834–1891), Czech poet, writer and journalist, was born in Prague, and grew up in a colourful part of the town called Malá Strana (Lesser Quarter). His first laurels came from the success of his collection of poetry called "Cosmic Songs" that documented his good astronomical knowledge. The song No. XXII "... are there frogs there, too?" was, on the occasion of the 26th General Assembly of the IAU in Prague, translated by Robert Russel into English. Jan Neruda was godfather of Josef and Jan Frič, the sons of the revolutionary Josef Václav Frič, who were born in Parisian exile. Both brothers shared an interest in astronomy with their godfather. When they came back to Bohemia, they started their astronomical observations, at first with the support of professor Vojtěch Šafařík. Later, they established a factory in Prague, which produced optical devices, and developed astronomical instruments. After the death of younger brother Jan, Josef built an ob-

servatory at Ondřejov near Prague. In 1928, Josef Jan Frič donated his observatory to the state.

After the establishment of the Czechoslovak Academy of Sciences in 1953, the former State Observatory in Clementinum, together with the Ondřejov Observatory, became the basis of the Astronomical Institute of the Czechoslovak Academy of Sciences. One historical root of this institution thus reaches to 1722, when Clementinum observatory was established by the Jesuits, and another to the Frič's foundation of the Ondřejov Observatory in 1898, which was inspired by the interest of his poetic godfather Jan Neruda.

### Current Facilities

The Astronomical Institute of the Academy of Sciences of the Czech Republic has a prominent position as the largest professional place in the Czech Republic. The names of the Institute's four scientific departments suggest a lot about its scientific profile: Solar Physics; Interplanetary Matter; Stellar Physics; and Galaxies and Planetary Systems.

The Solar Physics department focuses on active solar phenomena such as sunspots, solar flares and coronal mass ejections. The data coming from the instruments of the Ondřejov observatory, including optical and radio wavebands, are combined with X-ray and UV observations from satellites and space probes

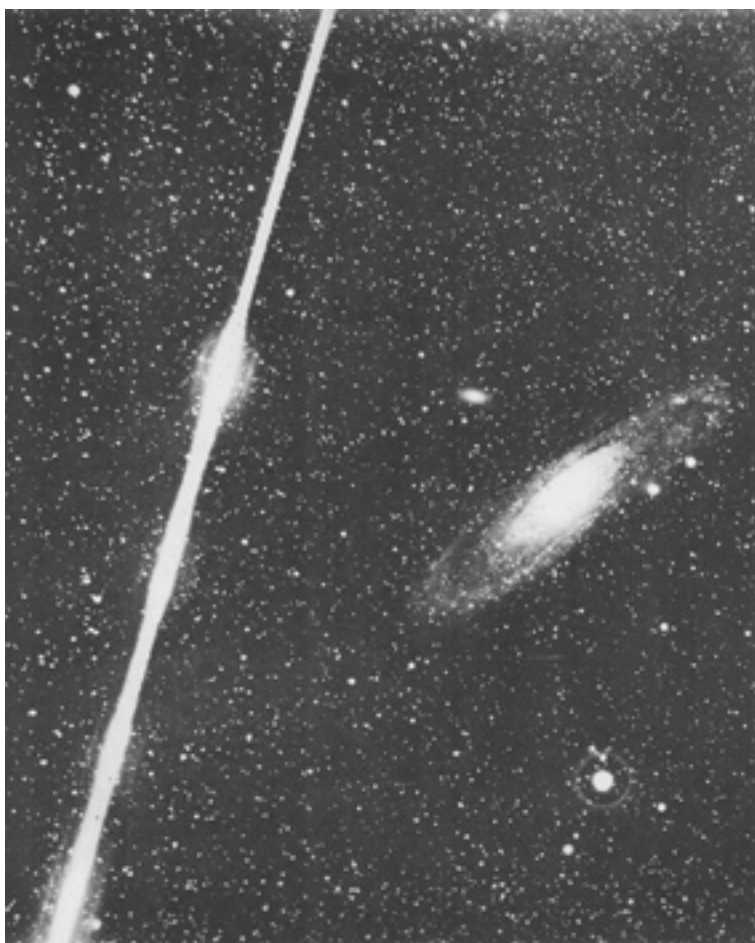
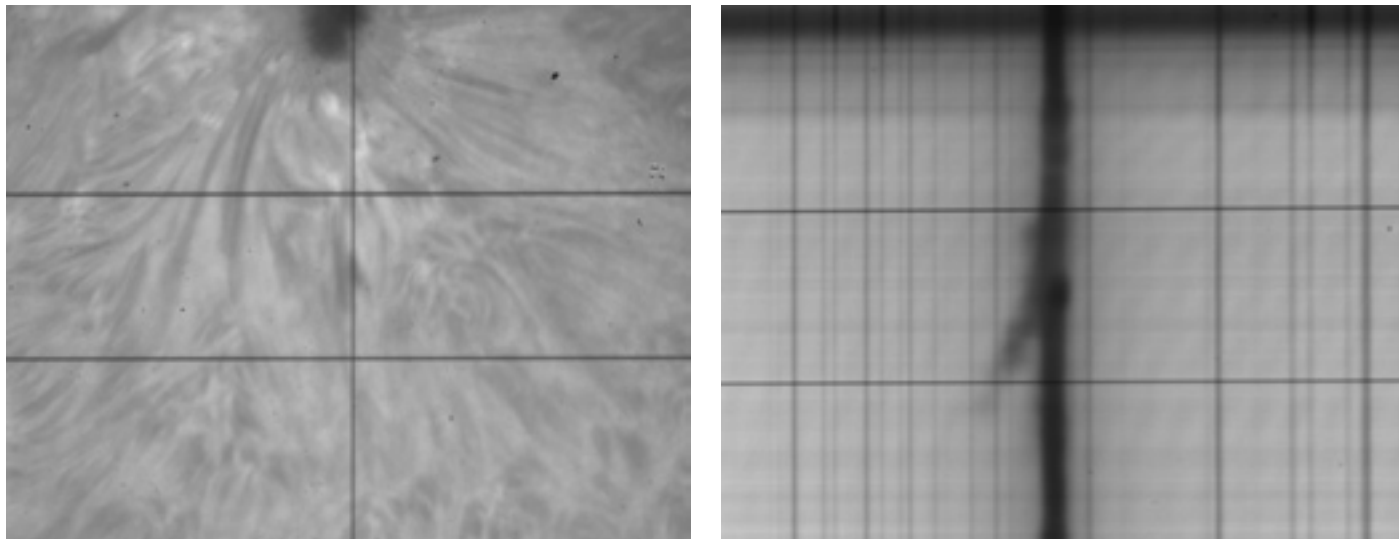


**Figure 4:** The observation of fireballs has a long tradition at the Ondřejov Observatory. The photograph taken on 12 September 1923 by Josef Klepešta shows the M31 galaxy in Andromeda with a fireball in front.

**Figure 5:** H $\alpha$  filtergram (left panel) and corresponding H $\alpha$  spectrum (right) of a solar active region as obtained by the Ondřejov large horizontal solar telescope HSFA2 on 4 July 2006. Note the Doppler shifted features in the spectrum (wavelength increasing to the right).



to have a complex multi-wavelength information on these fast non-equilibrium phenomena. The observations are compared to numerical simulations trying to discover the basic mechanisms ruling the Sun. The main goal is the study of magnetohydrodynamic and radiative processes in the solar plasma, which offers conditions unachievable in laboratories on Earth. The Sun-Earth relation and cosmic weather are also studied with a lot of geophysical and other practical applications.

The department of Interplanetary Matter operates the European network of all-sky cameras, which records meteors, particularly the brightest of them, which are called fireballs. This network holds the world's primacy in finding meteorites upon observation of their passage through the Earth's atmosphere. In 1959, parts of the meteorite Příbram were found upon calculation of its path through the Earth's atmosphere based on photographs taken by all-sky cameras. The network of all-sky fireball cameras and spectral cameras has been in continuous operation since 1963 and is currently the only one in the world. The atmospheric fragmentation and structural properties of meteoroids, chemical composition of meteoroids from spectroscopy, physics of meteor radiation and ionisation, and long-term activity of meteor showers from radar observations, are studied. In 1993 a new programme of CCD observations of asteroids using a dedicated 0.65-m telescope started with the focus on their

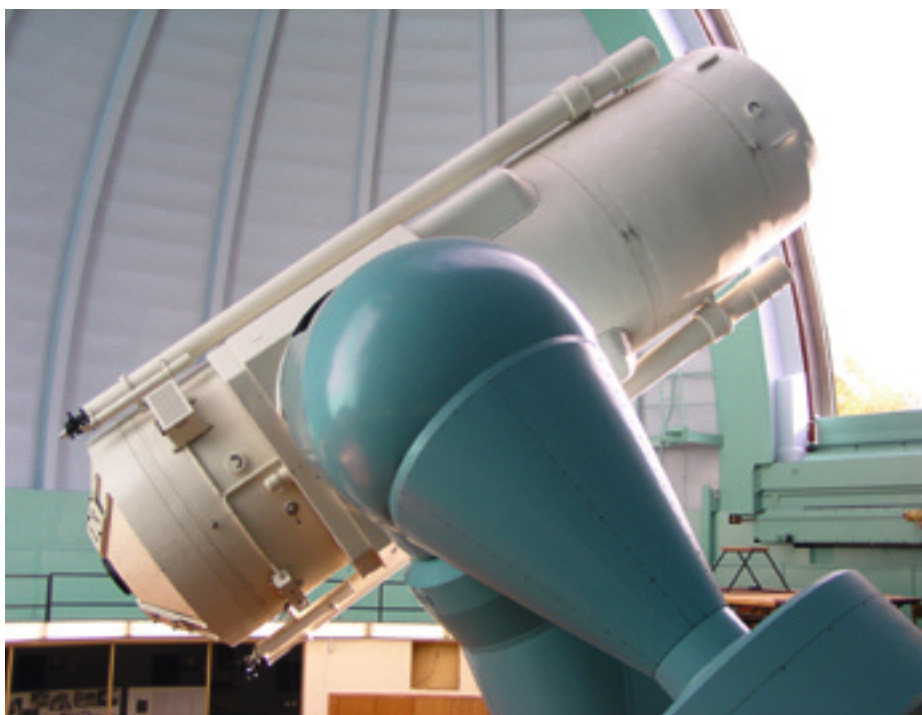


**Figure 6:** The 2-m telescope in Ondřejov.

rotation and the detection of near-Earth asteroids. In recent years, new discoveries have been made of several binary and very rapidly rotating asteroids.

The Stellar Physics department operates the largest telescope on the territory of the Czech Republic, which has a primary mirror of 202 cm diameter. The main focus is on the study of variable, espe-

cially binary stars. The photometric and spectral observations are combined to disentangle the orbital parameters of binaries. The use of spectroscopy requires the development of the theory of stellar atmospheres, as well as other methods of processing and evaluation of observational data. Interacting binaries are usually strong sources of X-ray radiation as observed from space probes.

Photo: J. Havelka, Astronomical Institute, Academy of Sciences of the Czech Republic

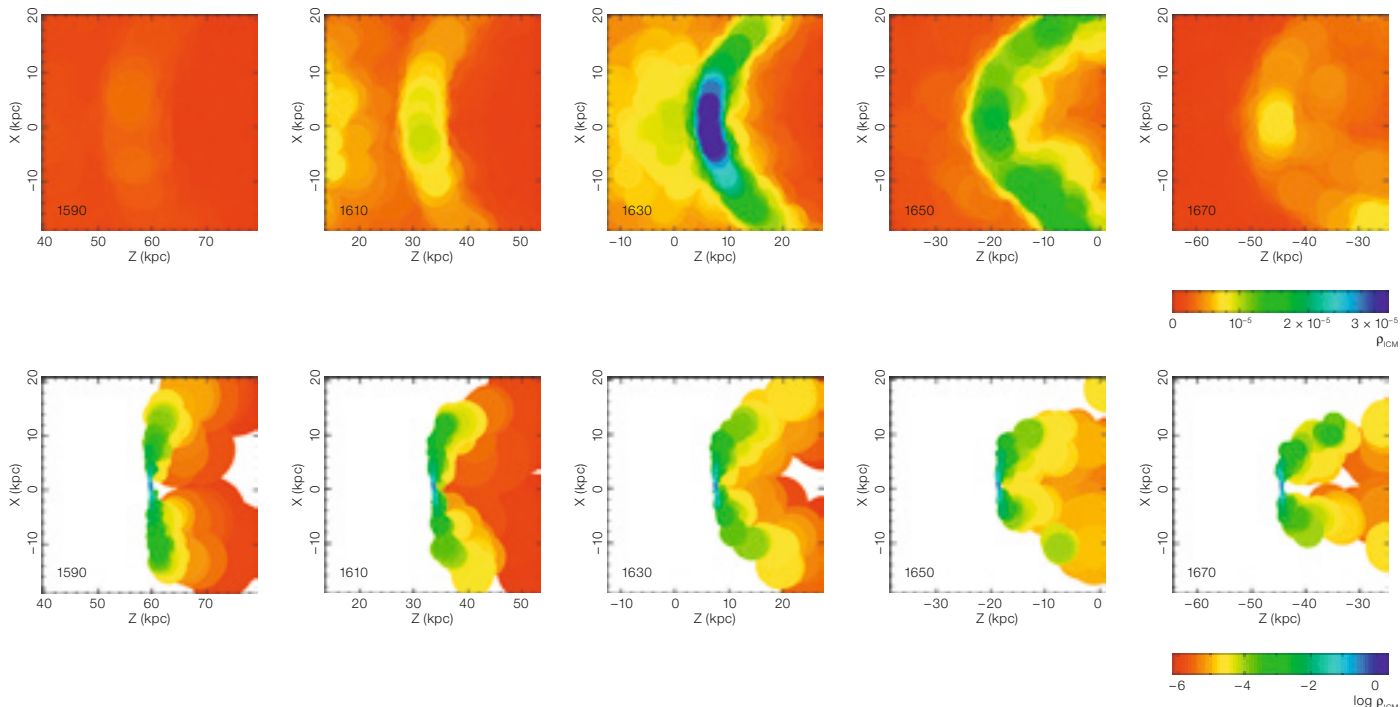


**Figure 7:** Gas stripping in galaxy clusters: formation of a bow shock in front of a galaxy as seen in simulations using N-body SPH with a gravity tree code. From Jáhym, P., 2006, Ph.D. Thesis, Charles University Prague, and Université Pierre et Marie Curie, Paris.

The department of Galaxies and Planetary Systems resides in the Prague part of the Astronomical Institute, but it has its own zenith telescope in Ondřejov. It deals with the study of the rotation of the Earth, and with the theoretical problems of Solar System dynamics and exoplanets. The trans-Neptunian bodies are studied including the resonance in the Kuiper Belt. Triggered star formation in the turbulent interstellar medium is studied both in observations and simulations. The influence of gas recycling on galaxy evolution across a Hubble time, including gravitational and hydrodynamic processes, is considered (see Figure 7 for example). Study of relativistic astrophysics includes accretion processes and resonances in discs surrounding black holes. An example is shown in Figure 8 where the predicted variations of the X-ray spectrum of an accretion disc at eight successive phases are plotted during the entire orbit of a single spot located at a distance of seven gravitational radii from the black hole and rotating clockwise. A distant observer is placed at an inclination of 30 de-

grees with respect to the disc normal and sees the system from the left side. Superposition of several tens of such spots then contributes to the source variability as the spots arise, trace some part of the orbit, and gradually fade away (c.f. Eckart et al. 2006).

In the Institute of Physics of the Academy of Sciences of the Czech Republic, a research group participates in the project of the Pierre Auger Observatory which is building an array of telescopes in Argentina to detect showers of high-energy cosmic rays. The contribution of the Czech Republic includes mainly the fabrication of hexagonal mirrors for two the Schmidt cameras observing Cherenkov radiation in the Earth's atmosphere.

The Astronomical Institute of the Charles University, which is an integral part of the Faculty of Mathematics and Physics, has mainly educational duties in teaching undergraduate and graduate courses of astronomy and astrophysics. The research areas include the spectroscopic properties of hot stars, particularly in binaries and multiple systems, and exploration of the nature of Be stars. Studies of physical properties, dynamics and evolution of small bodies of the Solar System include the Yarkovsky effect and

observations mainly deal with orbits and light curves of asteroids, including new discoveries of such bodies. Studies in cosmology, with special emphasis on the properties of gamma-ray bursts, are performed. Studies in history of astronomy focus particularly on the Bohemian region.

The Institute of Theoretical Physics of the Charles University is also a part of the Faculty of Mathematics and Physics. Students are educated in mathematics and computing, and in theoretical physics, including classical and quantum mechanics, elementary particle physics, thermodynamics, relativistic physics and cosmology. Research areas include gravitational collapse with small non-spherical perturbations, black-hole electrodynamics, theory of gravitational radiation, exact solutions of Einstein's field equations and cosmological perturbation theory.

The Institute of Theoretical Physics and Astrophysics at the Faculty of Sciences, Masaryk University in Brno, provides basic courses in astronomy and astrophysics at the undergraduate and graduate level. Research includes the physics of hot stars, non-LTE models of stellar atmospheres, variable stars, carbon stars, K-type giants and properties of atmos-

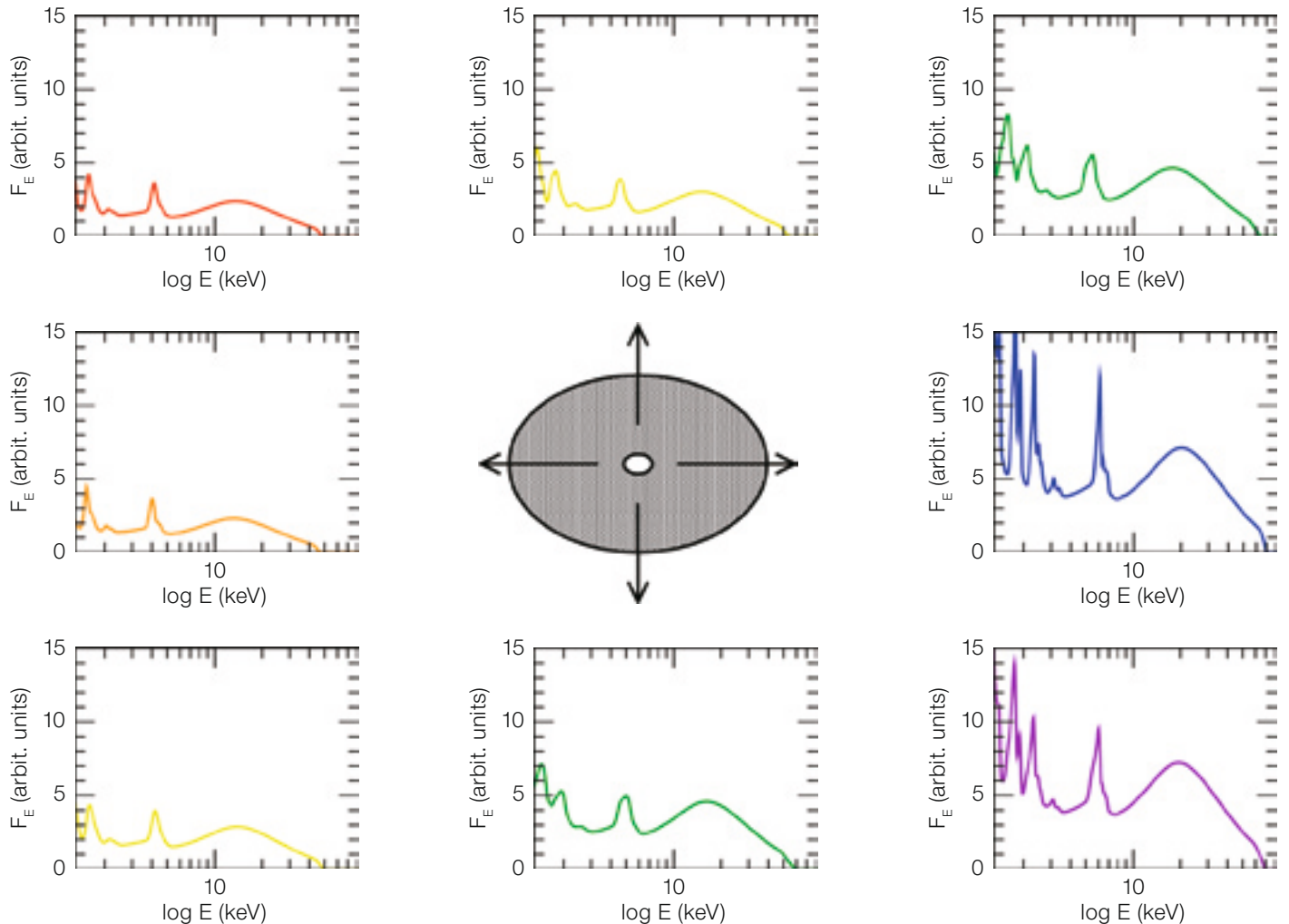


**Figure 8:** The predicted variations of the X-ray spectrum of an accretion disc around a galactic nucleus black hole are plotted. (From Goosmann R. W. et al., in "The X-ray Universe 2005", edited by A. Wilson, El Escorial, Madrid, Spain, in press.

pheric extinction. The Institute manages the Masaryk University Observatory at Kraví hora equipped with a 0.6-m reflector with a CCD camera.

The Relativistic Astrophysics Group of the Institute of Physics of the Silesian University in Opava is active in the fields of neutron stars, black holes and cosmology. The anisotropies of the CBR are explored as well as  $\Lambda$ -CDM cosmological models.

The Czech Republic can be proud of its unique net of planetaria and public observatories. Their primary goal is to provide natural science knowledge to a broad public and to demonstrate the sci-

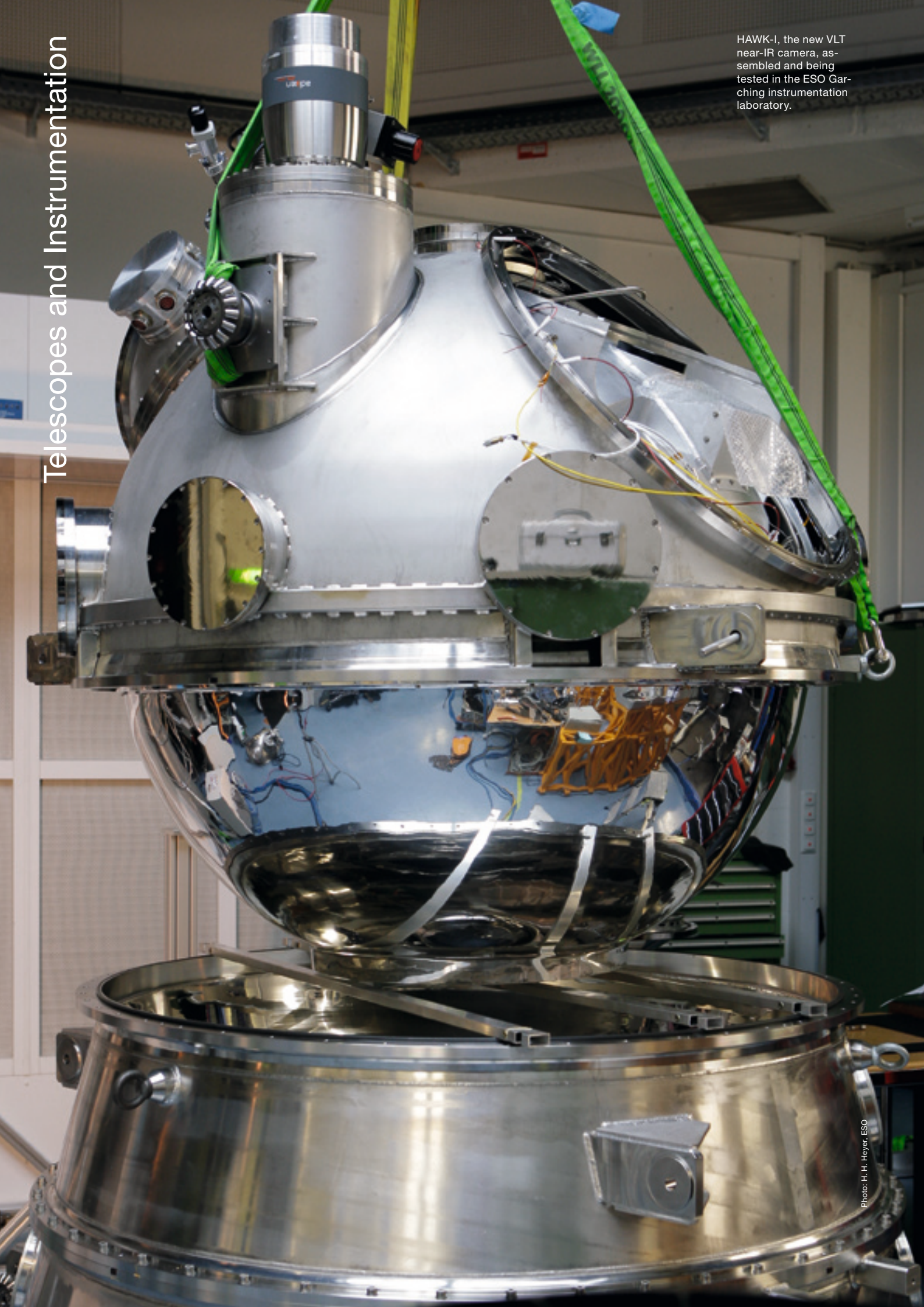
entific method by special astronomical research. The Klet' Observatory, which is equipped with a 1-m telescope with a CCD detector, has its research programme dedicated to the astrometry of asteroids with unusual orbits and comets, providing precise determination of their orbits. The main part of the work is devoted to the near-Earth orbits. The data are provided to the Central Bureau for Astronomy Telegrams of the IAU. Other observatories include the Nicolaus Copernicus Observatory and Planetarium in Brno, Štefánik Observatory and Planetarium in Prague, Rokycany Observatory, Úpice Observatory, Valašské Meziříčí Observatory, and others.

This brief review presents the past and current status of astronomy in the Czech Republic, which is the starting point for the entrance of the Czech Republic into ESO.

#### References

- Eckart A. et al. 2006, *The Messenger* 125, 2
- Hadrava P. 2006, "The European Southern Observatory and Czech Astronomy", Academia, Praha
- Palouš J., Vondrák J. and Šolc M. 2002, "Astronomy and Astrophysics in the Czech Republic", in "Organizations and Strategies in Astronomy III", ed. A. Heck, Kluwer, 163

HAWK-I, the new VLT near-IR camera, assembled and being tested in the ESO Garching instrumentation laboratory.



# FORS1 is getting Blue: New Blue Optimised Detectors and High Throughput Filters

Thomas Szeifert, Roland Reiss, Pedro Baksai, Sebastian Deiries, Carlo Izzo, Emmanuel Jehin, Mario Kiekebusch, Sabine Moehler, Kieran O'Brien, Emanuela Pompei, Miguel Riquelme, Gero Rupprecht, Tzu-Chiang Shen (all ESO)

Ground-based observations in the ultraviolet part of the electromagnetic spectrum are notoriously difficult owing to absorption of the atmosphere, of optical elements and the poorer efficiency of detectors. Now that CCD detectors with excellent UV response and cosmetic quality have become available, it was time to optimise FORS1 for imaging, low-resolution spectroscopic and polarimetric observations in the blue-UV. As a bonus, a new set of broadband filters with very high transmission and carefully defined filter bands were installed.

## FORS – A brief history

FORS1 and FORS2 are two of the first-generation VLT instruments that were built by an external consortium (Landessternwarte Heidelberg, Universitätssternwarte München and Universitätssternwarte Göttingen, all in Germany). FORS1 was the first of the scientific facility instruments and saw first light at the Cassegrain focus of VLT-ANTU, on 15 September 1998 (Appenzeller et al. 1998). FORS2 followed in 2000 on VLT-Kueyen. The FORSes also served on Melipal and Yepun; currently they are installed again on Antu (FORS2) and Kueyen (FORS1). They are amongst the most scientifically productive instruments of the VLT: more than 750 refereed papers have been published to date with both FORSes. Many of these papers have achieved high scientific impact factors as indicated by nearly 20 000 citations.

Soon after it entered regular science operations, FORS2 received a major upgrade when its original  $2k \times 2k$  Tektronix detector was replaced (effective April 2002) by a mosaic of two red-optimised MIT/LL CCDs. Further upgrades included several prototype volume-phased holographic gratings (VPHG) that greatly boosted its scientific productivity. We

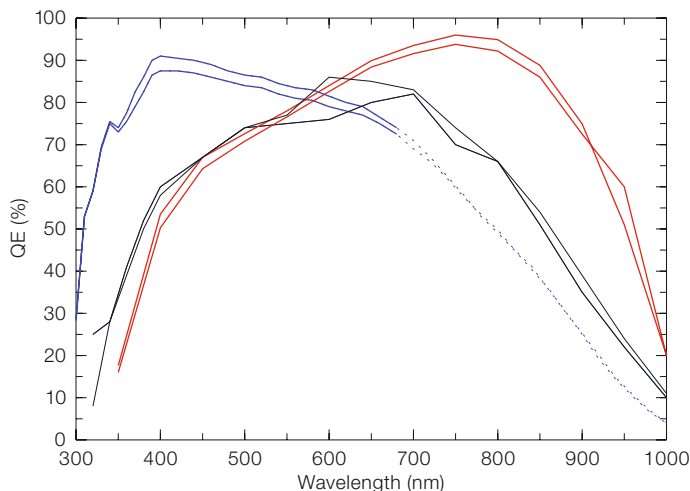


**Figure 1:** Comparison of the CCD efficiencies of FORS1 and FORS2 before and after the respective upgrades. Black: Tektronix CCDs; Red: FORS2 MIT CCDs; Blue: FORS1 E2V CCDs. The dotted part indicates the range affected by fringing (see text).

intended to follow this highly successful example by adding similar capabilities to FORS1. The first stage in this process was the addition of the 1200 B VPHG that opened new opportunities for stellar and extragalactic observations by doubling the spectral resolution at very high grism throughput.

## The upgrade

Following the purchase of the VPH gratings and the success of the new red detector mosaic of FORS2, it was clear that an upgrade of FORS1 with a blue-sensitive new mosaic would be a good complement to FORS2. The prospect of having the same detector format for both instruments was another strong driver: it allows essentially the same control and data-reduction software to be used with FORS1 and FORS2. When the hardware and the resources to carry out the upgrade became available, we seized the opportunity.

The Garching Optical Detector Team (ODT) prepared the hardware part of the upgrade, a pair of E2V blue-sensitive chips. ODT was in particular responsible for the selection and characterisation of the CCDs, the mounting and adjustment of the mosaic and the preparation of the detector control system (FIERA). The CCDs are named “Marlene”, formerly the detector in the UVES blue arm, and “Norma III”, one of the CCDs from the batch procured for OmegaCAM. The choice was motivated by a dramatic increase in the quantum efficiency of

these two chips in the blue-UV compared to that of the existing Tektronix CCD, as can be seen in Figure 1.

The significant boost in the quantum efficiency of these CCDs has been achieved by subjecting them to a treatment of soaking in synthetic air, combined with UV light flashing. The precise physics of this effect is not known, however, the effect is reproducible and sufficiently long-lived so that it can be applied to an instrument in regular science operations. For a description of the process see Baade et al. (2005). Additional reasons for choosing these new detectors are that they can be read out much faster and have a lower read-out noise level, which is crucially important for dark-time spectroscopy and narrow-band imaging in the blue and UV. Finally the cosmetic quality of these detectors is far superior to that of the generation of the Tektronix detector used up to now with FORS1.

The properties of the new CCD mosaic are: 4096 by 4096 pixels, 15  $\mu\text{m}$  square, binned  $2 \times 2$  by default. The pixel scale is 0.25” per (binned) pixel and the inter-chip gap width is 12.2”. The read-out noise as measured during the commissioning is about three electrons.

Strong support came from the Garching Integration and Cryo-Vacuum Department that prepared the cryostat and the various mechanical pieces required for the upgrade. An important part of the upgrade was the adaptation of the various pieces of software affected by

the upgrade: Observation Software (OS), templates and the Observer Support Software (OSS) tool FIMS. These upgrades were done by members of the Paranal software department who greatly benefited from the fact that FORS2 already uses a similar mosaic and similar control software. Finally, the Exposure Time Calculator (ETC) and data-reduction pipeline had to be adapted and tested.

Installation and Commissioning was a joint enterprise of the Paranal Science Operation Team and the Garching Instrumentation Division (see Figure 2). After two commissioning runs the upgraded system was certified in early April 2007 ready for science operations. This is the reason why the upgrade was only announced in the Call for Proposals (CfP) for Period 80. It would however have been hard to justify mothballing an excellent CCD system for six months and continuing operations with an old, inferior one. So it was decided to go already into P79 with the upgraded system and adjust the schedule where necessary at short notice in coordination with the PI's.

We also ordered a set of dichroic high throughput filters for the *U*, *B*, *V* and *g* bands to take further advantage of the new blue sensitivity of the mosaic. We specified a very high transmission, very carefully chosen central wavelengths and full width half maximum values so that the photometric flux can be nicely transferred to Vega magnitudes with standard stars selected from Landolt (1992). Colour corrections are typically smaller than 0.1 magnitudes. The resulting filter set (together with the already existing R\_SPECIAL, I\_BESS and z\_GUNN filters) either matches the Bessel (1990) definition of the UBVRI or the Sloan Digital Sky Survey (SDSS; Fukugita et al. 1996) *ugriz* systems. The latter system has achieved great acceptance in the scientific community due to the large impact of the SDSS. Figures 3 and 4 compare the old FORS1/2 filters with the new ones, the latter manufactured by Asahi (Japan). Note that *u*\_HIGH, *b*\_HIGH, *v*\_HIGH and R\_BESS filters are only offered with FORS1 and the R\_SPECIAL filter only with FORS2.

The new "HIGH" filters are available with FORS1 since April 2007 in Visitor Mode



Figure 2: Old (left) meets new (right) – the two detector systems side by side on their dedicated carriages next to FORS1 in the enclosure of Kueyen.

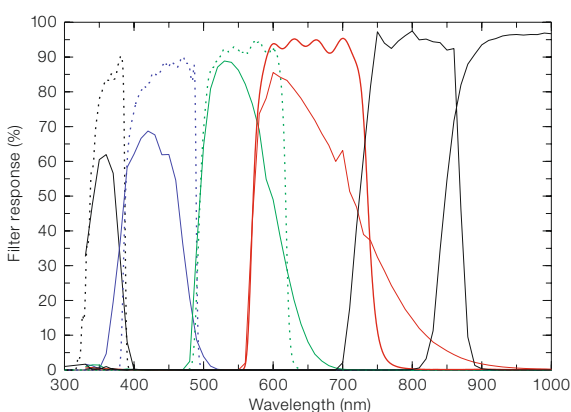


Figure 3: Transmission curves of the old (continuous lines) and new (dotted lines) FORS filters as measured in the ESO Optics Lab for Bessel *UBVRI* and *z*. The thin and thick red lines indicate the FORS1 R\_BESS and the FORS2 R\_SPECIAL filter, respectively.

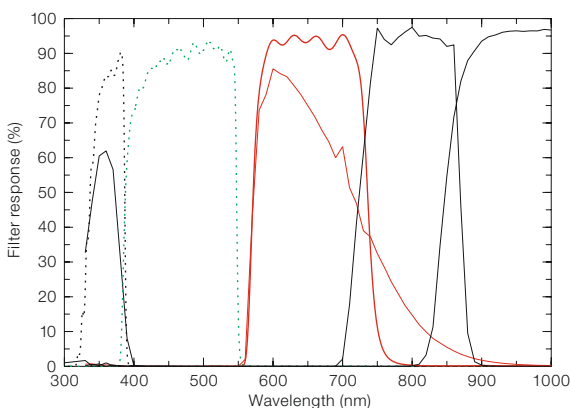


Figure 4: Transmission curves of the old (continuous lines) and new (dotted lines) FORS filters as measured in the ESO Optics Lab for SDSS *ugriz* filters. The thin and thick red lines indicate the FORS1 R\_BESS and the FORS2 R\_SPECIAL filters, respectively. The [O I] line at 557.7 nm falls exactly in the gap between *g* and *R*.

only, because they were not yet ready and characterised when the CfP for Period 79 went out in September 2006.

#### Let the game begin ...

The new detector system saw its first sky light on 30 January 2007. During a first commissioning run lasting three nights

we performed a thorough characterisation of the quantum efficiency, not only of the detectors but also of the new filters. Observations of numerous photometric and spectrophotometric standard stars proved that our expectations, based on the laboratory data, were correct. The new detector alone gave an improvement of 0.8 and 0.4 magnitudes in *U* and *B*, respectively, and the performance

dropped (as expected) only slightly in the *I*-band. Using, in addition, the new high throughput filters resulted in a spectacular gain of 1.3 mag. in *U* and 0.8 and 0.3 mag. in *B* and *V*.

The response given here has been calculated from the photometric zero points measured during the first commissioning run, according to the following strategy. First we calculated the Vega flux, integrated over the filter curves. From the Vega flux we calculated the zero points for 100% instrument and telescope throughput in magnitudes (27.41, 29.12, 29.21, 29.18, 28.78 in *UBVRI* and 27.93, 29.47, 29.33 and 29.90 in the *ubvgr* filters, respectively) for incoming photons/sec at the 8-m aperture of the VLT (see Table 1). The overall instrument response can then be easily derived from the measured photometric zero points at zero airmass. Similarly the Vega zero points at 100% response were calculated for the VIMOS *UBVRI* filters (27.93, 29.37, 28.96, 29.05 and 28.91 mag.) and for the FORS2 *R\_SPECIAL* filter (29.33 mag.). The response is then given in units of detected electrons per incoming photon including the telescope, the FORS longitudinal Atmospheric Dispersion Corrector (ADC), the instrument optics and detector response, but not the filter transmission. This response is given in parentheses in Table 1 and demonstrates the high performance of FORS1, FORS2 and VIMOS in all filters.

In addition the new *g*-band filter opens a new observation window. It collects the flux from the astronomical targets over a wide wavelength range where the night sky is very dark and the atmospheric transmission is high (390 nm to 550 nm).

A second commissioning run (five nights in March/April 2007) finally verified the functioning of the system in all supported observing modes (imaging, long-slit and multi-object spectroscopy, imaging and spectropolarimetry).

#### ... even with some adverse effects

There is however a significant price to pay for high quantum efficiency in the blue-UV: the fringe pattern at near-infrared wavelengths, beyond approxima-

Filter	FORS1 TEK	FORS1 e2v	FORS2 MIT	VIMOS e2v
<i>U</i>	25.20 (0.13)	26.53 (0.28)	n/a	26.5 (0.27)
<i>B</i>	27.70 (0.27)	28.48 (0.40)	27.70 (0.27)	28.20 (0.34)
<i>g</i>	n/a	28.89 (0.39)	n/a	n/a
<i>V</i>	28.05 (0.34)	28.33 (0.39)	28.10 (0.39)	27.90 (0.38)
<i>R</i>	28.00 (0.34)	27.96 (0.33)	28.40 (0.42)	27.90 (0.35)
<i>I</i>	27.15 (0.22)	26.99 (0.19)	27.70 (0.37)	27.0 (0.17)

tely 700 nm, increases significantly as compared to the old (somewhat thicker) Tektronix detector and the spatial frequency of the fringes also increases strongly. The fringing has a heavy impact on high signal-to-noise observations.

For imaging observations the fringes will remain at high amplitude in the sky background, on account of its OH emission-line spectrum, after flat fielding with the solar spectrum twilight flat fields. The sky background with fringes is best subtracted by obtaining an averaged sky image cleaned from astronomical sources, scaled to the sky level of the individual exposures. More commonly observers obtain "super flats" from the night sky airglow images observed in a jitter sequence. While this method leads to a more pleasing image with a flat sky background, it strongly compromises the photometric accuracy, which better matches a continuous or solar-type spectrum than the OH airglow spectrum.

In spectroscopy, flat fields obtained with continuous light calibration lamps can, at least partly, correct the fringes. In theory the light that is detected by every

**Table 1:** Zero points and instrument response for FORS1, FORS2 and VIMOS. Note that the VIMOS *U*-filter red cut-off is at 395 nm while it is at 385 nm for FORS1. Similar differences exist also for the other filters; therefore zero points do not allow a direct comparison of the absolute instrument response. The instrument response in detected electrons per incoming photon after eliminating the effect of the different filter sets is given in parentheses.

pixel has the same wavelength for targets, sky and flat field lamps. The correction should therefore be possible. In practice, however, the slightly different light path of the calibration light as compared to the telescope optical path, together with the small flexure of the FORS instrument, prevents perfect fringe correction using flat field spectra. In first tests, we obtained signal-to-noise ratios of up to 15 at wavelengths greater than 700 nm (see Figure 5).

Many scientific projects with FORS1 are focused on detecting extremely faint objects at very low signal-to-noise ratios or will concentrate on the shorter wavelength range after the blue optimisation. To demonstrate the performance of FORS1, Figure 6 shows a spectrum of a  $z = 2.42$  quasar of  $g = 20.4$  magnitudes which was obtained in only 15 minutes of integration time.

In both imaging and spectroscopy it is mandatory to apply jitter and nodding techniques to obtain good sky subtraction. The fringes however will not be corrected in the extracted spectra of science targets and standard stars by the nod-

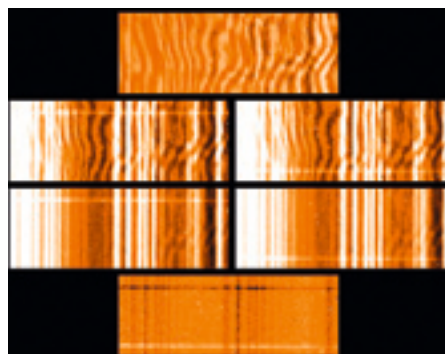
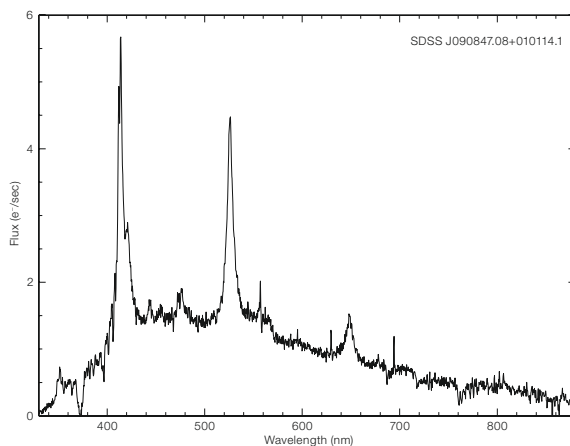


**Figure 5:** A demonstration of fringe correction with the new FORS1 detector. The top panel shows part of a spectroscopic (master) screen flat. The next two panels show parts of two bias-subtracted sections from 1200 s spectra taken with an offset along the slit (positions A (left), and B (right)). The two panels below show the same parts of the spectra, now divided by the master flat (top). Fringes are only partly corrected by the continuous light screen flat fields. The difference image of these two exposures (bottom) still contains significant sky background flux. A better result could be achieved using a sequence of four exposures (A-B-B-A).

ding technique. More details on this topic will be available on the FORS web pages. It should be noted that FORS2 has extraordinarily low fringe amplitude with its red-optimised MIT detector combined with the very low flexure it shares with its twin, FORS1. Users with strong requirements on fringe correction are therefore encouraged to choose FORS2.

In summary, the successful blue upgrade of FORS1 leads to a very promising complement to FORS2 that will further enhance the scientific productivity of this efficient and reliable pair of instruments.



#### Acknowledgements

We are grateful to: the FORS Instrument Operations Team (ESO) for continuous support through all stages of the upgrade project: Magda Arnaboldi, Paul Lynam, Palle Møller, Ferdinando Patat, Marina Rejkuba; the PAO Engineering Department for efficient support during the commissioning, in particular Roberto Castillo and Pascal Robert; and finally Walter Seifert (Landessternwarte Heidelberg) for his support in the definition of the new filter set.

#### References

- Appenzeller I. et al. 1998, *The Messenger* 94, 1  
 Baade D. and the Optical Detector Team 2005, in "Scientific Detectors for Astronomy", eds. J. E. Beletic, J. W. Beletic and P. Amico, *Astrophysics and Space Science Library*, Springer, 73  
 Bessel M. S. 1990, *PASP* 102, 1181  
 Fukugita M. et al. 1996, *AJ* 111, 1748  
 Landolt A. U. 1992, *AJ* 104, 372

**Figure 6:** Extracted, airmass-corrected spectrum of the quasar SDSS J090847.08+010114.1 (20.4 mag in *g*-band,  $z = 2.42$ ). Note that the spectrum (exposed for 15 minutes during dark time without order separation filter) is also shown in the red and near-infrared spectral range where the fringes are strongest. The strongest three emission lines (from left to right) are the hydrogen Lyman alpha line, C IV and C III lines.



VLT FORS1 image of the bubble nebula N76 around the hot binary star AB7 in the Small Magellanic Cloud, based on three exposures through narrow-band filters isolating doubly ionised helium (He II, in blue), doubly ionised oxygen ([O III], in green) and singly ionised hydrogen (H-alpha, in red). The image measures 400 by 400 arcseconds and north is up and east to the left. The binary system AB7 (the bright stellar image in the centre of the nebula) consists of one evolved massive Wolf-Rayet star and a companion O-type star. The very high temperature of the stars is responsible for the centred He II nebula (blue region enclosed within the yellow ring). To the north-east, just outside the nebula, a small network of green filaments is visible, a remnant of an earlier supernova explosion. See ESO PR 08/03 for more details.

# Towards Precision Photometry with FORS: A Status Report

Wolfram Freudling, Palle Møller, Ferdinando Patat, Sabine Moehler, Martino Romaniello, Emmanuël Jehin, Kieran O'Brien, Carlo Izzo, Eric Depagne, Emanuela Pompei, Dominique Naef, Gero Rupprecht, Arto Järvinen (all ESO)

The two *FOcal Reducer* and low-dispersion Spectrographs (*FORS*) are the primary imaging instruments for the VLT. Because they are not direct imaging instruments, the accuracy of photometry which can routinely be obtained is limited by significant sky concentration and other effects. This article reports on the progress of a long-term project to improve the photometric calibration of the FORS instruments.

The calibration plan for the FORS instruments calls for observations of photometric standards in each clear night. The primary purpose of these observations is to monitor instrument performance. The same data are also used to calibrate science observations for programmes where 5 to 10% photometric accuracy is sufficient. Two years ago we started the *FORS Absolute Photometry (FAP)* project

to characterise the photometric performance of the FORS instruments and investigate if and how the routine calibration of the instruments can be modified to offer improved photometric zero points (ZPs). An additional goal of this programme is to develop procedures to allow users to get more accurate photometric calibration.

The results are available as two internal ESO reports, Møller et al. (2005) and Freudling et al. (2006). In this article, we present a brief overview of the issues related to photometry with the FORS instruments, and the current status of *FAP*. Our work has so far concentrated on the FORS1 camera, but the most of the findings will equally apply for FORS2.

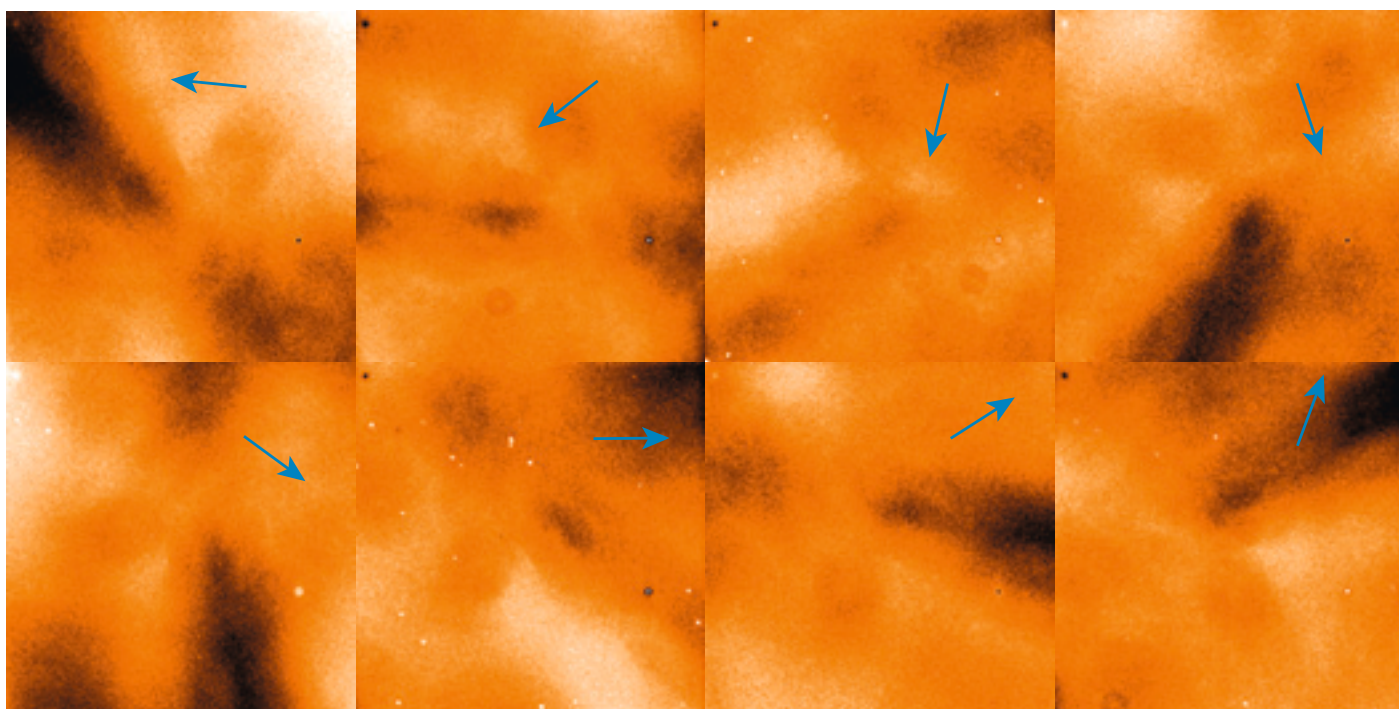
## Relative photometry with FORS1

Accurate photometry starts with reliable and stable flatfielding. We used the huge collection of twilight flats in the VLT archive to investigate the quality of the flatfields commonly used for the reduction of FORS images. In order to investigate the stability of the flatfields, we computed the mean of bias-subtracted flatfields, and divided each individual frame by this mean. This removed the stable part of the flatfields. Visual inspection

revealed that the structure in the flatfields consists of a temporally constant pattern, superimposed on large-scale fluctuations which rapidly change in time. The contrast of the constant pattern is higher in bluer bands. Interestingly, we found a correlation of some of the patterns with the adaptor rotator angle. The FORS instruments are mounted on adaptor rotators which compensate for the sky-field rotation inherent to the VLT alt-azimuth mounting. Part of the structure in the flat field rotates rigidly with the angle of the rotator. This is illustrated in Figure 1. This pattern in the flatfield must be external to FORS1 and might be due to reflections and/or asymmetric vignetting within the telescope or the adaptor itself.

A high signal-to-noise version of the rotating structure is shown in Figure 2. This image was created by counter-rotating *B* flatfields by an amount equal to the rotator angle and then computing the median of the rotated flatfields. If there was no correlation between the structure

**Figure 1:** A sequence of *B* FORS1 sky-flats divided by the median of all flatfields. The intensity scale range is 3%. The rotator adapter angles (-105, -73, -35, 0, +30, and +70) are indicated by a blue arrow in the upper right corner.



in the flatfields and the rotator angle, then the structure of the individual flatfields should average out and the median would be smooth and flat. Instead the opposite can be seen in Figure 2. A finger-like pattern, which is already visible in the individual flats shown in Figure 1, stands out with increased signal-to-noise. This demonstrates that this is a rotating feature. The peak-to-peak amplitude of the pattern in the median frame is about 1%. Inspection of individual images in the stack shows that the amplitude varies substantially among the individual flatfields.

Twilight flats, as routinely obtained each night, differ from each other by as much as 5%. If such flatfields are applied to science data, the relative photometric accuracy is limited to about 5%. Even when controlled for rotator angle, flatfields differ from each other by an amount which questions the feasibility of per-cent-level photometric accuracy with FORS1. A key question is whether these fluctuations reflect true differences in the end-to-end throughput of FORS1. In that case, relative and therefore absolute accuracy at the per cent level simply cannot be obtained with FORS1. A more likely explanation is that the flatfields are flawed and do not represent the throughput of FORS1. In that case, the task is to find the true flatfield which should be applied to data so that the photometric ZPs are constant over the whole detector.

We experimented with different procedures to remove the large-scale pattern from the raw observed flatfields. For the investigations described in the following sections, we used new observations to test the quality of the flatfields constructed in this manner, and compared them to the regular “master flats” produced by combining the routine twilight flats for that night.

The large variation in the flatfields was the motivation to take a closer look at possible variations of the ZP magnitudes across the detector when using the master flat. The goal was to derive a correction for the master flats and to find a quantitative estimate of the accuracy of the finally adopted flatfield. For that purpose, we observed standard fields with a 25-point dither pattern which placed one relatively bright star on a grid of po-

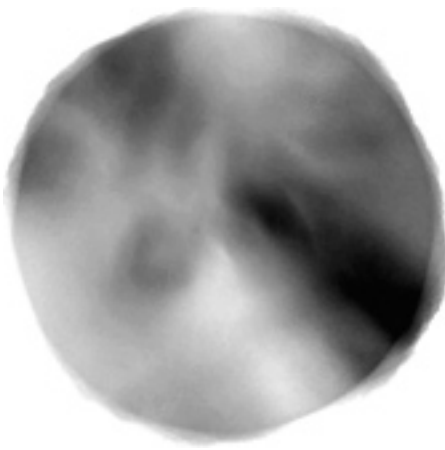


Figure 2: A stack of all *B* sky flats after applying a rotation around the geometrical centre with an amplitude equal to the adapter rotator angle. The intensity scale range is 1%.

sitions across the CCD. This approach is often nicknamed the “1000 points of light” approach. In addition, we took images of the same fields rotating the whole frame.

Ideal data sets for calibrating images with suspected ZP variations across the detectors are fields which contain suitable photometric standards over the whole dithered region. We therefore selected regions within Stetson fields (Stetson, 2000, 2006) as our targets, which contain a large number of photometric standards suitable for 8-m-class telescopes. These fields proved to be useful for our purpose, and we will investigate whether all current FORS calibration fields can be replaced with appropriately selected pointings within the Stetson calibration fields.

The simplest and most direct way to investigate relative ZP changes with dithered data is to compare the relative instrumental magnitudes of individual standard stars which are observed at positions all across the detectors. A much more sensitive method is to use the measured magnitudes of any star which has been observed at two or more different dither positions. Each individual star might only provide relative ZP shifts for a few positions on the detector. By combining the information from many stars, the ZP variations over the whole detector can be reconstructed. We used singular value decomposition (SVD) to construct such an image of the ZP varia-

tions from our dithered observations. The details of the formalism are described in Freudling et al. (2007). This image can then be used to correct the flatfield, or be applied as a second-order flatfielding step to the science data. The flatfield correction frame for the R filter is shown in Figure 3. The peak-to-peak flatfielding error at the position of the observed stars is about 30 mmag. It should be emphasised that the amplitude of the correction frame depends on the flatfield used to process the imaging data, and that the correction frame therefore only applies to that particular flatfield.

We tried several methods to remove the fluctuating and rotating features, described above, from the master flats before computing the correction frame. The most successful approach was to remove the large-scale pattern by dividing each flat-field by a smoothed version of itself. This procedure lowers the amplitude of the necessary correction to the flat-fields derived from observations of standard stars, and therefore improves the overall flat-fielding.

So far we have derived flatfield corrections for three data sets taken more than two years apart. The overall shape and amplitude of the correction frames were stable over that period. We therefore conclude that the best flatfielding with FORS1 can be obtained by: (1) removing large-scale features from the master flats; (2) applying a correction frame derived from observations of standard fields.

#### Absolute photometry with FORS1

Nightly ZPs for FORS instruments have so far been computed assuming a constant extinction for each night. The extinction, however, varies substantially from night to night, even when the nights are photometric. Therefore, ZPs derived using a mean extinction depend on the airmass of the measured standard field and are not useful for accurate photometry. The true instrumental photometric ZP above the atmosphere, as derived from extrapolation of the extinction curves, probably varies much more slowly than the night-to-night variations of the extinction. Therefore, better photometric ac-

curacy can be obtained by fitting the extinction coefficients for several nights simultaneously, assuming that the instrumental ZP does not change. Such a scheme can be included in the computation of the flatfielding correction, so that a photometric solution is simultaneously obtained with the relative flatfield correction.

The measured magnitudes of repeatedly observed stars can also be used to estimate short-term fluctuations in the extinction during the night. Each of the more than 1000 individual stars observed with our dither pattern can be used for this purpose. When the weighted average of all stars is used, changes in the extinction can be measured with an accuracy of about 1 mmag. An estimate of fluctuations in the extinction is an automatic by-product of the fitting procedure described above.

One of the tools to independently assess the quality of the night is the “VLT Astronomical Site Monitor” (ASM) which can be accessed at <http://archive.eso.org/asm/ambient-server>. We found that, at least in the one photometric night used for *FAP*, the measured scatter of about 6.8 mmag is very similar to the flux rms measured by the ASM monitor. It is tempting to conclude that the rms from the ASM can be used as a proxy for expected rms fluctuations of the ZP. We plan to further investigate the usefulness of the ASM to judge the photometric quality of the night.

Understanding the achievable accuracy of photometry requires understanding the total error budget. In particular, it is important to understand the accuracy of our procedures for flatfielding. We used the residuals of the extinction solution for a detailed investigation of the error estimates.

Measurement errors were computed for each measured magnitude from the read-out and Poisson noise, both for the pixels used to compute the stellar flux and for those used to estimate the local background. The error estimates range from 2 to 30 mmag. Errors in the listed standard magnitudes were taken from Stetson (2000) and Stetson (2006), which are based on repeated observations in



Figure 3: R-band flatfield correction frame.

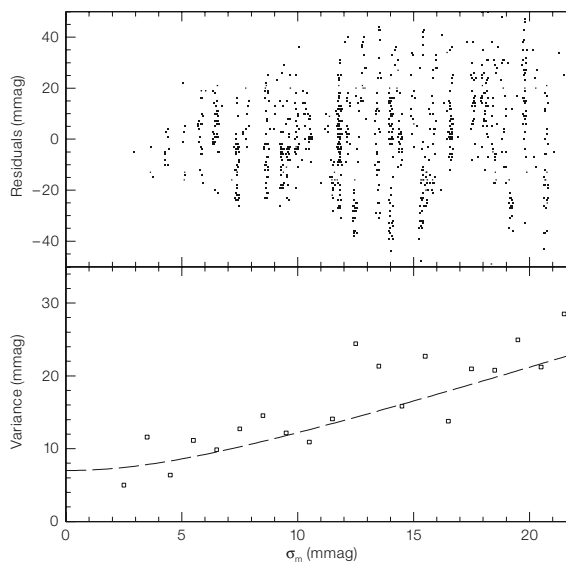


Figure 4: Upper panel: Residuals from the extinction solution as a function of the estimated magnitude error. The magnitude error includes the measurement error from the current observations as well as estimated uncertainties for the magnitudes of standard stars. Lower panel: The variance of the residuals as a function of magnitude error. The superimposed line is an error model, which includes statistical errors as well as extinction fluctuations.

different nights. Above, we estimated that extinction fluctuations during the photometric night for this programme were  $\approx 6.8$  mmag. In Figure 4 we demonstrate that extinction variations, statistical errors and errors in the standard magnitudes account for most of the residuals of our photometric solution. A detailed analysis suggests an upper limit on residual flatfielding and other sources of errors of about 3 mmag. This demonstrates that precision photometry with per-cent-level accuracy is indeed possible with FORS1.

One of the important goals of this project is to define a set of guidelines on how to achieve a per-cent-level photometric

accuracy. The uncertainty in the photometric ZP is obviously an important factor which determines the final accuracy of the magnitudes. The *FAP* observations contain a large number of standard stars on each individual image, and the number of calibration images is much larger than the number realistically taken for the calibration of normal science observations. An important part of the photometric guidelines will therefore be to find the necessary minimum number of standard fields needed to achieve a certain photometric accuracy.

*FAP* imaged four different Stetson fields in a single photometric night, which were

used to derive a photometric extinction solution. The magnitude and colour range, and the consistency of derived ZPs is similar for all fields. To estimate the errors on the ZPs from sets of only two standard field observations, we recomputed the ZPs from subsets of the *FAP* data. We used every combination of two standard fields which were taken with a difference in airmass of at least 0.7. The distribution of the resulting ZPs is shown in Figure 5. The distribution has an almost Gaussian peak but also a long non-Gaussian tail. In about 10 % of all cases, the errors on the resulting ZPs is larger than 3%. This shows that the observation of only two standard fields is insufficient to photometrically calibrate a night to per-cent-level accuracy.

We then repeated the experiment using three standard fields. At most one of the fields in each set was at an airmass less than 1.3, and the differences between minimum and maximum airmass was larger than 0.7. The resulting distribution of ZPs is plotted in Figure 5. Also shown is a Gaussian with the same mean, standard deviation and normalisation as the ZP distribution. It can be seen that the distribution resembles closely a Gaussian with a standard deviation of 11 mmag. In contrast to the previous experiment with only two standard fields, all ZP errors are less than 3%. This result strongly suggests that the use of three photometric standard fields, chosen with

the strategy outlined above, leads to an accuracy for the magnitude ZP of about 10 mmag.

The scatter in the ZPs also suggests that errors are almost Gaussian when three different standard fields are used. The error budget discussed above implies that the dominant error on the mean magnitude of all stars in any of the standard fields are fluctuations in the extinction, if the number of standard stars in each field is large enough and the exposures sample the airmass between 1 and 2 uniformly. For a typical magnitude uncertainty of 10 mmag, about 30 or more standard stars per field are needed. This is one of the reasons to use the Stetson standard fields as opposed to fields with fewer stars with known magnitudes.

#### The past and future FORS1 photometric systems

In April 2007 FORS1 was upgraded with a new CCD mosaic and a new set of broad-band filters (see article on page 9). During February and March 2007 we therefore carried out an intensified version of our usual photometric calibration plan, where we employed all the tools and methods developed during the *FAP*. This data set includes dithers and rotations which makes it possible to derive flatfield corrections directly from the calibration data. The calibrations obtained

during those two months will therefore serve to determine the best possible, and final, photometric characterisation of the now retired system which has been used since the start of VLT operation.

This “Final Effort” on the retired FORS1 photometric system will also serve as a model for the design of our future FORS calibration plan. Our pilot programme has shown that per-cent-level photometry with FORS is indeed feasible. The key requirement for this is the ability to compute the flatfield corrections. In order to make this possible for a large number of programmes, those corrections must be determined directly from the calibration plan data, which in turn places more demands on our calibration plan. In particular there needs to be a large number of moderately faint standards in each field. We are currently investigating whether appropriate regions for this purpose can be found within the Stetson standard fields. Using these fields will therefore require that we measure U-Band magnitudes for the standards in those fields. (Stetson, 2006).

*FAP* has shown that it is possible to achieve per-cent-level photometry with FORS1 with moderate effort. Over the next year, we plan to prepare new photometric standard fields suitable to obtain more accurate photometric solutions and simultaneously derive flatfield corrections. If this programme proves to be successful, we plan to incorporate new flatfielding algorithms into the FORS pipeline.

#### References

- Freudling W. et al. 2006, “The FORS Absolute Photometry Project”, VLT-TRE-ESO-13100-4006
- Freudling W. et al. 2007, in “The Future of Photometric, Spectrophotometric, and Polarimetric Standardization”, ed. C. Sterken, ASP Conference Series 364, 113
- Møller P. et al. 2005, “FORS: An assessment of obtainable photometric accuracy and outline of strategy for improvement (FORS IOT Secondary Standards Working Group)”, VLT-TRE-ESO-13100-3808
- Stetson P. B. 2000, PASP 112, 925
- Stetson P. B. 2006, fields listed at <http://cadwww.dao.nrc.ca/cadcbn/wdbi.cgi/astrocat/stetson/query>

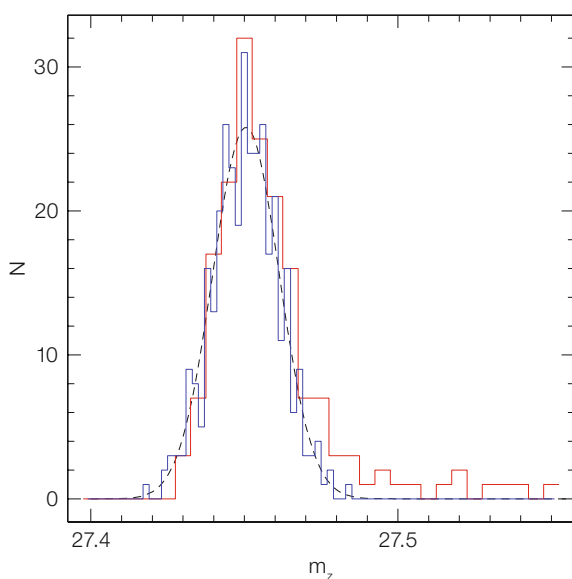


Figure 5: Distributions of zero points determined from two and three standard observations (red and blue histograms respectively). The dashed line is a Gaussian with a  $\sigma$  of 11 mmag.

# Exploring the Near-Infrared at High Spatial and Spectral Resolution: First Results from CRIRES Science Verification

Ralf Siebenmorgen<sup>1</sup>  
 Alain Smette<sup>1</sup>  
 Hans Ulrich Käußl<sup>1</sup>  
 Andreas Seifahrt<sup>1</sup>  
 Stefan Uttenthaler<sup>2</sup>  
 Arjan Bik<sup>1</sup>  
 Mark Casali<sup>1</sup>  
 Swetlana Hubrig<sup>1</sup>  
 Yves Jung<sup>1</sup>  
 Florian Kerber<sup>1</sup>  
 Jorge Melnick<sup>1</sup>  
 Alan Moorwood<sup>1</sup>  
 Jean-François Pirard<sup>1</sup>  
 Hugues Sana<sup>1</sup>  
 Elena Valenti<sup>1</sup>  
 Lowell Tacconi-Garman<sup>1</sup>  
 Michael Hilker<sup>1</sup>  
 Francesca Primas<sup>1</sup>  
 Pedro J. Amado<sup>3</sup>  
 Andrés Carmona<sup>1</sup>  
 Ewine F. van Dishoeck<sup>4</sup>  
 Cédric Foellmi<sup>1</sup>  
 Miwa Goto<sup>5</sup>  
 Roland Gredel<sup>5</sup>  
 Eike Günther<sup>6</sup>  
 Bengt Gustaffson<sup>7</sup>  
 Don Kurtz<sup>8</sup>  
 Christopher Lidman<sup>1</sup>  
 Hendrik Linz<sup>5</sup>  
 Fabrice Martins<sup>9</sup>  
 Karl Menten<sup>10</sup>  
 Claire Moutou<sup>11</sup>  
 Poul E. Nissen<sup>12</sup>  
 Dieter Nürnberger<sup>1</sup>  
 Ansgar Reiners<sup>1</sup>

- <sup>1</sup> ESO  
<sup>2</sup> Institut für Astronomie, University Vienna, Austria  
<sup>3</sup> Gr-IAA, Instituto de Astrofísica de Andalucía, Granada, Spain  
<sup>4</sup> Universiteit Leiden, the Netherlands  
<sup>5</sup> Max-Planck Institute for Astronomy, Heidelberg, Germany  
<sup>6</sup> Thüringer Landessternwarte (TLS), Tautenburg, Germany  
<sup>7</sup> Uppsala University, Sweden  
<sup>8</sup> University of Central Lancashire, Preston, United Kingdom  
<sup>9</sup> Max-Planck Institute for Extraterrestrial Physics, Garching, Germany  
<sup>10</sup> Max-Planck Institute for Astronomy, Bonn, Germany  
<sup>11</sup> Laboratoire d'Astrophysique Marseille (LAM), France  
<sup>12</sup> University of Aarhus, Denmark  
<sup>13</sup> Hamburger Sternwarte, Universität Hamburg, Germany

The VLT cryogenic high-resolution infrared echelle spectrograph CRIRES offers high spatial, spectral and temporal resolution spectroscopy from 1 to 5  $\mu\text{m}$ . Highlights from among the 29 pilot studies of the CRIRES science verification (SV) runs are summarised.

The VLT cryogenic high-resolution infrared echelle spectrograph CRIRES (Käußl et al. 2004) is located at the Nasmyth focus A of UT1 (Antu). It provides a resolving power of up to 100 000 in the spectral range from 1 to 5  $\mu\text{m}$ . CRIRES can boost all scientific applications aiming at fainter objects, higher spatial resolution (for extended sources), spectral and temporal resolution. Spectral coverage is maximised through a mosaic of four Aladdin III InSb arrays providing an effective  $4096 \times 512$  detector array in the focal plane. A MACAO (Multi-Applications Curvature Adaptive Optics) system can

be used to increase both spatial resolution and signal-to-noise ratio.

The scientific potential of the CRIRES instrument is demonstrated by the many results obtained during three science verification observing campaigns which have been performed in August, October 2006 and in February 2007. Twenty-nine pilot studies were granted observing time totaling 20 000 s integration time. The principal investigators (PI) and project titles of the successfully executed SV programmes are given in Table 1. Individual projects range from studies of the Earth's atmosphere, disc structure around young stars, brown dwarfs (BD), extra-solar planets to pulsation and wind properties of massive stars, asymptotic giant branch stars (AGB), structure of the Galaxy and astroseismology. In this article some of the highlights are presented in a sequence beginning with young stars, brown dwarf stars and planets,

**Tabel 1:** CRIRES science verification runs: principal investigator (PI) and project title is given for each programme.

ID	PI	Title
1	Amado	NIR spectroscopy of pulsating stars?
2	Bik	Circumstellar discs around massive young stellar objects
3	Carmona	Probing the gas in the inner 50 AU of proto-planetary discs
4	Foellmi	Distances to late-type stars
5	Goto	H <sub>2</sub> and CO observation toward Superantennae
6	Günther	CRIRES for high precision RV of late-type stars
7	Gustaffson	CNO abundances in Bulge giants
8	Käußl	Search for OH in the disc around HD 163296
9	Kerber	Determining the atmospheric precipitable water vapour content
10	Kjaer	High resolution infrared spectrum of SN 1987A
11	Kurtz	High time-resolution precision radial velocities of peculiar A stars
12	Lidman	A high-resolution spectral atlas of the night sky
13	Linz	Disc winds and envelopes associated with BN-type objects
14	Martins	The most massive stars in the GC: binarity and metallicity
15	Melnick and Gredel	Molecular hydrogen in Doradus 30
16	Moutou	Transmission spectroscopy of transiting extrasolar planets
17	Nissen	The abundance of sulfur in metal-poor stars
18	Nürnberger	Weighing a high mass protostellar candidate
19	Reiners	FeH spectroscopy in ultra-cool dwarfs – CRIRES or UVES?
20	Sana	Can IR solve the wind clumping question?
21	Seifahrt	Effective temperatures and gravities of low-mass stars and BD
22	Siebenmorgen	Astrochemistry in dust formation regions
23	Siebenmorgen	Roadmap of astrochemistry during massive star formation
24	Siebenmorgen	Bound on time dependency of the fine structure constant
25	Smette	Na I D and Ca II in a $z \sim 2$ damped Ly $\alpha$ system
26	van Dishoeck	CO emission from transitional protoplanetary discs
27	Uttenthaler	The C/O and C <sup>12</sup> /C <sup>13</sup> ratios and three dredge-up in bulge AGB stars
28	Uttenthaler	Titanium Oxide band heads in the J-band
29	Valenti	Chemical composition of evolved populations in LMC and NGC 1866

followed by massive and Asymptotic Giant Branch stars to targets outside the Galaxy. Finally CRILES calibration issues are mentioned.

### Discs around massive young stellar objects and extrasolar planets

The known circumstellar discs around massive young stellar objects T Cha and IRAS 16164–5046 were studied by van Dishoeck [ID 26] and by Bik [ID 2], respectively. The CO first-overtone emission in the *K*-band probes high-temperature gas ( $T = 3000$  K) and the velocity profile of IRAS 16164–5046 suggests that the hot gas is located in a rotating disc within 10 AU of the central star. The CO-fundamental transitions in the *M*-band probe lower-temperature gas ( $T = 50$ –500 K) and therefore different regions in the circumstellar material. Figure 1 shows three transitions of the  $^{12}\text{CO}$  spectrum of IRAS 16164–5046. The R(7) line is more sensitive to higher temperature compared to R(0). The spectra reveal two absorption components; a saturated blue component which could be caused by an outflow or wind, and a red, unsaturated component which changes in intensity from the higher to the lower energy level. This extra red absorption could be a cold envelope surrounding this object.

A full *L*- and *M*-band (3600–5100 nm) wavelength scan of the spectrum of the extremely red and massive protostar W33A was performed, aiming to achieve a first road map of the astrochemistry occurring during the formation process of massive stars. A section of it, corresponding to the spectral region near 4200 nm, is shown by Käufel et al (2007). Figure 2 compares the rich CO line system (near 4730 nm) to the broad Br $\alpha$  and Pfy lines. Derived radial velocities (RV) for CO, Br $\alpha$  and Pfy lines are  $\sim 31$  km/s confirming earlier estimates (Roueff et al. 2006).

Carmona [ID 3] obtained *K*-band spectra of the classical T Tauri star LkH $\alpha$  264. They confirm the previous discovery of the ro-vibrational  $v = 1-0$  S(1) H $_2$  line. In addition, thanks to the enhanced sensitivity of CRILES, they detect at 2223.3 nm the  $v = 1-0$  S(0) H $_2$  transition. However, the spectra do not reveal the  $v = 2-1$  S(1) H $_2$  line. The line ratios of 1–0 S(0)/1–0 S(1)

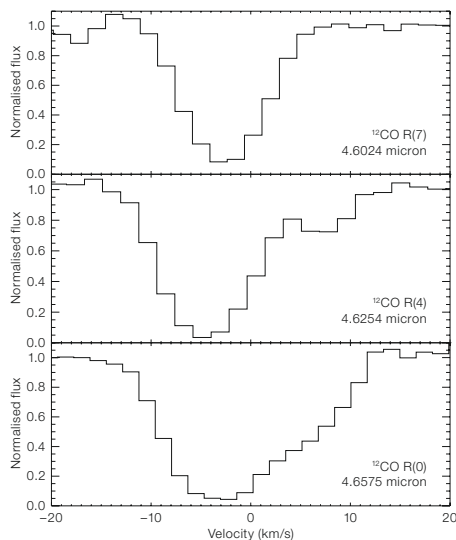


**Figure 1:**  $^{12}\text{CO}$  profile of the massive young stellar object IRAS 16164–5046. From top to bottom, lines R(7), R(4) and R(0) are plotted. The R(0) line is more sensitive to cold material than the other two. Two components can be identified, one belonging to the cold envelope and the other component caused by a wind or outflow (Bik et al.).

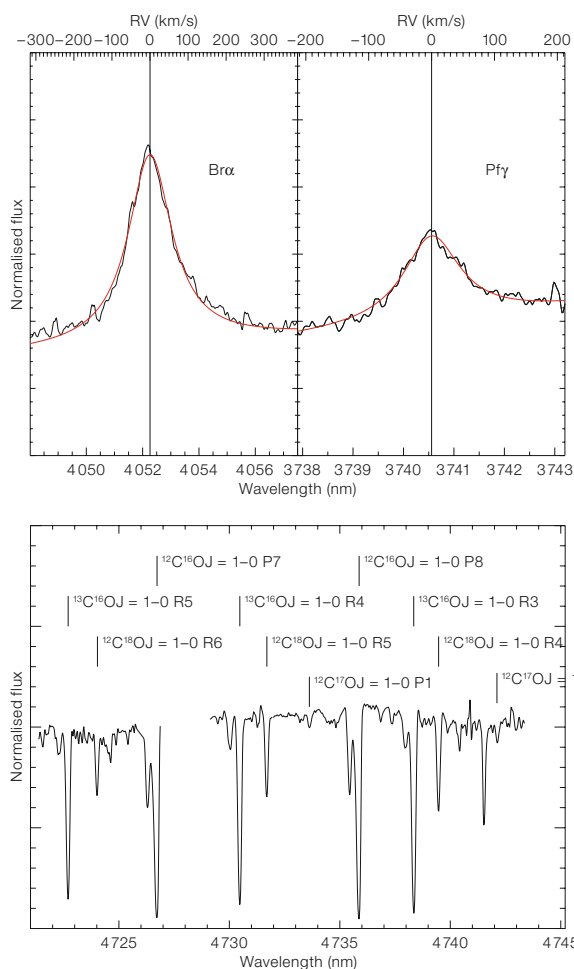


**Figure 2:** Line flux and RV of the Br $\alpha$  and Pfy (top) and various CO isotopes (bottom) of the protostar W33a (Siebenmorgen et al.).

$= 0.33 \pm 0.1$  and  $2-1 \text{ S}(1)/1-0 \text{ S}(1) < 0.2$  indicate that the  $\text{H}_2$  emitting gas is at temperature below 2000 K and most likely thermally excited by UV photons. Both detected lines have a FWHM of  $\sim 20$  km/s and are spatially unresolved. The mean FWHM of the PSF in the continuum is  $\sim 0.36''$  in the  $\text{H}_2$   $1-0 \text{ S}(1)$  spectrum, constraining the  $\text{H}_2$  emitting region to the inner 50 AU of the disc at an assumed distance of 300 pc. The  $v = 1-0 \text{ S}(1)$  and the  $v = 1-0 \text{ S}(0)$   $\text{H}_2$  lines in LkH $\alpha$  264 are single peaked. Modelling of the  $v = 1-0 \text{ S}(1)$  line shape indicates that the disc has a relatively small inclination. The best model fit suggests that the disc surrounding LkH $\alpha$  264 is inclined by  $20^\circ$  relative to the line of sight (Figure 3).

Late-type objects of spectral type M and later exhibit extremely interesting absorption bands. In particular, the molecular band of FeH shows sharp absorption lines that can be used for precision spectroscopy, a rare feature for late-type stars and brown dwarfs. These lines appear in the spectral range close to  $\approx 1000$  nm, at the red end of the UVES spectral coverage and at the blue one of CRIRES. A performance test of both instruments in this overlapping region was carried out by Reiners [ID 19] on GJ 2005A, a M5.5 star, observed with CRIRES and MACAO, while Gl 406, a star of the same spectral type, was observed with UVES. The FeH absorption of both stars resembles each other very closely. The UVES data were taken at a resolution of 50000, and for comparison CRIRES data were rebinned to match this lower resolution. The UVES exposure of Gl 406 ( $V = 13.54$ ) yielded a SNR of 60 after 200s whereas the CRIRES spectrum on the much fainter star GJ 2005 A ( $V = 15.42$ ) gives a SNR of 50 after 480 s. Therefore, in this overlapping wavelength region, UVES requires roughly twice the observing time of CRIRES to reach the same SNR for similar flux levels and spectral resolution.

The closest T dwarf to the Sun (3.26 pc),  $\epsilon$  Ind B, is an ideal system to improve our understanding of substellar objects by detailed spectral measurements. The two members of this extreme cool brown dwarf binary have spectral type T1 and T6.5 and masses of  $\sim 47$  and  $28 M_{\text{Jup}}$ , respectively. The CRIRES spectroscopy campaign by Seifahrt [ID 21] concentrat-

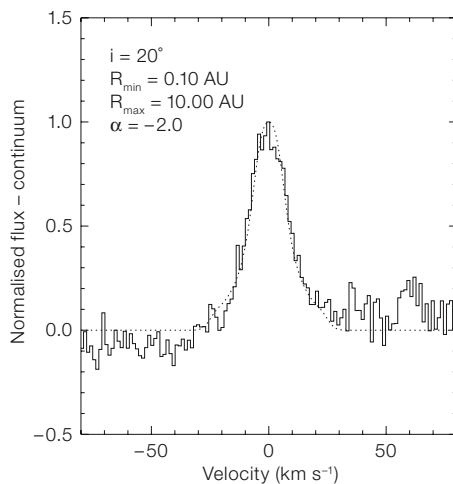


**Figure 3:**  $\text{H}_2$   $v = 1-0 \text{ S}(1)$  line detected in LkH $\alpha$  264 at 2121.8 nm and model (dashed) assuming that the emission originates in a circumstellar disc. The fit parameters  $R_{\text{min}}$  and  $R_{\text{max}}$ , the inner and outer radius of the emitting region,  $\alpha$ , the power law exponent of the intensity ( $I(R) \propto R^\alpha$ ) and  $i$ , the inclination angle (Carmona et al.), are listed.

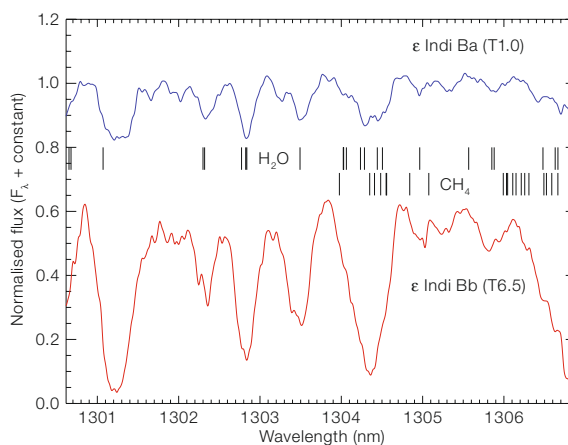


**Figure 4:** Cut-out of the high-resolution spectrum of the binary components  $\epsilon$  Ind Ba (top) and Bb (bottom). Lines of water vapour ( $\text{H}_2\text{O}$ ) and methane ( $\text{CH}_4$ ) are marked. Note the increase in line strength for both species between the T1 dwarf (Ba) and the T6.5 dwarf (Bb) and the strong line broadening by the high projected rotational velocity  $v \sin i \sim 28$  km/s (Seifahrt et al.).

ed on a K I line at 1252.5 nm, water vapour and methane ( $\text{CH}_4$ ) features at wavelengths close to the peak flux of T dwarfs. For the first time in natural-seeing observations, spectra of both binary components, separated by  $\sim 0.9''$ , have been obtained with spectral resolution of  $R \sim 50000$  (Figure 4). The S/N of the spectra are between 20–60 (per pixel) which is in close match to the predictions of the CRIRES exposure time calculator (ETC). Detailed comparison of the spectra to synthetic atmospheric models as well as to existing T dwarf models are in progress. In particular, the relative radial velocity of  $\epsilon$  Indi Ba-Bb will improve their orbital parameters.

Precise radial velocity (RV) measurements are important in many astrophysical objects. In particular, they have led to the discovery of more than 200 extra-solar planets. Carrying out equivalent measurements at infrared wavelengths

has several advantages: indeed, late-type stars and brown dwarfs are much brighter at infrared wavelengths while the RV-jitter caused by stellar activity is about one order of magnitude smaller in the infrared than in the optical regime (Martins et al. 2006). Günther [ID 6] observed the MOV star GJ9847 in two different nights, obtaining spectra with the  $\text{N}_2\text{O}$ -absorption cell, as well as template spectra without. Simulations predict that the simultaneous wavelength reference allows a radial velocity precision of better than 30 m/s to be achieved. Even though improvements in the data analysis are still possible this accuracy is already achieved. The basic idea of the procedure is the same as for the  $I_2$ -cell method in the optical, which has been used for many years for planet detection. The main difference is that the influence of the telluric absorption lines has to be carefully removed. This is achieved by dividing the spectrum by a reference star free of

absorption features, e.g. a B-type star. This technique is illustrated in Figure 5 for the M0V star GJ 9847.

The SV programme by Moutou [ID 16] aimed at detecting the absorption signature of a planetary atmosphere, during a transit of the extrasolar planet in front of its parent star. This requires high spectral resolution to deblend the planetary features from the stellar ones at a certain epoch. For such transiting systems, one expects to detect a  $K_1$  absorption feature in the near-IR. Unfortunately during the execution of the programme, the CRIRES observing sequence could not fully meet the time critical window that lasted a little more than two hours. The data however show differences from one spectrum to the other and a longer lasting sequence is allocated in P79.

#### Massive stars, Asymptotic Giant Branch stars and Galactic structure

The Pistol star, located close to the Galactic Centre, is the most luminous star in the Galaxy. Unless it is actually made up of various components, it is also the best candidate to be the most massive star. The very high resolving power of CRIRES was used by Martins [ID 14] to investigate the presence of a spectroscopic companion, as well as to constrain the abundance of a few key elements (Si, Mg and Fe). Data were obtained during the February run and are currently being analysed with atmospheric models. They will reveal whether the Pistol star is truly a very massive star, and will provide the ratio of alpha elements to Fe, a quantity which critically depends on the chemical enrichment history and the IMF in the Galactic Centre.

Information on star interiors can be obtained through the determination of the frequencies of pulsation modes as they emerge at the stellar surface, a technique known as asteroseismology. Amado et al. [ID 1] tested the feasibility of asteroseismology in the NIR. For 3.5 hours, they continuously observed the strongly photometric  $\delta$  Scuti variable star, 1 Mon and searched for the presence of line profile or equivalent width variations due to the pulsations.

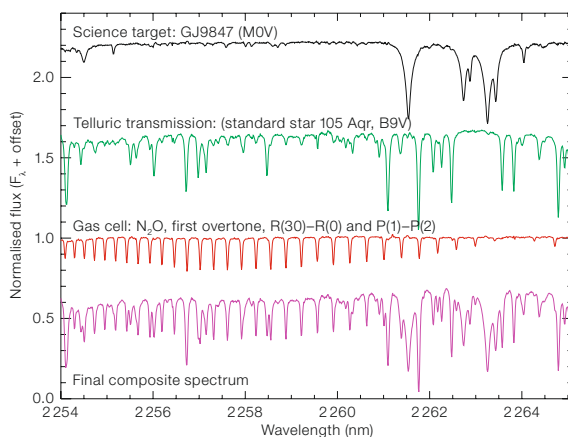


Figure 5: From top to bottom and shown as indicated: the normalised spectrum of GJ9847; the telluric standard star; the  $N_2O$  gas cell; and the final composite spectrum (Günther et al.).

O-type stars are among the brightest and most luminous stellar components of a galaxy. Through their radiation and wind momentum, they largely influence their surroundings as well as their host galaxies. However, our knowledge of these objects is still fragmentary. One of the currently most critical questions is related to the exact properties of their stellar winds, which determine their mass-loss rates, and thus their evolution to become supernovae. CRIRES allows to significantly increase the number of accessible diagnostic lines. Sana [ID 20] acquired a high S/N ratio spectrum of  $\zeta$  Pup, an O4 supergiant and one of the closest O-type stars. The comparison of the observed line profile with the one predicted from atmospheric models should provide tight constraints on its wind properties and, more specifically, on its clumping factor. Using ESO and IUE archives, a multi-wavelength analysis covering the whole spectral range from the UV to the near-IR domain is foreseen. The complementarity of the diagnostic lines in these various wavelength ranges should help to obtain a self-consistent view of the atmosphere of this massive star.

Nissen [ID 17] choose extreme metal-poor stars in the Galactic halo to study the abundance of Sulphur, an  $\alpha$ -element, considered an important diagnostic for galactic chemical evolution (see the article by Nissen et al. on page 38). Infrared observations of atomic lines in the near-infrared are an important complement to visible (UVES) spectra, as they can be less sensitive to details of the atmospheric models and may have substantially larger oscillator strengths. An impressive spectrum with a S/N of 330

was achieved (Nissen et al. 2007 – the first published refereed paper from CRIRES).

The infrared absorption spectra of  $H_3^+$  and CO were observed by Goto [ID 5] toward the luminous infrared source in the Quintuplet cluster GCS 3-2 and is shown in Figure 6. Note the distinct absorption profiles of  $H_3^+$  R(1,1)<sup>l</sup> and CO R(1) along the same line of sight. While CO mostly probes the gas in molecular clouds in the Galactic arms along the line of sight, the  $H_3^+$ , responsible for R(1,1)<sup>l</sup>, occurs both in arm clouds and in the gas at the Galactic Centre region. The pedestal component of R(1,1)<sup>l</sup> is almost identical with the broad absorption band of R(3,3)<sup>l</sup> obtained at Subaru and Gemini South. R(3,3)<sup>l</sup> however exclusively samples the gas in the Galactic Centre. The population of  $H_3^+$  in the metastable state (J,K) = (3,3), 361 K above the ground state, attests to the presence of warm ( $T \sim 250$  K) and diffuse gas ( $N_H \sim 100/cm^3$ ) in the central molecular zone, which was unknown before (Oka et al. 2005).

Uttenthaler [ID 27] obtained *H*- and *K*-band spectra of a handful of bulge AGB stars to determine the C/O and  $^{12}C/^{13}C$  ratios. These ratios are influenced by a deep mixing event called the third dredge-up (3DUP) which occurs on the AGB. If 3DUP has occurred in a given star, the  $^{12}C/^{13}C$  ratio should be high (compared to the solar value of  $\sim 89$ ), otherwise it should be low ( $< 10$ ). As an example the CRIRES spectrum of M794 reveals a strong  $^{12}CO$  4–2 band head but weak  $^{13}CO$  lines (e.g. at 2354.25 and 2355.1 nm), so that this star has a rather low  $^{12}C/^{13}C$  ratio. Further support that

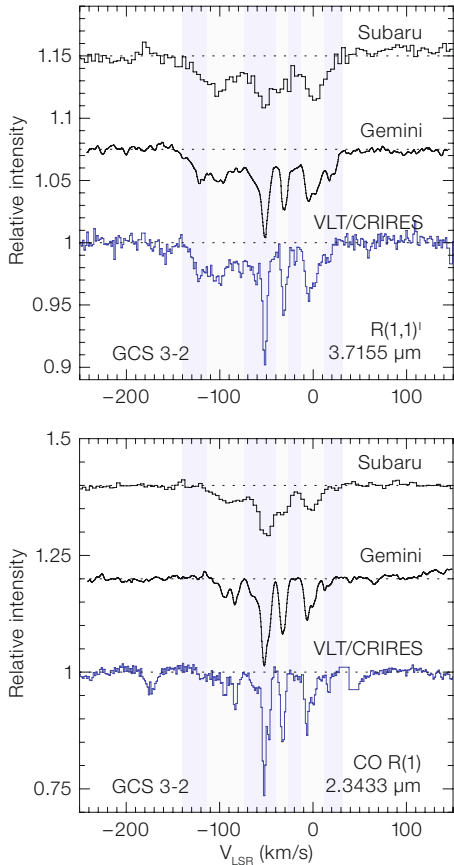


**Figure 6:** Infrared absorption spectra of  $H_3$  R(1,1) and CO R(1) towards the Quintuplet cluster GCS 3-2 observed with three different high-resolution spectrographs. The performance of IRCS at the Subaru telescope (with spectral resolving power  $R = 20\,000$ ) and Phoenix at Gemini South ( $R = 75\,000$ ) is compared to that of CRIRES at the VLT ( $R = 100\,000$ ). The higher velocity resolution of CRIRES is the obvious advantage among the other instruments on 8-m-class telescopes.

discriminated by obtaining the ages of a considerable number of Bulge red giant stars using the ratios of heavy element abundances, in combination with their kinematics, as a chronometer. The main reason for observing in the IR (see Ryde et al. 2005) is the much smaller interstellar extinction so that the whole Bulge is observable and not just a few windows transparent at optical wavelengths. Only the near-IR offers all the indicators necessary for accurate determination of the important C-N-O molecular equilibrium in the atmospheres of cool stars, through the simultaneous observation of many clean CO, CN and OH lines. The goal with the SV run was to test the method. The result was successful, even though, only three Bulge stars could be observed. Figure 7 shows the CRIRES spectrum of one of them, Arp 4203. The wavelength range 1531–1570 nm was recorded and only a 1/4 of the spectrum is shown for clarity. From the derived abundances, the findings are that, e.g., the giant star Arp 4203 is depleted in C, enriched in N,

M794 has not experienced a 3DUP is given by the non-detection of Technetium, a radioactive indicator for this process. Interestingly, as determined from UVES spectra, this star shows Lithium in its atmosphere, which is rather surprising for a previously classified low-mass AGB star. Most probably another mixing process – called cool bottom processing – is at work in this star, reducing the  $^{12}\text{C}/^{13}\text{C}$  ratio almost down to its equilibrium value.

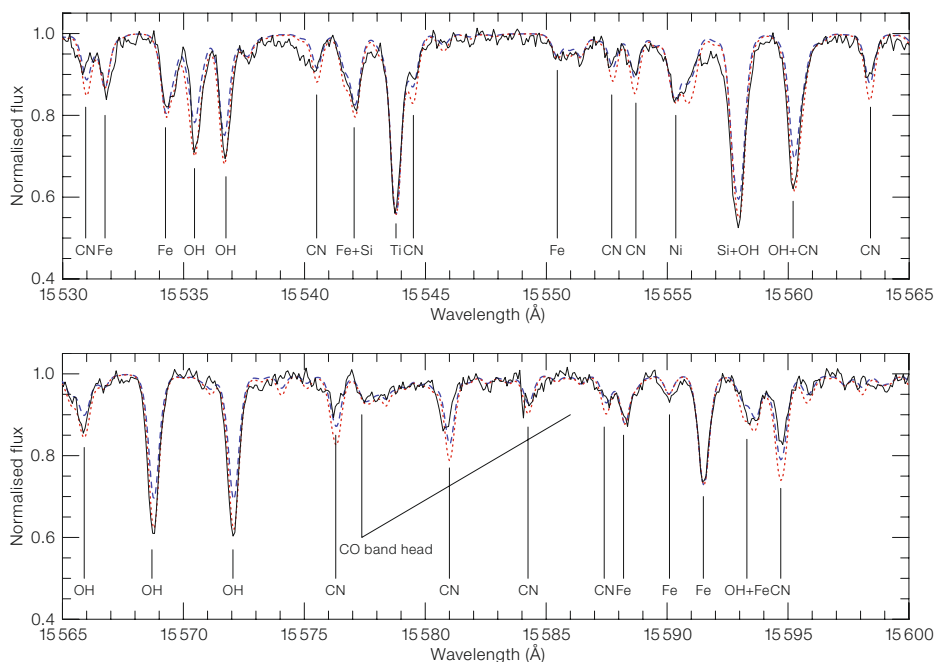
Gustafsson [ID 7] studied the CNO abundances in bulge giants, first, as a SV trial run and subsequently in an allocated programme in period P79. The team is a large international collaboration including members from Australia, Brazil, Chile, France, Germany and Italy. Studying the Milky Way Bulge is particularly important and, as an ultimate goal, should answer the question of whether it is the Galaxy's oldest region, perhaps together with the Halo. Alternatively, it could have been gradually formed, at least partially, from stars and gas in the disc that migrated inwards. These hypotheses can be

with an excess of O relative to Fe but compatible with the alpha elements (Mg, Si and Ca). The C and N abundances are signs that matter exposed to the CN cycle (which conserves the sum of C and N nuclei) has been dredged up to the stellar surface. The sum of the abundances of C, N, and O is close to that expected from a non-processed old star, formed with an excess of oxygen and alpha elements relative to iron. The preliminary elemental abundances are presented in Ryde et al. (2007), while a full analysis will be presented in a forthcoming paper.

### Outside the Galaxy

Two extragalactic SV projects were executed. Siebenmorgen [ID 24] tried to constrain variations in the fine structure constant,  $\alpha = e^2/hc$  by observing the [O III] doublet redshifted to  $z \sim 2$ . The QSO 1148-001 was selected as it shows a bright doublet unresolved at low resolution. Unfortunately, the lines are too broad when observed at a resolution of

**Figure 7:** Two sections of the CRIRES spectrum of Arp 4203 are presented (full line, black) together with models with nitrogen increased by +0.4 dex (dashed, blue) relative to the best fit, and when oxygen is instead decreased by 0.2 dex (dotted, red). For clarity the best-fit model is not shown (Gustafsson et al.).



50000 and no useful constraint could be derived.

A second project focused on the ISM of proto-galaxies at  $z > 2$  (Smette [ID 25]). The NaI and CaII absorption lines are common features in the ISM of our Galaxy, but so far they have never been observed in the ISM of objects with redshifts larger than one. CRIRES offers the possibility to extend the study of the ISM by means of these important lines for damped Lyman-systems (DLA) at high  $z$ . These lines provide important information regarding the velocity structure of the gas. NaI can be compared with the low-ionisation lines seen in UVES spectra to better constrain the ionisation conditions. At low redshift, CaII is often seen in turbulent material such as the one seen in the merging galaxies. Comparison between NaI and CaII is also a very good indicator of the clumpiness of the gas. The QSO HE0251-5550, chosen from the H/ESO DLA survey (Smette et al. in prep.), has a hydrogen column density  $\log(N_{\text{H I}}) = 20.7$  DLA in its spectrum and a redshift of  $z = 2.3$ , allowing the search for NaI and CaII doublets with CRIRES. Although the object is bright enough in  $R$ -band to close the AO loop, though with little improvement in image quality, the faintness of the QSO ( $H = 14.6$ ) made guiding somewhat difficult, as insufficient flux is reflected back from the slit jaws to the slit viewer detector. The spectra covering the NaI lines reached the expected S/N but did not reveal the lines, probably because of the low metal abundance of this system. Unfortunately, the seeing degraded during the promising, yet challenging, observations of the CaII lines and the spectra have an unusably low S/N. Despite the non-detection, these observations were a good test of the feasibility to observe such 'faint' targets with CRIRES, in particular, when the high resolution allows one to avoid the effects of telluric lines.

### Calibration of CRIRES data: CRIRES and the Earth's atmosphere

Observing with CRIRES as well as calibrating and reducing CRIRES data revealed multiple challenges that the science verification programmes helped to identify. A large number of the problems that the CRIRES team met during the execution of the programmes have been solved in time for science operations, while work is still going on for others.

For example, the high-resolution capabilities of the instrument are a challenging aspect when it came to the development of a precise ( $\sigma(v) \sim 70\text{m/s}$ ), robust and automatic wavelength calibration procedure. The pipeline, now in use to assess the quality control of the data, uses as first guess the wavelength solution provided by a physical model of the instrument, which is accurate to about 1–2 pixels. It then cross-correlates data with other catalogues such as telluric features computed by HITRAN or OH line lists. In addition, CRIRES supports high-accuracy wavelength calibration by means of gas cells and a ThAr hollow cathode lamp (Kerber et al. 2007).

But an accurate and precise wavelength calibration relies on a large number of lines on each detector. Ideally, these lines should be observed simultaneously with the target. Such is the case for observations through gas cells. In several spectral bands, the sky lines are very numerous. However, little is known of their apparent wavelength stability which could limit their use for high-accuracy wavelength calibration. Such a study – the feasibility of using OH lines to calibrate CRIRES data – is at the base of the proposal of Lidman [ID 12], as this molecule shows a rich ro-vibration spectrum. Before CRIRES, OH sky line spectra had only been systematically obtained with spectral resolutions of 10000 or less. CRIRES spectra of the OH lines were taken during evening twilight, which is the time when they are at their brightest. In a single 300-s exposure it is possible to see up to a dozen lines on a single detector and up to four times that number over the entire mosaic. In order to assess their wavelength stability, data over several nights were obtained, immediately followed by a ThAr spectrum. A quick in-

spection of the  $R \sim 100\,000$  spectra reveals that CRIRES resolves doublets which are seen as single lines at spectral resolution of 10000 (see Figure 9 in Siebenmorgen and Smette 2007). However, even at a resolution of 100000 CRIRES does not resolve individual lines. Also, a number of sky lines appear that are not listed in available catalogues and *vice versa*.

CRIRES is also helping ESO in preparation for the next generation of giant telescopes. Kerber [ID 9] tested a method to measure the atmospheric content of precipitable water vapour (PWV) using the equivalent widths of  $\text{H}_2\text{O}$  absorption lines in the near-IR which are imprinted onto the spectra of early-type stars. An accurate and efficient method to determine the PWV is highly valuable for any thermal IR instrument at an E-ELT. For quantitative measurements, unblended water lines are selected to have a minimum dependence of their absorption coefficient at a temperature of  $\sim 300\text{K}$ . CRIRES spectra of bright stars were observed on several nights during SV. On some of these nights routine measurements with VISIR (see Smette et al. 2007) can be used to establish the PWV from mid-IR data allowing for comparison across wavelength and method. Very acceptable agreement between both methods and instruments is found.

### References

- Carmona A. 2007, Ph.D. Thesis, University of Heidelberg
- Käufl H. U. et al. 2004, SPIE 5492, 1218
- Käufl H. U. et al. 2007, The Messenger 126, 32
- Kerber F. et al. 2007, ASP Conference Series 364, ed. C. Sterken, 461
- Martins F. et al. 2006, ApJ 644, L75
- Nissen et al. 2007, A&A, accepted, astro-ph/0702689
- Oka et al. 2005, ApJ 632, 882
- Roueff et al. 2006, A&A 447, 963
- Ryde N. et al. 2007, astro-ph/0701916
- Ryde N. 2005, in: "High Resolution Infrared Spectroscopy in Astronomy", ESO Astrophysics Symposia, (eds.) H. U. Käufl, R. Siebenmorgen and A. F. M. Moorwood, Springer, 365
- Siebenmorgen R. and Smette A. 2007, CRIRES User's Manual, <http://www.eso.org/instruments/crires/doc/>
- Smette A., Horst H. and Navarrete J. 2007, Proceedings of the 2007 ESO Instrument Calibration Workshop, Springer-Verlag, in press, <http://www.eso.org/gen-fac/meetings/cal07/presentations/smetteCal07.pdf>

# The First Active Segmented Mirror at ESO

Frédéric Gonté, Christophe Dupuy, Christoph Frank, Constanza Araujo, Roland Brast, Robert Frahm, Robert Karban, Luigi Andolfato, Regina Esteves, Matty Nylund, Babak Sedghi, Gerhard Fischer, Lothar Noethe, Frédéric Derie (all ESO)

The Active Phasing Experiment (APE) is part of the Extremely Large Telescope Design Study which is supported by the European Framework Programme 6. This experiment, which is conducted in collaboration with several partners is a demonstrator to test and qualify newly-developed phasing sensors for the alignment of segmented mirrors and test the phasing software within a telescope control system to be developed for a future European Extremely Large Telescope. The segmentation of a primary mirror is simulated by a scaled-down Active Segmented Mirror of 61 segments which has been developed in-house.

## Background

In order to gain experience with the phasing of segmented mirrors, in particular to develop new optical phasing sensors and to test the interface with the rest of the wavefront control system, ESO decided to perform an optical-bench type experiment, named the Active Phasing Experiment (APE). This project is part of the Extremely Large Telescope Design Study (ELTDS) which is supported by the European Framework Programme 6. The project is performed in close collaboration with the Istituto Nazionale di Astrofisica di Arcetri, the Instituto de Astrofísica de Canarias (IAC) and the Laboratoire d'Astrophysique de Marseille (LAM), and the industrial firm Fogale. The core optical element of APE, simulating the segmented primary mirror in a large telescope, is a scaled-down Active Segmented Mirror (ASM) with 61 segments which can all be controlled in piston, tip and tilt. The pupil of the telescope is re-imaged onto the ASM. The optical beam is then re-adapted to behave like the VLT output beam and distributed to the four phasing sensors to be tested in the experiment.

The design and integration phases of APE, which started in 2005, have been completed and the test phase will start in June 2007 during which time APE will be installed at the focus of one of the VLT unit telescopes in 2008.

Initially the APE team wanted to contract the design and manufacture of the ASM to a private company. However, when no company could be found which could meet the rather stringent requirements, it was decided to develop the ASM in-house, involving ESO groups in Integration, Optics, Electronics, Software and the ELT Project Office.

## Design and integration

The current design of the primary mirror of the European Extremely Large Telescope consists of 984 hexagonal segments (Gilmozzi and Spyromilio 2007). Each segment has a diameter of around 1.5 m and the size of the gaps between the segments is approximately 4 mm. In order to achieve the performance required for high-resolution imaging with extreme Adaptive Optics (AO), the hexag-

onal mirrors have to be aligned with a precision better than 15 nm rms. It was clearly not feasible to produce a scaled-down version of the full primary mirror. However, from a statistical point of view, a mirror with approximately 50 segments is already representative of a mirror with many more segments in terms of the study of issues like alignment algorithms or the effect of misalignments on image quality. The main requirements for the ASM can be summarised as:

- 61 segments in four rings around the central segment
- Segment size 17 mm to minimise the size of the re-imaged pupil and the relay optics on the optical bench
- Three degrees of freedom for rigid body movements, that is piston, tip and tilt for each segment
- Precision of displacement better than 2 nm (similar to an ELT)
- Range of displacement more than 15  $\mu\text{m}$  (similar to an E-ELT)
- Size of the gaps between segments between 80 and 150  $\mu\text{m}$  (scaled-down from the gap size in the ELT primary)
- Surface form quality better than 15 nm RMS (similar to the required surface quality of a real segment with active shape control)
- Operational temperature between 0°C and 25°C
- Possibility to exchange a segment in case of failure.
- Optical fibres to be inserted in two of the hexagonal mirrors (central mirror and one of the perimeter mirrors) to align APE with high efficiency

A segment unit, shown in Figure 1, consists of a base, three actuators, three springs and a hexagonal mirror. The 61 modules were assembled on a base plate (Figure 2). Since the precision of positioning the surfaces of the hexagonal mirrors relative to the base plate is better than 15  $\mu\text{m}$ , it is necessary to be able to actively align all the mirrors. Among the set of candidates for the commercially available actuators, only piezo actuators could fulfil the ASM requirements. Since this type of active segmented mirror is the first of its kind it was decided to start development in mid-2005 with a prototype of only seven segments.

Figure 1: Each segment is integrated separately. It is composed of one base, three piezo-actuators, three springs and a hexagonal mirror.



Photo: H. Heyer, ESO

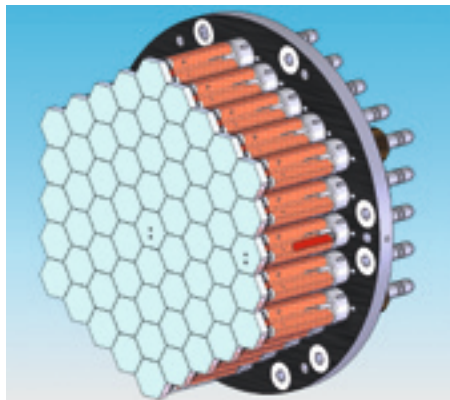


Figure 2: Mechanical design of the ASM made by Christoph Frank. The 61 segments are seen with the three actuators per segment, the module base, the support plate and the connectors behind the support plate. The fibres inserted in the central mirror and one of the mirrors on the right side of the ASM can also be seen.

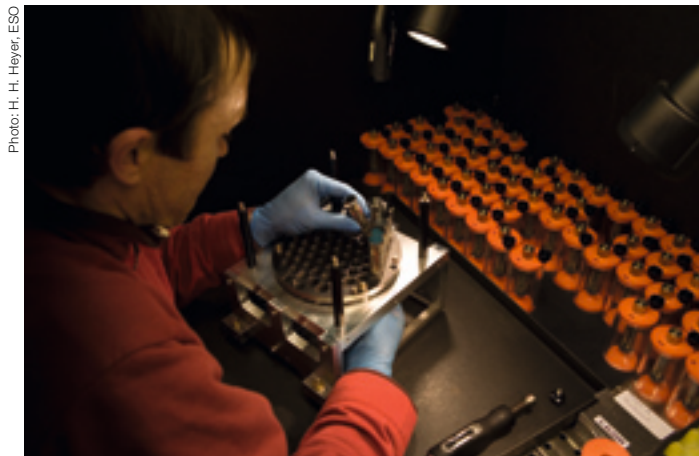


Figure 3: Integration of the ASM (having a plug and play concept) by Christophe Dupuy. Each segment is added one by one on a support polished plate which has a surface flatness better than 2 microns.

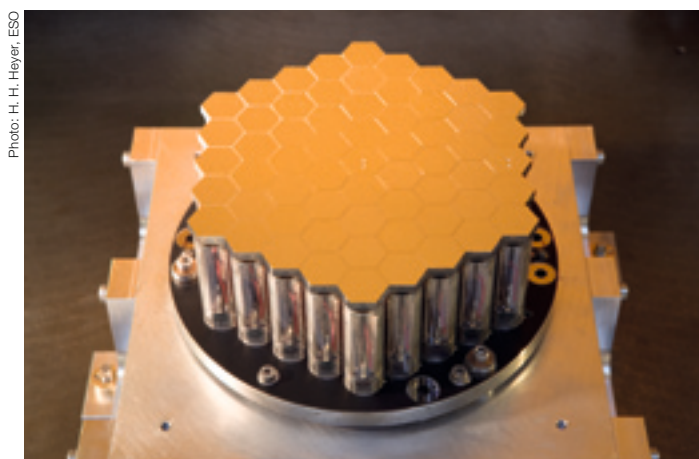


Figure 4: Photo of the fully assembled ASM.

The mechanical design has been made by Christoph Frank. The integration has been conducted by Christophe Dupuy for the opto-mechanical parts (see Figure 3), by Roland Brast for the drive electronics and by Robert Frahm for the software. The tests were performed by Constanza Araujo. Information obtained during the tests of the seven-segment prototype was used to improve the final design.

### Current tests

Several features have been tested on the fully integrated ASM (Figure 4), for example fatigue of the components, eigen-frequencies, speed and hysteresis of the positioning, drift of an actuated position, resolution and accuracy of the positioning, quality and cosmetics of the surfaces of the segments. The fully integrated ASM has fulfilled and, in some cases, even surpassed the specifications. Figure 5 shows an interferogram of the surface of the ASM while being tested. The tips and tilts of the segments have been selected such that the letters of the acronym ASM appear in the interferogram.

During the APE experiment, the ASM will be driven in closed loop based on signals

obtained by an Internal Metrology system which consists of a two-wavelength interferometer developed by Fogale. The seven-segment prototype has been used to test the closed-loop system and achieved a performance better than 5 nm rms for the alignment errors at the intersegment borders.

The fully integrated ASM has now fulfilled and, in some areas, even surpassed the specifications. The success of this realisation now provides the possibility to fully test future phasing sensors of the E-ELT within the Active Phasing Experiment.

### References

Gilmozzi R. and Spyromilio J. 2007, *The Messenger* 127, 11

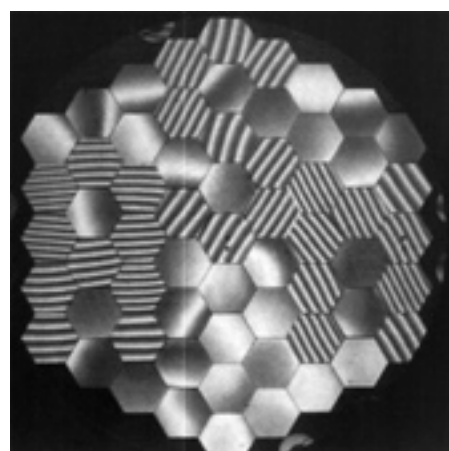


Figure 5: Interferogram of the surface of the ASM. Some segments have been tip-tilted to create fringes on some selected segments to write on it the acronym ASM.

# Progress of the ALMA Project

Christoph Haupt, Hans Rykaczewski (ESO)

An overview of the current status of the ALMA project and the progress over the last two years is presented. The main focus is on the European deliverables, but the contributions of North America and Japan are also mentioned.

## Science Objectives of ALMA

The Atacama Large Millimeter and Submillimeter Array (ALMA) will provide an unprecedented combination of sensitivity, angular resolution, spectral resolution, and imaging fidelity at the shortest radio wavelengths for which the Earth's atmosphere is transparent. The three major scientific goals for ALMA can be summarised as: to detect spectral line emission from CO or CII at a redshift of  $z = 3$  in less than 24 h of observation; to image gas kinematics in protostars and protoplanetary discs at a distance of 150 pc, enabling the study of the physical, chemical and magnetic field structures; to provide images with an angular resolution of  $0.1''$ .

## Developments over the last two years

The agreement to construct ALMA was signed in 2002 by the North American community, represented through the National Science Foundation (NSF), and the European community, represented through ESO. After three years of detailed design studies and prototype research, it became evident that the project could not be realised within the original time-scale and within the available funds foreseen at the time of signing the agreement. The management and scientists involved in ALMA were therefore charged to develop a new configuration of the project within their foreseen budget, while still maintaining the prime scientific objectives.

During this period in-depth studies and large efforts were made to define the "re-baselined" ALMA project. A major element in cutting the cost was the reduction of the number of antennas from 64 to 50 (with an ultimate goal of 64). Fortuna-



Photo: H. Heyer, ESO

Figure 1: The Road between Chilean Highway No. 23 and ALMA.

tely, the results of testing of the prototypes for the receiver cartridge showed that several of the receivers significantly exceeded their noise temperature requirements, thus partially offsetting the loss in sensitivity through the reduced number of antennas. Independent advisory and review committees, focusing on the technical performance as well as on the cost of the project, confirmed the scientific importance of the modified ALMA project, based on the new affordable costs. By the end of 2005 the re-baselined project and the new budget were approved by the ESO Council. The North American partners received approval from their Funding Agency (NSF) by the middle of 2006.

In parallel, Japan, through the National Astronomy Observatory of Japan (NAOJ), continued to define and formulate their participation in the ALMA project. The European and North American partners in ALMA spent a considerable amount of time with their Japanese partners in identifying the Japanese participation and reviewed various subsystems, in particular correlator, receivers and antennas. Details on the partnerships were defined and an official, trilateral agreement between ESO, the NSF, and the National Institute for Natural Sciences (NINS, Japan) was signed in summer 2006. NAOJ will provide four antennas of 12 metres diameter, twelve antennas of 7 metres diameter, two receiver bands for all 66 antennas of ALMA and the Atacama Compact Array (ACA) Correlator. Approval of funds required for the Japanese participation

in ALMA is expected by summer 2007. With the inclusion of the Japanese partners ALMA becomes a truly global astronomy facility.

## The ALMA Site

The ALMA Array Operations Site (AOS) will be located at a unique place: the Altiplano de Chajnantor, a plateau at an altitude of 5 000 metres in the Atacama Desert in Chile. This location was selected for reasons of dryness and altitude.

The ALMA Operations Support Facilities (OSF), located at an altitude of about 2 900 metres and 28 km away from the AOS will be the base camp for the everyday, routine operation of the observatory.

Constructing and operating the ALMA Observatory within the ambitious scientific goals and the unprecedented technical requirements in this environment, with its harsh living conditions, will be one of the real challenges.

Construction of the OSF and AOS sites and their access required substantial effort from the ALMA project. The OSF site, located at 2 900 metres altitude, is about 15 km away from the nearest public road, the Chilean highway No. 23 and the AOS is another 28 km away from the OSF site. A road of 43 km length was constructed to access the OSF and AOS (Figure 1), with sufficient width to regularly transport the antennas between the OSF and AOS for maintenance.

The OSF is the centre of activities of the ALMA construction project. Presently all ALMA Site contractors and their staff are accommodated at the OSF. Work is organised in 20 day working/10 day rest periods. Special camps have been erected and can now accommodate the maximum required capacity of 500 workers.

During the construction period, the OSF will become the focal point of all antenna Assembly-Integration-Verification (AIV) activities. Antenna assembly will be done at the OSF site at three separate areas, one each for the antennas provided by North America (Vertex), Japan (Melco) and Europe (AEM Consortium). AIV activities will be carried out at the OSF, after preliminary acceptance of the antennas, and prior to moving them to the AOS.

Ultimately, the OSF and its Technical Facilities will become the centre of all day-to-day scientific activities. During the operations phase of the observatory it will be the workplace of the on-site astronomers and of the technical teams responsible for maintaining proper functioning of the ALMA telescope and its equipment.

ESO signed the contract for the construction of the OSF Technical Facilities in August 2006. Construction work has advanced (see Figure 2) and during this time no major problems or delays have occurred. As specified in the construction schedule, foundations have been prepared and the superstructures of the buildings were completed in March 2007. Provisional Acceptance of all facilities is foreseen for the first quarter of 2008.

The AOS Technical Building (Figure 3) will be delivered by the North American ALMA partner. Inside the building, construction work and furnishing is expected to be completed by summer 2007. Human operations at the AOS will be limited to an absolute minimum, due to the high altitude. The AOS Technical Building will house the Back-End electronics and the Correlator. Digitised signals received from the radio telescopes will be processed here and further transmitted to the data storage facilities located at the OSF. The AOS building will become usable for installing technical equipment in June 2007.



Figure 2: Construction work on the OSF Technical Buildings.



Figure 3: The AOS Technical Building.

### The ALMA Antennas

Major performance requirements of each antenna are 2" absolute pointing over the whole sky, 0.6" offset pointing, a 25-micron rms overall surface accuracy and the ability to fast switch over a 2-degree range in less than 1.5 seconds. These requirements are at least comparable to those of existing submillimetre radio telescopes; however all of these, except the APEX antenna which is very similar to an ALMA prototype antenna, are protected from the weather by shelters.

The antennas are critical for the ALMA project and their quality and performance are a major contributor to the overall functionality of ALMA. In view of the technical criticality of the antenna specification, three prototypes were supplied by the AEC Consortium (procured by ESO), Vertex RSI (procured by NRAO for North America) and Mitsubishi Electrical Company (procured by NAOJ, Japan). All three

prototypes were extensively tested at the ALMA Test Facility in Socorro, New Mexico (see the image on the front cover). Various groups of international experts, both internal and external to ALMA, reviewed the performance of the prototype antennas and concluded that the performance expected at the ALMA site conforms to the technical requirements for all three designs.

Following a Call for Tender for the antennas, the North American partners of the ALMA project, through Associated Universities Incorporated (AUI), signed a contract to supply up to 25 antennas, with options to increase the contract to 32 antennas, with Vertex RSI on 11 July 2005. Similarly, on 6 December 2005, the ESO Director General signed a contract (see ESO PR 31/05) with the AEM Consortium (Alcatel Alenia Space France, Alcatel Alenia Space Italy, European Industrial Engineering S.r.l., MT Aerospace) for the supply of 25 ALMA antennas (as the Eu-

ropean share of the project), also with options to increase the number of antennas to 32. The four total power antennas of 12 m diameter, equipped with nutators, to be provided by Japan, have been ordered from Mitsubishi Electrical Company. The twelve remaining antennas of 7 m diameter will be ordered in the course of the year 2007 by NAOJ.

The first antenna to be supplied by Vertex RSI is expected to be ready for provisional acceptance in Chile in the second half of 2007. The first antenna to be supplied by the AEM Consortium is expected by the third quarter of 2008. Despite the delayed delivery of the AEM antennas, both suppliers are expected to deliver their 25th antenna by the end of 2011. Acceptance for the first antenna from Japan is expected to take place in December 2007.

The Preliminary Production Design Review for antennas to be produced by Vertex RSI was held in September 2006, the corresponding review for AEM antennas was held at the end of January 2007.

### The ALMA Antenna Transporters

The antenna array at an altitude of 5000 m can be reconfigured by relocating antennas on the stations located on the Chajnantor plateau. The configurations can be changed from a compact one, in which all antennas operate within an area of 160 m × 250 m, to an extended configuration for which the maximum separation between antennas reaches about 15 km. In order to move antennas, each with a mass of around 100 tons, the ALMA project has designed a special transport vehicle (Wilson 2006). Two vehicles will be needed to cover the operational relocation requirements. These transporters will move antennas between the assembly and maintenance area at the OSF and the AOS and at the AOS between different antenna stations for reconfiguration of the array. By means of the transporter (Figure 4) the antennas can be positioned to an accuracy of a few millimetres on the high-precision station interface.

The mass of the antennas, their high-precision and the hostile, high altitude envi-

Figure 4: ALMA Antenna Transporter.



Photo: Scheuerle Fahrzeugfabrik GmbH

ronment impose severe requirements on these vehicles. Each transporter will have a mass of about 150 tons, and dimensions of about 10 × 15 × 6 m (width × length × height). The contract for the production of these truly unique transporters was signed by ESO with Scheuerle Fahrzeugfabrik GmbH (Germany) on 22 December 2005. The first of the transporters will roll out of the hangar and will be tested in summer 2007 (see Figure 4) to be transported and delivered to the OSF in the fourth quarter of 2007. The second vehicle is expected to be delivered about six months after the first one.

### The ALMA Front-End

The ALMA Front-End system is the first element in a complex chain of signal reception, conversion, processing and recording. The Front-End is designed to receive signals in ten different frequency bands (Table 1). In the initial phase of operation the antennas will be equipped with six bands. These are Bands 3, 4, 6, 7, 8 and 9. It is planned to equip the antennas with the missing bands at a later stage of ALMA operation.

The ALMA Front-Ends are superior to almost all existing systems. Indeed, development work for the ALMA prototypes has also led to improved receivers for existing millimetre and sub-millimetre observatories.

They are comprised of numerous elements (Figure 5), produced at different locations in Europe, North America and Japan. In the initial phase of construction ALMA decided, after the prototyping and developing stage, to build a set of eight pre-production units before moving to full production. This initial phase started in the years 2004 and 2005. Some components were successfully and completely pre-produced by the end of 2006 and the rest are expected to be completed in the course of 2007.

The largest single element of the Front-End system is the cryostat, a vacuum vessel with the cryo-cooler attached. The cryostats will house the receivers, which are assembled in cartridges and can relatively easily be installed or replaced. The corresponding warm optics, windows and IR filters were delivered by the Institut de Radio Astronomie Millimétrique (IRAM, France). The operating temperature of the cryostats will be as low as 4 K.

ESO and the Rutherford Appleton Laboratory (RAL, UK) launched a development and pre-production programme for the manufacture of eight completely operational cryostats. Six cryostats (Figure 6) have been fully assembled. The remaining two units are in manufacture and the Cryostats production contract was signed in April 2007.

A development and pre-production phase was also launched for the six dif-

Table 1: The ten frequency bands of ALMA.

ALMA Band	Frequency Range (GHz)	Receiver Noise Temperature (K) over 80 % of the RF Band	at any RF Frequency	To be produced by <sup>1</sup>	Mixing scheme
1	31.3–45.0	17	26	to be decided	Single Side Band
2	67–90	30	47	to be decided	Single Side Band
3	84–116	37	60	HIA	Dual Side Bands
4	125–163	51	82	NAOJ	Dual Side Bands
5	163–211	65	105	OSO (6 only)	Dual Side Bands
6	211–275	83	136	NRAO	Dual Side Bands
7	275–373	147	219	IRAM	Dual Side Bands
8	385–500	196	292	NAOJ	Dual Side Bands
9	602–720	175	261	NOVA	Double Side Band
10	787–950	230	344	NAOJ (to be confirmed)	Double Side Band

ferent receiver cartridges (Table 1). The technical specification of the various receiver cartridges are demanding, set at the state of the art or even beyond at the time of definition. The development programmes were successful, meeting essentially all of the requirements – and sometimes substantially exceeding them – specifically for the receiver noise temperatures. This is a very important achievement as to some extent the better noise performance and higher sensitivity partially compensate the loss in collecting area.

In the frame of the European FP6 programme, ESO is leading a group of European institutes to develop and build six Band 5 receiver cartridges and to develop associated software. This project was approved by the European Community at the end of 2005. In parallel, NAOJ is leading activities related to the development of Band 10 receivers. The Band 9 cartridge was built by NOVA in the Netherlands and is shown in Figure 7. The receivers for Band 10 are still in an R&D phase; it is expected that in 2008 a final decision will be made on implementing this ALMA band with the highest frequency.

Pre-production of the cryogenic low-noise amplifiers for Band 7, 4–8 GHz, and for Band 9, 4–12 GHz, receivers has been successfully completed by Centro Astronómico de Yebes (CAY, Spain). Amplifier series production for Band 7 commenced in February 2007 by Spanish industry.

Water Vapour Radiometers (WVRs) are needed to provide a correction of the phase fluctuations due to atmospheric water vapour fluctuations. The development of two prototype WVRs, at Cam-

<sup>1</sup> IRAM Institut de Radio Astronomie Millimétrique (Grenoble, France)  
 HIA Herzberg Institute of Astrophysics (Victoria, Canada)  
 NAOJ National Astronomical Observatory of Japan (Mitaka, Japan)  
 NOVA Nederlandse Onderzoekschool voor Astronomie (Groningen, the Netherlands)  
 NRAO National Radio Astronomy Observatory (Charlottesville, USA)  
 OSO Onsala Space Observatory/Chalmers University (Onsala, Sweden)

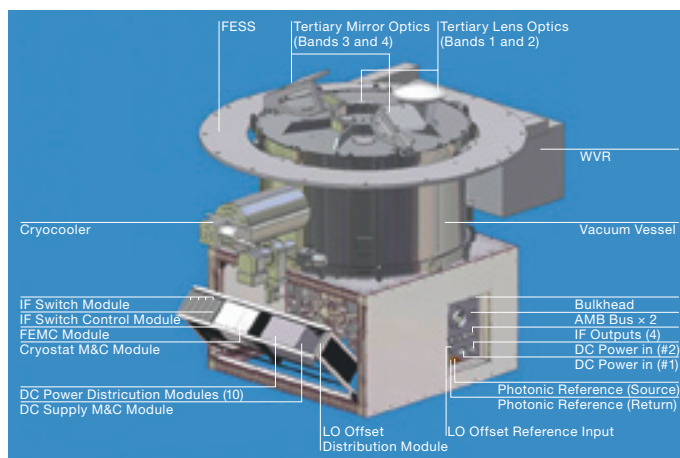
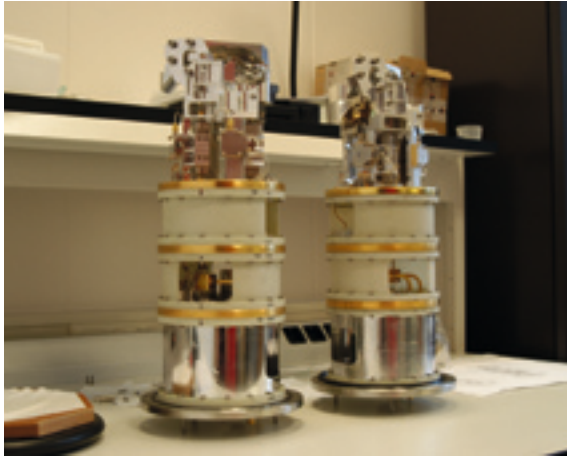


Figure 5: Schematic of the ALMA Front-End System.

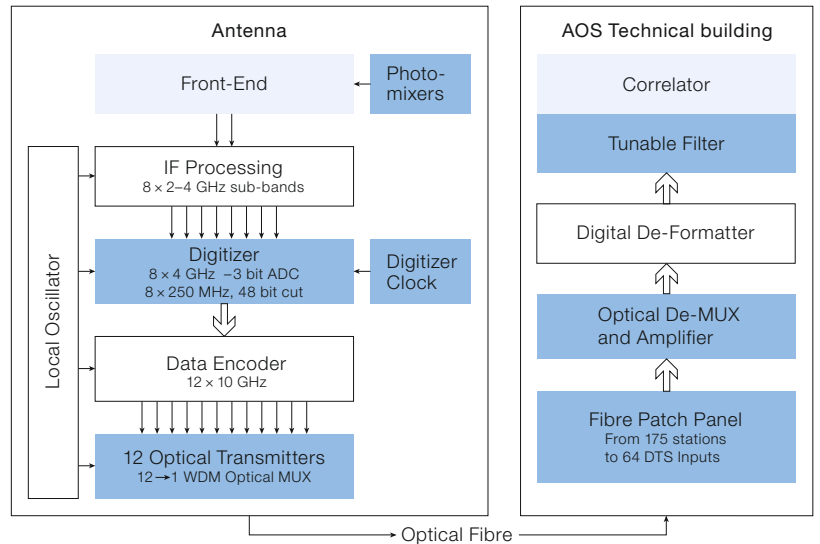


Figure 6: ALMA Cryostat pre-production at RAL/UK.

**Figure 7:** ALMA Band 9 Cartridges ready for delivery, at NOVA in the Netherlands.



**Figure 8:** Schematic of ALMA Signal Processing and data transfer from the Front-End to the Correlator. Parts to be provided by ESO are shaded in dark blue.



bridge University (UK) and Onsala Space Observatory (Sweden), was completed and both underwent intensive testing at the Sub-Millimeter Array (SMA) on Mauna Kea (Hawaii). The performance of both prototypes meets the requirements and demonstrated the atmospheric correction method. The Call for Tender for the final detailed design and full WVR production was issued in February 2007 to industry in ESO member states and production should commence in mid-2007.

### The ALMA Back-End

The ALMA Back-End systems deliver signals generated by Front-End units installed in each antenna to the Correlator installed in the AOS Technical Building. Signal processing and data transfer is schematically shown in Figure 8. In each of two orthogonal linear polarisations an intermediate frequency (IF) of 8 GHz bandwidth can be processed and recorded at any time. Analogue data, produced by the Front-End electronics, are processed and digitised before being formatted for the transmission through the optical transmitter units and multiplexers. All these elements are installed in the receiver cabins of each antenna. Optical signals are then sent through optical fibres to the AOS Technical Building. The total distance in the most extended antenna configuration is about 15 km. At the AOS Technical Building the incoming optical signals are de-multiplexed and de-formatted before entering the Correlator.

The European deliverables in the ALMA Back-End project are a number of components, which are produced by several European institutes, working closely with ESO, and NRAO. These deliverables are: digitizer chips and digitizer assembly; digitizer clock assembly; optical data transmission system; fibre patch panel; optical multiplexers (MUX) and de-multiplexers (De-MUX); Erbium-Doped Fibre Amplifiers (EDFA), and photonic local oscillator photomixers.

Development and pre-production of these components has been successfully completed; the components will be integrated at NRAO in Socorro and installed in the European and North American prototype antennas for tests at the ALMA Test Facility ATF.

An example of one of the various Back-End components produced in Europe is the 4 GHz digitizer in its final layout (see Baudry et al. 2006, Figure 3). The clock rate is 4 GHz, allowing an input bandwidth of 2 GHz. The digitization uses three levels to preserve the signal-to-noise ratio. During the prototype and development phase, the initial layout was optimised in order to reduce the number of parts and the assembly costs. The final digitizers show an improved performance and a higher reliability. This work was carried out in close collaboration between ESO and the University of Bordeaux. The first units have been shipped to Socorro for final acceptance and integration with tests at the ATF.

### The ALMA Correlator

The ALMA Correlator, to be installed in the AOS Technical Building, is the last component in the receiving end of the data transmission. It takes as input the digitized signals from the individual antennas and outputs amplitude and phase on all of the interferometer baselines in each of a large number of spectral channels. It is a very large data-processing system, composed of four quadrants, each of which can process data coming from up to 16 different antennas. The complete correlator will have 2912 printed circuit boards, 5200 interface cables, and more than 20 million solder joints. The first quadrant was completed at NRAO in the third quarter of 2006. Work on the second quadrant is progressing on schedule.

Integral parts of the Correlator are Tunable Filter Bank (TFB) cards, which allow a major increase in the flexibility by subdividing the frequency range into 32 independently configurable sub-channels. Four TFB cards are needed for the data coming from a single antenna. The TFB cards have been developed and optimised by the University of Bordeaux over the last few years. Prototypes and pre-production units were extensively tested and their performance was critically reviewed in the first half of 2006. In the meantime, series production is progressing and the first batch of 108 out of 560 TFB cards has been produced.

## System Engineering and Integration

An important ALMA-wide activity is the System Engineering and Integration (SE&I) task, which covers coordination of activities across the project. One of the prime objectives of SE&I is to ensure that modules and equipment produced for an ALMA subsystem, often in different locations of the world, fit physically and functionally together. SE&I is also responsible for the ALMA system design, technical budgets and for ensuring the system integrity, and hence has to ascertain that all interfaces between the various subsystems are completely understood, well defined, rigorously reviewed and properly documented.

In order to achieve the tasks mentioned above, the SE&I team takes a central role in the preparation and management of project performance and engineering requirements and Interface Control Documents ICD. SE&I is also very active in organising, holding and chairing technical reviews of the project, which could be internal to ALMA or external, reviewing the status and progress of the design and manufacturing of ALMA components by industry or scientific institutes. Product and Quality Assurance is another task and will receive a high visibility specifically during the manufacturing phase.

The SE&I group is also leading the activities related to Prototype System Integration and the testing at the ALMA Test Facility (ATF) in Socorro (see front cover). During the years 2007 and 2008 the ATF will serve as a facility where ALMA hardware and software will be integrated into an operational system using the two prototype antennas from Europe and North America. In a joint effort with the ALMA Science team, first fringes were recorded in March 2007 (see ESO PR 10/07). The ATF is also used for training integration and operations personnel for Chile and for qualifying equipment needed for acceptance tasks in Chile, such as the Optical Pointing Telescope and the Holography System.

Another major activity for the coming years is the Assembly, Integration and Verification (AIV) at the OSF. Equipment acceptance has already started and AIV at the OSF will begin with the antenna

delivery in the middle of 2007 for which preparations are currently ongoing.

## Computing

The development of a unified software system for the ALMA Observatory is another important activity which requires intensive interactions with all of the ALMA engineering project teams. The nature of software development calls for a common approach and policy from the very beginning – not only with respect to the engineering teams, but also between the European and North American partners. In contrast to some cases of hardware oriented activities, where specialised instruments are provided, this project requires entire software packages to be developed under a single management and organisation.

ALMA Software Development is managed as a truly integrated, trilateral organisation. The European, North American and Japanese Executives have identified individual work packages under a common leadership.

Work in Europe is organised through ESO. The centre of European software development and management is at ESO's headquarters in Garching. Many software packages are developed by ESO in collaboration with European institutes who have experienced and qualified staff developing and testing the required software. Table 2 gives an overview of software projects carried out by various European institutes in association with ESO.

Major computing subsystems for which ESO has direct responsibility include:

- ALMA Common Software (ACS), the infrastructure used by all other software;
- Archive, both Front-End and science archive, collecting not only science data, but also any other information used by the ALMA observatory software;
- Integration and test activity, to get a coherent and tested software system out of the many subsystems;
- High Level Architecture activity, responsible for the design of the ALMA software and consistency of its interfaces;

**Table 2:** Software Development in European Institutes.

Software Activity	Institute <sup>2</sup>
Science Software Requirements	IRAM
Pipelining	UKATC, MPIfR
Archiving	Man. Un./JBO
Observing Preparation	UKATC
Offline Data Processing	MPIfR, CNRS
Telescope Calibration	IRAM, IEM-CSIC
ALMA Common Software	OAT

<sup>2</sup> IRAM	Institut de Radio Astronomie Millimétrique (Grenoble, France)
UKATC	United Kingdom Astronomy Technology Centre (Edinburgh, United Kingdom)
MPIfR	Max-Planck-Institut für Radioastronomie (Bonn, Germany)
Man. Un.	University of Manchester (Manchester, United Kingdom)
JBO	Jodrell Bank Observatory (Macclesfield, United Kingdom)
CNRS	Observatoire de Paris & Centre National de la Recherche Scientifique (Paris, France)
IEM-CSIC	Instituto de Estructura de la Materia (Madrid, Spain)
OAT	Osservatorio Astronomico di Trieste

- Executive subsystem, which provides the operator user interfaces;
- Observatory Support Software, which provides the support tools needed by time allocation teams and the support for data packages;
- Software engineering activity, which maintains the standards to be used in hardware and software.

Figure 9 shows as an example the Operator Master Console. This is part of the Executive subsystem, for which ESO is responsible.

## Acknowledgements

We would like to thank Claus Dierksmeier, Stefano Stanghellini, Gie Han Tan, Fabio Biancat Marchet and Gianni Raffi for helping to prepare this article.

## References

- Baudry A. et al. 2006, *The Messenger* 125, 37  
 Wilson T. 2006, *The Messenger* 123, 19  
 Haupt C. et al. 2006, *Proc. SPIE* 6271, 14

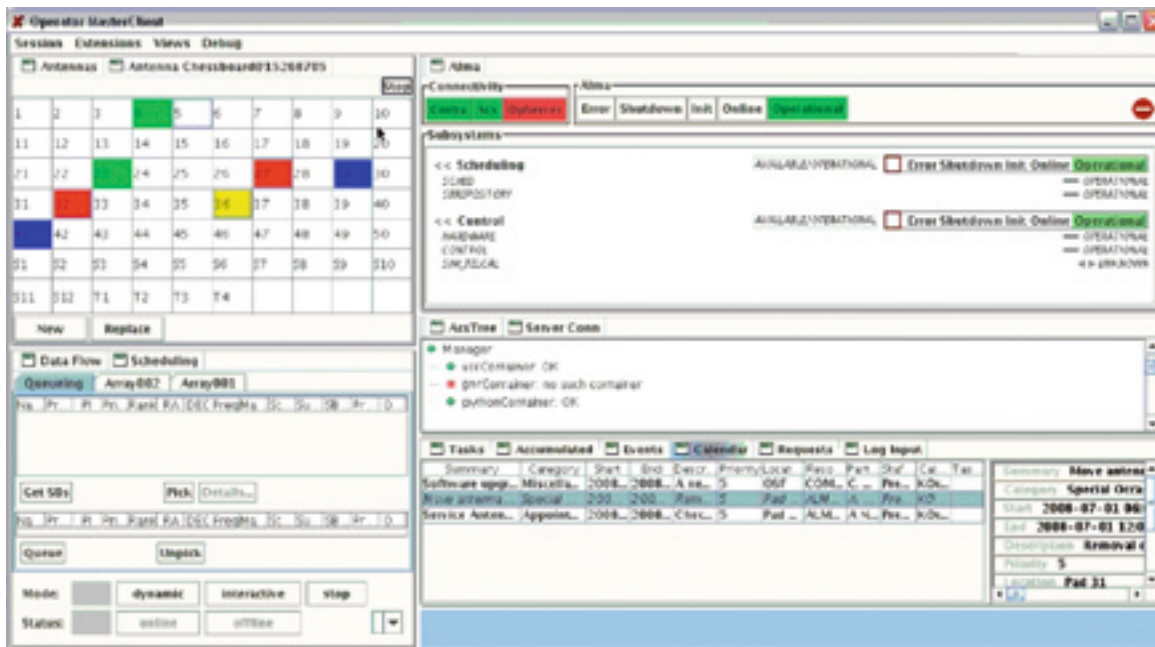


Figure 9: The ALMA Operator Master Console.

## ALMA European Project Scientist Appointed

Tom Wilson (ESO)

The new ALMA European Project Scientist is Dr. Leonardo Testi. He took up the appointment in May 2007. Leonardo Testi received his Ph.D. from the University of Florence in 1997. Subsequently he was a postdoctoral fellow at the Owens Valley Radio Observatory of Caltech. In 1998 he joined staff of the Arcetri Astrophysical Observatory, and later on of INAF, for which he also served on the Science Council. Leonardo has been chair of the European ALMA Science Advisory committee and a member of the ALMA Science Advisory committee, so he well knows the details of the project as well as the science that can be carried out with ALMA.

Leonardo's main scientific interest is the study of circumstellar discs around newly formed stars. It is believed that many of these discs of dust and gas will develop into planetary systems, so such studies are complementary to the optical searches for extrasolar planets being carried out, for example, with HARPS and the ESO 3.6-m telescope. The major drawbacks to present-day studies of circumstellar discs are sensitivity and angular resolution. With ALMA, the sensitivity will be more than 40 times better, and the angular resolution more than 5 times better, than current instruments. Thus ALMA will allow breakthroughs in this area, as well as for studies of star formation, galaxy evolution and dynamics, Solar System science and cosmology.

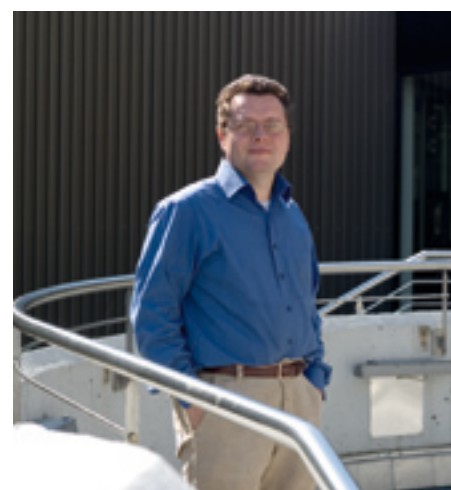


Photo: H. Hoyer, ESO

Dr. Leonardo Testi



FORS1 colour composite image of the H<sub>II</sub> region NGC 2081 in the Large Magellanic Cloud taken with the new blue CCD. Three filter images isolating emission lines of [O II], [O III] and H-alpha were combined.

# Hunting for Frozen Super-Earths via Microlensing

Jean-Philippe Beaulieu<sup>1,3</sup>  
 Michael Albrow<sup>1,4</sup>  
 Dave Bennett<sup>1,5</sup>  
 Stéphane Brillant<sup>1,6</sup>  
 John A. R. Caldwell<sup>1,7</sup>  
 Johannes J. Calitz<sup>1,8</sup>  
 Arnaud Cassan<sup>1,9</sup>  
 Kem H. Cook<sup>1,10</sup>  
 Christian Coutures<sup>1,3</sup>  
 Stefan Dieters<sup>1,11</sup>  
 Martin Dominik<sup>1,2,12,13</sup>  
 Dijana Dominis-Prestler<sup>1,14</sup>  
 Jadzia Donatowicz<sup>1,15</sup>  
 Pascal Fouqué<sup>1,16</sup>  
 John Greenhill<sup>1,11</sup>  
 Kym Hill<sup>1,11</sup>  
 Matie Hoffman<sup>1,8</sup>  
 Uffe G. Jørgensen<sup>1,17</sup>  
 Stephen Kane<sup>1,18</sup>  
 Daniel Kubaš<sup>1,6</sup>  
 Jean-Baptiste Marquette<sup>1,3</sup>  
 Ralph Martin<sup>1,19</sup>  
 Pieter Meintjes<sup>1,8</sup>  
 John Menzies<sup>1,20</sup>  
 Karen Pollard<sup>1,4</sup>  
 Kailash Sahu<sup>1,21</sup>  
 Christian Vinter<sup>1,17</sup>  
 Joachim Wambsganss<sup>1,9</sup>  
 Andrew Williams<sup>1,19</sup>  
 Kristian Woller<sup>1,17</sup>  
 Marta Zub<sup>1,9</sup>  
 Keith Horne<sup>1,2,12</sup>  
 Alasdair Allan<sup>2,22</sup>  
 Mike Bode<sup>2,23</sup>  
 Daniel M. Bramich<sup>1,2,24</sup>  
 Martin Burgdorf<sup>2,23</sup>  
 Stephen Fraser<sup>2,23</sup>  
 Chris Mottram<sup>2,23</sup>  
 Nicholas Rattenbury<sup>2,25</sup>  
 Colin Snodgrass<sup>2,6</sup>  
 Iain Steele<sup>2,23</sup>  
 Yiannis Tsapras<sup>2,23</sup>

- <sup>1</sup> PLANET Collaboration
- <sup>2</sup> RoboNet Collaboration
- <sup>3</sup> Institut d'Astrophysique de Paris, CNRS, Université Pierre et Marie Curie, Paris, France
- <sup>4</sup> University of Canterbury, Department of Physics and Astronomy, Christchurch, New Zealand
- <sup>5</sup> University of Notre Dame, Department of Physics, Notre Dame, Indiana, USA
- <sup>6</sup> ESO
- <sup>7</sup> McDonald Observatory, Fort Davis, Texas, USA

- <sup>8</sup> Boyden Observatory, University of the Free State, Department of Physics, Bloemfontein, South Africa
- <sup>9</sup> Astronomisches Rechen-Institut (ARI), Zentrum für Astronomie, Universität Heidelberg, Germany
- <sup>10</sup> Lawrence Livermore National Laboratory, Livermore, California, USA
- <sup>11</sup> University of Tasmania, School of Mathematics and Physics, Hobart, Tasmania, Australia
- <sup>12</sup> Scottish Universities Physics Alliance, University of St Andrews, School of Physics and Astronomy, St Andrews, United Kingdom
- <sup>13</sup> Royal Society University Research Fellow
- <sup>14</sup> University of Rijeka, Physics Department, Faculty of Arts and Sciences, Rijeka, Croatia
- <sup>15</sup> Technische Universität Wien, Austria
- <sup>16</sup> Observatoire Midi-Pyrénées, Laboratoire d'Astrophysique, Université Paul Sabatier, Toulouse, France
- <sup>17</sup> Niels Bohr Institutet, Astronomisk Observatorium, København, Denmark
- <sup>18</sup> Department of Astronomy, University of Florida, Gainesville, Florida, USA
- <sup>19</sup> Perth Observatory, Perth, Australia
- <sup>20</sup> South African Astronomical Observatory
- <sup>21</sup> Space Telescope Science Institute, Baltimore, Maryland, USA
- <sup>22</sup> eSTAR Project, School of Physics, University of Exeter, Devon, United Kingdom
- <sup>23</sup> Astrophysics Research Institute, Liverpool John Moores University, Birkenhead, United Kingdom
- <sup>24</sup> The Isaac Newton Group of Telescopes, Santa Cruz de La Palma, Canary Islands
- <sup>25</sup> The University of Manchester, Jodrell Bank Observatory, Macclesfield, Cheshire, United Kingdom

In order to obtain a census of planets with masses in the range of Earth to Jupiter, eight telescopes are being used by the combined microlensing campaign of the PLANET and RoboNet collaborations for high-cadence photometric round-the-clock follow-up of ongoing events, alerted by the OGLE and MOA surveys. In 2005 we detected a planet of 5.5 Earth masses at 2.6 AU from its parent 0.22  $M_{\odot}$  M star. This object is the first member of a new class

of cold telluric planets. Its detection confirms the power of this method and, given our detection efficiency, suggests that these recently-detected planets may be quite common around M stars, as confirmed by subsequent detection of a  $\sim 13$  Earth-mass planet. Using a network of dedicated 1–2-m-class telescopes, we have entered a new phase of planet discovery, and will be able to provide constraints on the abundance of frozen Super-Earths in the near future.

The discovery of extrasolar planets is arguably the most exciting development in astrophysics during the past decade, rivalled only by the discovery of the cosmic acceleration. The unexpected variety of giant exoplanets, some very close to their stars, many with high orbital eccentricity, has sparked a new generation of observers and theorists to address the question of how planets form in the context of protostellar accretion discs. Planets are now known to migrate and maybe even be ejected, via planet-disc and planet-planet interactions. We are beginning to discover how our Solar System fits into a broader community of planetary systems, many with very different properties. Microlensing-based searches play a critical role by probing for cool planets with masses down to that of Earth. Of key interest is how planets are distributed according to mass and orbital distance (Figure 1) as this information provides a crucial test for theories of planet formation. Core accretion models (Ida and Lin, 2005) are today the best description for the formation of planetary systems: the accretion of planetesimals leads to the formation of cores, which then start to accrete gas from the primitive nebula. This scenario predicts that for M dwarf stars there is a preferential formation of Earth- to Neptune-mass planets in 1–10 AU orbits. These planets are expected to form within a few million years. More massive planet (Jupiter) formation is hampered by a longer formation time (10 Myr) during which the gas evaporates and is no longer available to be accreted.

There is a wide variety of planets and at first sight it appears that our system is very special. However, our view of the whole picture is still blurred by observational biases inherent to the detection

techniques using transits and radial velocities. Both methods are more sensitive to massive planets close to their parent star. Doppler measurements and the space transit missions, such as COROT, can already, or will shortly, be able to detect Neptune-mass planets close to their parent star. Direct detections fill the other extreme of very large separations which are unknown in our Solar System. It is therefore necessary to use different techniques, each probing different areas of the planet-mass versus orbital distance parameter space.

Already with ground-based observations, the microlensing technique is sensitive to cool planets with masses down to that of the Earth orbiting 0.1–1  $M_{\odot}$  stars, the most common stars of our Galaxy, in orbits of 1–10 AU. Currently, over 700 microlensing events towards the Galactic Bulge are alerted in real time by the OGLE and MOA surveys each year. During these events, a source star is temporarily magnified by the gravitational potential of an intervening lens star passing near the line of sight, with an impact parameter smaller than the Einstein ring radius  $R_E$ , a quantity which depends on the mass of the lens, and the geometry of the alignment. For a source star in the Bulge, with a 0.3  $M_{\odot}$  lens,  $R_E \sim 2$  AU, the projected angular Einstein ring radius is  $\sim 1$  mas, and the time to transit  $R_E$  is typically 20–30 days, but can be in the range 5–100 days.

A planet orbiting the lens star generates a caustic structure in the source plane, with one small caustic around the centre of mass of the system, the central caustic, and one or two larger caustics further away, the planetary caustics. If the source star happens to reach the vicinity of one of the caustics, its magnification is significantly altered as compared to a single lens, resulting in a brief peak or dip in the observed light curve.

The duration of such planetary lensing anomalies scales with the square root of the planet's mass, lasting typically a few hours (for an Earth) to 2–3 days (for a Jupiter). These two caustics (Figure 2) provide two modes for detection. When the central caustic is approached for all events with a small impact angle between source and lens star, corresponding to a large peak magnification of the event,

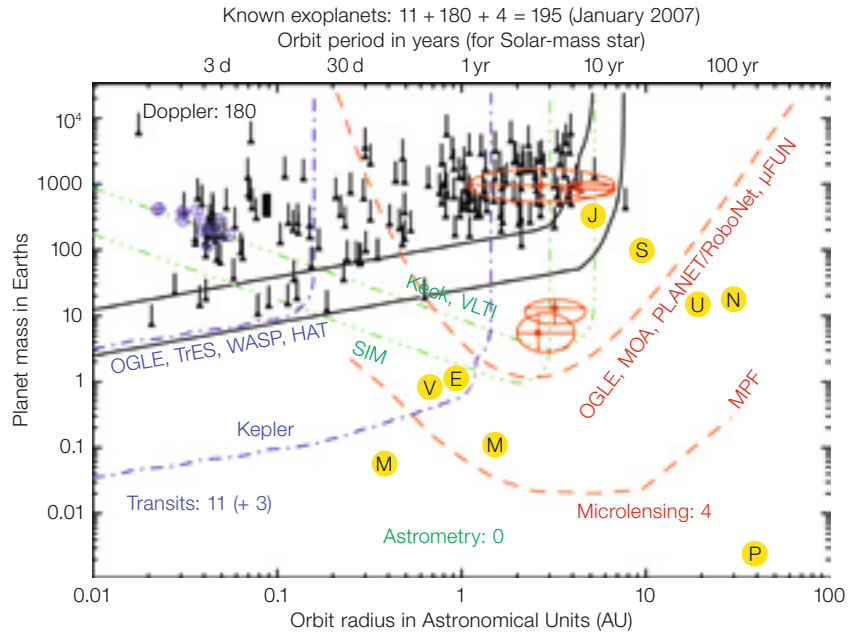
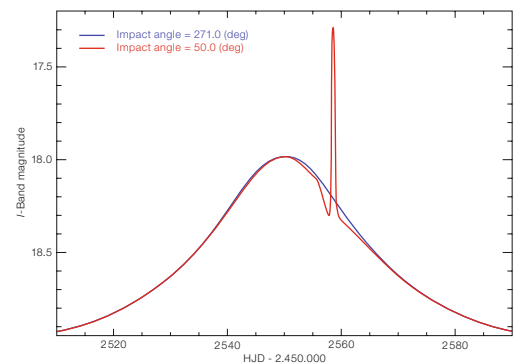
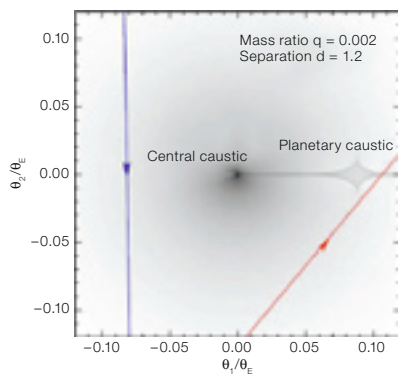


Figure 1 (above): Exoplanet discovery space (planet mass versus orbit size) showing the 8 planets from our Solar System (labelled as letters), 180 Doppler wobble planets (black triangles), 11 transit planets (blue circled crosses), and 4 microlensing planets (red circled crosses). Also outlined are the regions that can be probed by different methods: Doppler, transits; astrometry; and microlensing from the ground and space. Microlensing is a cost-efficient way to measure the mass function of cool planets down to the mass of the Earth.

Figure 2 (below): The left panel shows the caustic structure of a star/planet lens, with two possible trajectories of a source star. The right panel shows the corresponding observed light curves. Hitting the planetary caustic, or passing close to it, induces a short-lived but clearly detectable photometric signal.



the detection of planets in such events becomes highly efficient (Griest and Safizadeh 1998). In contrast, planetary caustics are only approached for a specific range of orientations of the source trajectory, but the characterisation of a planetary signal is much easier for such configurations.

The inverse problem, finding the properties of the lensing system, is a complex nonlinear one within a wide parameter

space to derive the planet/star mass ratio  $q$ , and the projected separation  $d$  in units of  $R_E$ . In general, model distributions for the spatial mass density of the Milky Way, the velocities of potential lens and source stars, and a mass function of the lens stars are required in order to derive probability distributions for the masses of the planet and the lens star, their distance, as well as the orbital radius and period of the planet, by means of Bayesian analysis.

The observational challenge is to monitor ongoing microlensing events, detected by the OGLE and MOA survey telescopes, with a fleet of telescopes to achieve round-the-clock monitoring and detect real-time deviations in the photometric signal. The telescopes belonging to our network together with their locations are shown in Figure 3. During the coming three Galactic Bulge seasons (from May to September 2007, 2008, 2009 in the southern hemisphere) we are planning to use the eight telescopes of the PLANET/RoboNET networks: Danish 1.5-m at La Silla (Chile), Canopus 1.0-m at Hobart and Bickley 0.6-m at Perth (Australia), Rockefeller 1.5-m at Bloemfontein and SAAO 1.0-m at Sutherland (South Africa). These are the standard telescopes of the PLANET network, to which were added in 2004 two robotic telescopes of the UK RoboNet network, North Faulkes 2-m in Hawaii and Liverpool 2-m in Canary islands, joined in 2006 by the South Faulkes 2-m in Australia.

### Observing strategy, and description of the reduction pipelines

A typical observing season of the Galactic Bulge starts at the beginning of May every year and lasts four months. Among the 691 alerts available in 2006 (579 from OGLE-III and 112 additional from MOA-II), about 180 are available every night in the middle of the season. Of these, around 20 targets can be monitored by 1-m-class telescopes, whereas the Danish 1.54-m and the 2-m telescopes can follow more events. Therefore, we must apply some criteria to select our 20 targets for every observing night. This is done by one member of the collaboration acting as a coordinator, the so-called 'homebase'. Depending upon the current magnification, the source brightness, and the time of the last observation, a priority algorithm assigns a worth to each of the events and suggests sampling rates, with the goal to maximise the planet detection efficiency. If the magnification of one event becomes very high, it may become the sole designated target during that night. While these suggestions are directly submitted to intelligent agents steering the robotic telescopes of the RoboNet network, the homebase currently tunes them using our experience gained, before



Figure 3: The different telescopes of the PLANET/RoboNet network.

instructing observers at the PLANET telescopes by means of a web page. We plan to embed our experience into future advanced versions of the priority algorithm and further automate this process.

At the beginning of the night, the observer finds on the PLANET web pages the list of targets with sampling intervals set up by the homebase. He then defines the exposure times for each target and reports them on our private web page, so that the homebase can estimate the observing load at each telescope. Typical sampling intervals are 0.5, 1, and 2 hours, according to the priority of each event. However, in case of a high magnification event, when the sensitivity to a planet is maximal, the sampling interval can be reduced to a few minutes, to the exclusion of all other candidate objects.

At the end of the exposure, the image is pre-processed (bias, dark removed and flatfielded), gets a standard name and is passed to an on-line pipeline. Starting in 2006, on all the PLANET telescopes, we shifted from a DoPhot-based on-line pipeline to an image subtraction pipeline based on ISIS (Alard 2000). This robust implementation, named WISIS, has two main tasks: *process* takes all available images of a given event, chooses the best template and subtracts all images from that template after convolving the reference point spread function (PSF) with the kernel to mimic the current PSF. The *update* task only processes new images using a previously chosen template.

In the case of OGLE, which has accumulated many images of a given field before a microlensing event is detected there, the template is built from a set of the best images and is not held fixed throughout the season. But in our case, we start observing an event when receiving the OGLE or MOA alert, so we have to build the template 'on the fly'. This generates problems when new images appear after a few nights, which are better than the first template. We then have to re-run the *process* routine on all images of the event. A different image subtraction pipeline is used on the RoboNet telescopes, but it follows the same philosophy.

The typical uncertainty of the on-line photometry is 1.2% for an  $I = 17.8$  mag Galactic Bulge star at the Danish 1.5-m telescope, and allows an on-line detection of a deviating signal. When this appears, excitement grows and an alert to homebase is issued. Homebase then prompts an off-line reduction of the event images, which are regularly uploaded to the Paris central archive. The off-line reduction is done with our other image subtraction pipeline, pySIS, which facilitates 'fine-tuning', so as to get the best possible photometry but is more difficult to automate for real-time use. If the off-line reduction confirms the deviation, an alert is issued to the microlensing community to intensify observations and maximise the chances of a good characterisation of the deviation, which is absolutely necessary for future modelling of the event. Moreover, all photometric data are made public immediately, as assistance to all teams in order to maximise the planet hunting community's success.

### The discovery of the frozen superEarth OGLE-2005-BLG-390Lb

On 11 July 2005, the OGLE Early Warning System announced the microlensing event OGLE 2005-BLG-390, with a relatively bright G4III giant as the source star. PLANET/RoboNet included it in its list of targets and started to monitor it on 25 July. The microlens peaked at a magnification  $A_{\max} = 3$  on 31 July. We were planning to continue to monitor it until the source exited the Einstein ring, when on 10 August observers at the Danish telescope noticed a measurement deviating

by 0.06 mag from the point source point lens prediction. They then took a second measurement, deviating by 0.12 mag. OGLE data became available, confirming the deviation seen in Chile. In order to check the nature of the deviation, home-base increased the proposed sampling rate at the automated Perth telescope. Perth started to observe this event continuously as soon as the target was within reach. South Africa was clouded out, and when observations resumed in Chile, it was clear that the anomaly was over. Different telescopes continued to observe the microlensing event. Perth data – which were received only with some delay – finally confirmed the short-duration deviation with a good coverage of six additional data points. Combined with two additional independent data points from the MOA team (Mt. John, New Zealand), the evidence of a well-covered short-term deviation from a point-lens light curve was on record (see Figure 4).

Frenetic modelling activities started and it became clear very quickly that we had discovered a low-mass planet. The analysis has proven to be rather straightforward for this event involving the transit of a large source star over a planetary caustic (Figure 5). The modelling of the photometric data yields the mass ratio  $q = 7.6 \pm 0.7 \cdot 10^{-5}$ , and the projected planet separation  $d = 1.61 \pm 0.008$  (in units of RE, the Einstein ring radius). We performed a Bayesian analysis using Galactic models and a mass function in order to derive probability distributions for the lens parameters (see Figure 2 from Beaulieu et al. 2006) and a constraint on the nature of the lens (low-mass main-sequence star or stellar remnant). The median values yield a host star of mass  $0.22^{+0.21}_{-0.11} M_{\odot}$  located at a distance of  $6.6 \pm 1.1$  kpc within the Galactic Bulge, orbited by a  $5.5^{+5.5}_{-2.7}$  Earth mass planet at an orbital separation of  $2.6^{+1.5}_{-0.6}$  AU (Figure 6, and the artist view of the planet by Herbert Zodet in ESO Press Release 02/06).

#### Planet detection efficiency

The detection efficiency of the experiment can be determined from all collected data, and comparison with the detections (or the absence of such) allows conclusions about the planet abundance

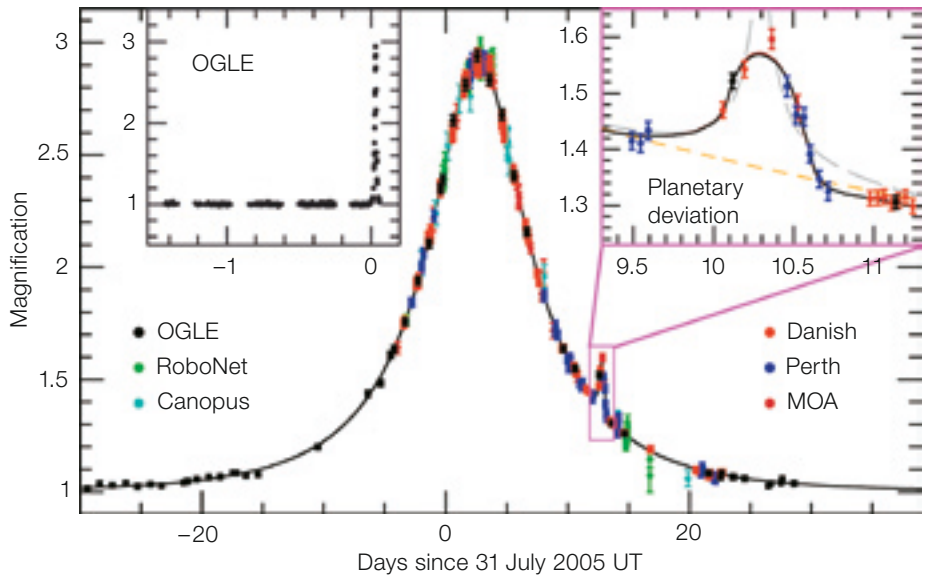


Figure 4: Light curve of OGLE-2005-BLG-390Lb, showing a brief planetary anomaly lasting for less than a day observed by four telescopes. The lens star is a  $\sim 0.22 M_{\odot}$  Galactic Bulge M dwarf orbited by a  $\sim 5.5$  Earth-mass planet at  $\sim 2.6$  AU with a

period of  $\sim 10$  years (plotted as solid line). The best alternative model is a binary source star but is rejected by the data. The dashed line is the point source lens model without the planetary deviation (Beaulieu et al. 2006).

around the probed stars. The first attempts were done on individual high-magnification events using a point-source approximation, and then were applied to a sample of the 42 well-covered microlensing events acquired by PLANET in 1995–1999 (Gaudi et al. 2002). Less than 1/3 of the lenses are orbited by Jupiters with orbits in the range 1–5 AU. We are currently working on an analysis combining 11 years of data (1995–2005). We calculate the detection efficiency of each microlensing light curve to lensing companions as a function of the mass ratio and projected separation of the two components, now taking into account extended source effects. We use the same Bayesian analysis as for determining probability densities for the lens star and planet properties (Dominik 2006). Figure 7 gives the mean detection efficiency of PLANET combining 14 well-sampled events from 2004. For Jupiter-mass planets, the detection efficiency reaches 50%, while it decreases only with the square-root of the planet mass until the detection of planets is further suppressed by the finite size of the source stars for planets with a few Earth masses. Nevertheless, the detection efficiency still remains a few per cent for planets below 10 Earth masses, made of rock and ice. As of today, four planets have been de-

tected by microlensing, two of which are Jupiter analogues (Bond et al. 2004, Udalski et al. 2005) and one Neptune (Gould et al. 2006), where the perturbation is due to the central caustic, and one rocky/icy planet of 5.5 Earth mass named OGLE-2005-BLG-390Lb (Beaulieu et al., 2006) via a planetary caustic. They are overplotted on Figure 7. So the era of discovery of frozen Super-Earths has been opened by the microlensing technique. One of the consequences of the discovery of such a small planet, is that these small rock/ice planets should be common.

#### Obtaining more information about these planets

Unlike other techniques, microlensing does not offer much chance to study the planetary system in more detail because the phenomenon only occurs once for each star. Only a significant statistical sample will allow us to reach firm conclusions and finally answer the question of how special is our own Solar System. Additional information about a specific event can be obtained once the lens star is directly detected. Here, we must wait many years till the relative motion of the source and lens stars separate them on the sky.

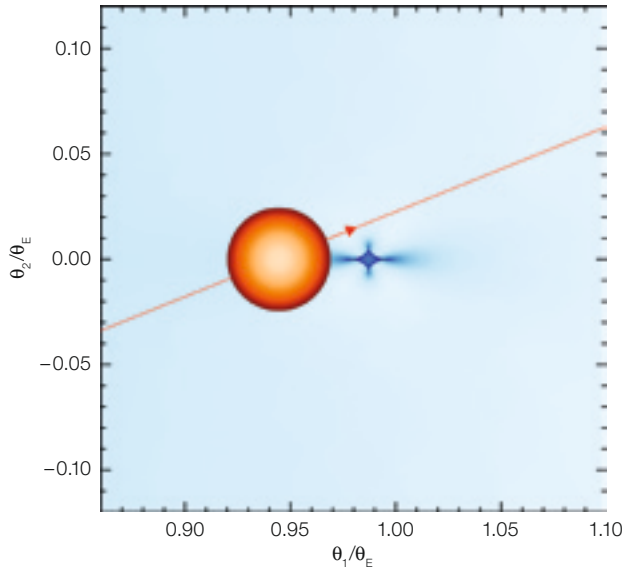


Figure 5: The source star and the planetary caustic of OGLE-2005-BLG6390. Notice the small size of the planetary caustic compared to the source star.

Bennett et al. (2006) using HST images have detected the lens star in the microlensing event OGLE-2003-BLG-235/MOA-2003-BLG-53, and therefore the uncertainty on the planetary parameters have been greatly reduced. This could be achieved too with HST or adaptive optics for OGLE-2005-BLG-169. In the case of the lens OGLE-2005-BLG-390La, the observation is much more difficult since we would need to detect a K ~ 22 mag object at about 40 mas (in five years) from a star that is 10 mag brighter. In the coming years, statistics about frozen Super-Earth planets orbiting M and K dwarfs will be obtained, complementing the parameter space explored by space transit missions like COROT and KEPLER or aggressive ground-based Doppler search, like those using the CORALIE, SOPHIE and HARPS instruments.

#### Acknowledgements

Microlensing follow-up observations would not happen without the alert systems of the OGLE and MOA collaborations. We are very grateful to OGLE and MOA, and to the observatories that support our science (ESO, Canopus, CTIO, Perth, SAAO, Boyden) via the generous allocations of time that make this work possible. The operation of Canopus Observatory is in part supported by a financial contribution from David Warren, and the Danish telescope at La Silla is operated by IDA financed by SNF. The RoboNet project is funded by the UK STFC. HOLMES

is supported by the Agence Nationale de La Recherche. KHC work performed under auspices of US DOE, by UC, LLNL under contract, W 7405-Eng-48. NJR acknowledges financial support by a PPARC PDRA fellowship and is partially supported by the European Community's Sixth Framework Marie Curie Research Training Network Programme, Contract No. MRTN-CT-2004-505183 ANGLES.

#### References

- Alard C. 2000, A&AS 144, 363
- Beaulieu J. P. et al. 2006, Nature 439, 437
- Bennett D. P. et al. 2006, ApJ 647, 171
- Bond I. A. et al. 2005, ApJ 606, 155
- Dominik M. 2006, MNRAS 367, 669
- Gaudi B. S. et al. 2002, ApJ 566, 463
- Gould A. et al. 2006, ApJ 644, L 37
- Griest K. and Safizadeh N. 1998, ApJ 500, 37
- Ida S. and Lin D. N. C. 2005, ApJ 626, 1045
- Udalski A. et al. 2005, ApJ 628, 109

Figure 6: Perturbation of the image of the source star by the planetary caustic observed with an ideal telescope. The time interval between the images is 0.1 day. The image scale is 30 microarcsec (Bennett and Williams).

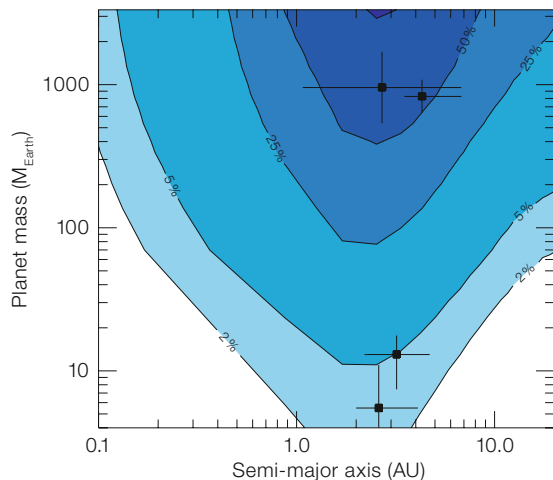
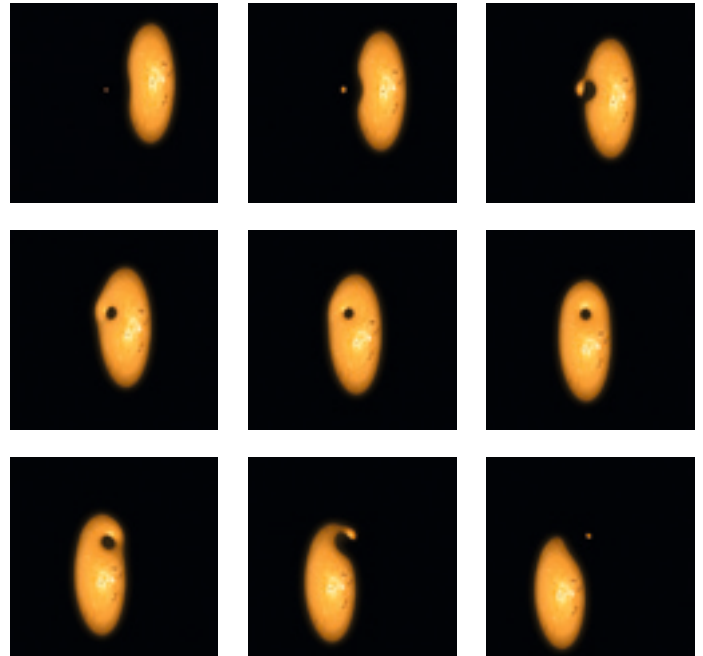


Figure 7: Average detection efficiency of planets as a function of mass and orbital separation (assuming circular orbits) in the 14 favourable events monitored by PLANET in 2004 (preliminary analysis) along with the planets detected by microlensing as of 2006 marked as points.

#### Relevant websites

- PLANET: <http://planet.iap.fr/>
- RoboNet: <http://www.astro.livjm.ac.uk/RoboNet/>
- MicroFUN: <http://www.astronomy.ohio-state.edu/~microfun/>
- MOA website: <http://www.phys.canterbury.ac.nz/moa/>
- OGLE website: <http://www.astrouw.edu.pl/~ogle/>

# Sulphur Abundances in Metal-Poor Stars – First Result from CRILES Science Verification

Poul Erik Nissen<sup>1</sup>  
 Martin Asplund<sup>2</sup>  
 Damian Fabbian<sup>2</sup>  
 Florian Kerber<sup>3</sup>  
 Hans Ulrich Käufel<sup>3</sup>  
 Max Pettini<sup>4</sup>

<sup>1</sup> Department of Physics and Astronomy,  
 Aarhus University, Denmark

<sup>2</sup> Research School of Astronomy and  
 Astrophysics, Australian National Uni-  
 versity

<sup>3</sup> ESO

<sup>4</sup> Institute of Astronomy, University of  
 Cambridge, United Kingdom

Sulphur is the tenth most abundant element in the Universe and plays an important role in studies of the chemical enrichment and star-formation history of distant galaxies. Due to the lack of suitable sulphur lines in the visible part of stellar spectra there is, however, still no agreement on the abundance of sulphur in Galactic metal-poor stars, and we are therefore uncertain about the nucleosynthetic origin of sulphur. New observations of infrared sulphur lines with the cryogenic high-resolution infrared echelle spectrograph (CRILES) at ESO's VLT are helping to solve this problem.

Abundance ratios of elements in celestial objects are usually given on a logarithmic scale with the corresponding solar ratio as the zero point. From the ratio between the number of iron and hydrogen atoms, we define the *metallicity* of a star as  $[Fe/H] \equiv \log(N_{Fe}/N_H)_{Star} - \log(N_{Fe}/N_H)_{Sun}$ , and in order to get information on the nucleosynthesis of an element X, we are studying how the quantity  $[X/Fe] \equiv \log(N_X/N_{Fe})_{Star} - \log(N_X/N_{Fe})_{Sun}$  varies as a function of  $[Fe/H]$ . For example, one finds that magnesium has a constant *overabundance*  $[Mg/Fe] = +0.3$  dex (corresponding to a factor of two) in Galactic halo stars with metallicities in the range  $-4 < [Fe/H] < -1$ , whereas  $[Mg/Fe]$  declines continuously to zero in disc stars with  $-1 < [Fe/H] \leq 0$ . A similar trend is found for  $[Si/Fe]$ . This can be explained if Mg and Si are made primarily by  $\alpha$ -capture reactions (i.e. successive captures of  $\alpha$ -particles) in Type II supernovae (SNe), whereas iron is made

by silicon burning in both Type Ia and Type II SNe. The point is that Type Ia SNe are not contributing with iron until the disc phase of our Galaxy, because their occurrence is delayed by about one billion years relative to Type II SNe, due to the lower progenitor mass of Type Ia SNe.

Sulphur is an element with an even number of protons ( $Z = 16$ ) like Mg and Si ( $Z = 12$  and  $14$ ), and nucleosynthesis calculations predict that S is made in the same way as Mg and Si in Type II SNe. Hence, we expect  $[S/Fe]$  to have the same trend with  $[Fe/H]$  as  $[Mg/Fe]$  and  $[Si/Fe]$ . Sulphur abundances derived from the weak Si I line at 869.5 nm by Israelian and Rebolo (2001) and Takada-Hidai et al. (2002) showed, however, an increasing trend of  $[S/Fe]$  towards low metallicities, with  $[S/Fe]$  reportedly reaching values as high as  $+0.8$  dex (a factor of six higher than the S/Fe ratio in the Sun) at  $[Fe/H] = -2.0$ . They suggested that such high S/Fe ratios might be due to an enhanced sulphur production in supernovae with a very large explosion energy, so-called hypernovae. Nissen et al. (2004), on the other hand, used the stronger Si I lines at 921.3 and 923.8 nm to derive a near-constant  $[S/Fe] \sim +0.3$  for halo stars in the metallicity range  $-3 < [Fe/H] < -1$ , as expected if normal Type II SNe are the sole source of sulphur. More recently, Caffau et al. (2005) proposed a dichotomy of  $[S/Fe]$  among Galactic halo stars with both *high* and *low*  $[S/Fe]$  values, which would imply a very complicated evolution of the sulphur abundance in our Galaxy.

A reason for the diverging  $[S/Fe]$  results may be that errors in determining sulphur abundances are larger than claimed by the authors of the cited papers. In this

connection, we note that the 869.5 nm Si I line is very weak in metal-poor halo stars and hence the measured strength of the line may be affected by irregular fringing variations of the CCD detector response, which are difficult to correct by flat-fielding. The stronger r<sub>1</sub> lines at 921.3 and 923.8 nm are less affected by such errors, but they occur in a spectral region hampered by numerous telluric lines that are often blended with the sulphur lines.

## CRILES observations

CRILES is a cryogenic, infrared echelle spectrograph designed to provide a resolving power  $\lambda/\Delta\lambda$  of up to 100 000 between about 950 nm and 5 000 nm as described in detail by Käufel et al. (2006). The commissioning of this VLT instrument opens up a new opportunity for independent determinations of sulphur abundances in metal-poor stars based on high-resolution observations of the Si triplet at 1.046  $\mu$ m. As part of the science verification of CRILES, a spectrum around the infrared triplet was obtained for the halo dwarf star G29-23 ( $V = 10.19$ ,  $[Fe/H] = -1.7$ ) on 6 October 2006. The entrance slit width of CRILES was set at 0.4 arcsec, which corresponds to a resolving power of 50 000 with four detector pixels per spectral resolution bin  $\Delta\lambda$ . In order to improve the removal of sky emission and detector dark current, the observations were performed in nodding mode with a shift of 10 arcsec between the two settings of the star on the slit. The exposure time was 2400 s. The seeing was rather poor (about 1.3 arcsec) but adaptive optics was applied to improve the stellar image, and the combined spectrum has a very satisfactory signal-to-noise ratio  $S/N \sim 330$  per spectral dispersion pixel. This is considerably

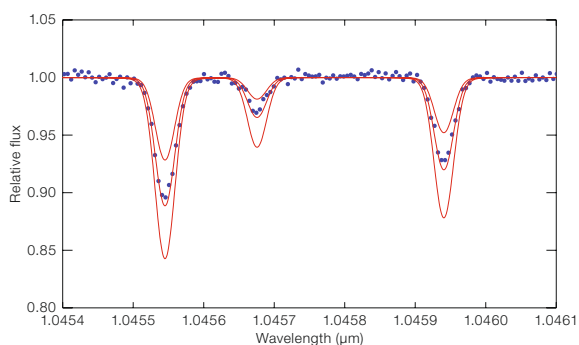


Figure 1: The CRILES spectrum of the metal-poor ( $[Fe/H] = -1.7$ ) dwarf star G29-23 around the 1.046  $\mu$ m Si triplet (dots) compared with synthetic model-atmosphere line profiles for three sulphur abundances corresponding to  $[S/Fe] = 0.0, +0.3$  and  $+0.6$ , respectively.

better than our earlier UVES spectrum of the same star (observed under similar conditions and with the same exposure time), which has S/N  $\sim 200$  around the S I lines at 921.3 and 923.8 nm. Furthermore, unlike the UVES near-IR spectrum, the CRIRES spectrum at 1.046  $\mu\text{m}$  is not plagued by telluric lines and fringing residuals.

The CRIRES spectrum of G29-23 is shown in Figure 1 in comparison with synthetic profiles of the sulphur lines for three values of [S/Fe]. Details of the model-atmosphere calculations and the determination of the iron abundance, which is based on Fe II lines, can be found in Nissen et al. (2007). As can be seen from the Figure, the synthetic profile corresponding to [S/Fe] = +0.3 provides an excellent fit to the CRIRES data for all three S I lines.

### Comparison with UVES observations

In Figure 2, the UVES spectrum of G29-23 is shown for the sulphur lines at 869.5, 921.3 and 923.8 nm. Telluric lines were removed by dividing by a scaled B-type star spectrum as described in Nissen et al. (2007). Again, the synthetic profile corresponding to [S/Fe] = +0.3 fits the data very well, but it is clear that the [S/Fe] value obtained from the weak 869.5 nm line is rather uncertain.

Although one should not put too much weight on a single star, the CRIRES spectrum of G29-23 provides an important check of the sulphur abundances obtained from UVES spectra for 40 halo stars in the upper panel of Figure 3, the UVES data indicate that [S/Fe] lies around a plateau of +0.3 dex if local thermodynamic equilibrium (LTE, i.e. a Boltzmann distribution of the atoms over the possible atomic energy states) is assumed when deriving the S abundances. If non-LTE corrections based on the statistical equilibrium calculations of Takeda et al. (2005) are taken into account, the plateau decreases to about +0.2 dex as shown in the lower panel of Figure 3.

The scatter of [S/Fe] around this plateau is remarkably small,  $\pm 0.07$  dex only, and no star has an enhanced S/Fe ratio

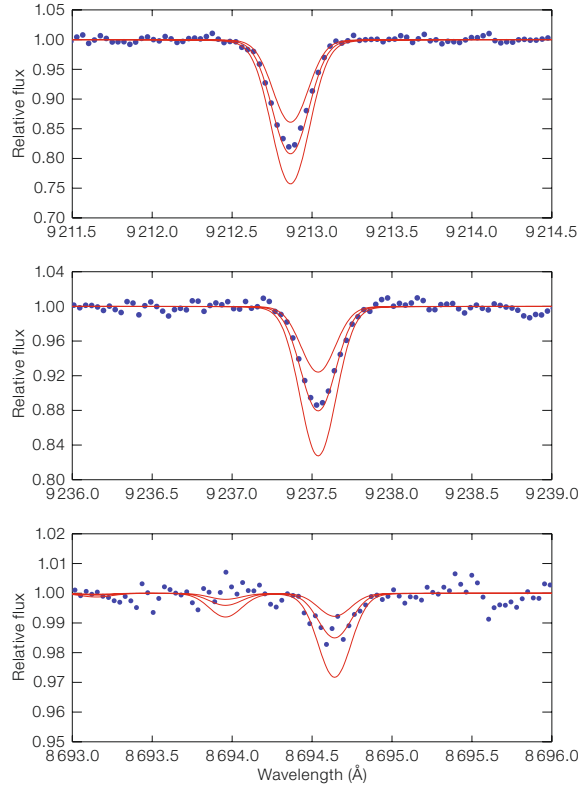


**Figure 2:** The UVES spectrum of G29-23 around the S I lines at 921.3, 923.8, and 869.5 nm (dots) compared with synthetic line profiles for three sulphur abundances corresponding to [S/Fe] = 0.0, +0.3 and +0.6, respectively.

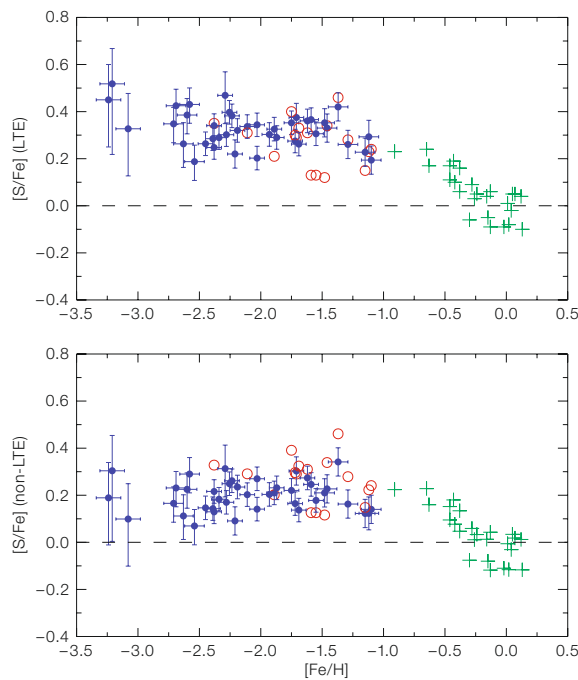


**Figure 3:** [S/Fe] versus [Fe/H] for Galactic stars. Disc stars ([Fe/H] > -1) from Chen et al. (2002) are shown with green crosses. For the halo stars ([Fe/H] < -1), blue circles with error bars show data based on sulphur abundances derived from the 921.3, 923.8 nm S I lines, and red circles show data from the weak 869.5 nm S I line. In the upper panel LTE has been assumed in deriving the S abundances, whereas the lower panel includes non-LTE corrections from Takeda et al. (2005).

( $[S/Fe] > +0.60$ ) as claimed by Israelian and Rebolo (2001), Takada-Hidai et al. (2002) and Caffau et al. (2005). Our results suggest that sulphur in the Galactic halo was made in the same way as Mg and Si, i.e. by  $\alpha$ -capture processes in massive SNe.

### The S/Zn ratio of Damped Lyman-alpha systems

The sulphur abundances derived by Nissen et al. (2007) were combined with zinc abundances determined from the 472.2 and 481.1 nm Zn I lines. Both S and Zn are among the few elements which are not readily depleted onto dust in the interstellar medium. For this reason, they are key to studies of metal enrichment in distant galaxies, particularly those detected as damped Lyman-alpha systems (DLAs) in the spectra of high-redshift quasars. Assuming that sulphur behaves like other  $\alpha$ -capture elements and that Zn follows Fe, the S/Zn ratio has been used to estimate the timescale of the star-formation process in DLAs. In particular, it has been argued that a solar S/Zn ratio indicates that Type Ia SNe have contributed to the chemical enrichment and that the age of a DLA system with a solar-like S/Zn therefore must be at least one billion years.

Before such a conclusion can be made, it is important to clarify the trend of  $[S/Zn]$  among Galactic stars. Figure 4 shows the results from Nissen et al. (2007). It is found that the trend of  $[S/Zn]$  depends quite critically on whether LTE is assumed or not. When the non-LTE corrections of Takeda et al. (2005) are applied,

there is an overall decrease in  $[S/Zn]$  at all but the highest values of  $[Zn/H]$  considered here. Furthermore, non-LTE effects are most significant at low metallicities with the result that, apparently,  $[S/Zn]$  reverts to solar values when  $[Zn/H] < -2$ . Such behaviour is unusual but, given our current limited understanding of the nucleosynthesis of Zn, cannot be excluded.

Taken at face value, the lack of a strong metallicity trend in the lower panel of Figure 4 would indicate that the usefulness of the S/Zn ratio as a 'clock' of the star-formation history is rather limited. The question that remains concerns the accuracy of the non-LTE calculations by Takeda et al. (2005); they depend critically on the rather uncertain cross-section for inelastic collisions with neutral hydrogen atoms, which tend to enforce an LTE population of the energy levels (Asplund 2005). Future observations of the forbidden sulphur line at 1.082  $\mu$ m in

cool halo giants may be particularly helpful in this connection. This line is formed close to LTE in cool stars, because nearly all sulphur atoms are in the lower energy level of the line (the ground state of the S I atom), and the number of atoms in the upper level is determined by collisions rather than radiative transitions. The forbidden line is very weak, but thanks to the efficiency and high resolution of CRIFES, precision measurements will be possible at metallicities as low as  $[Fe/H] \sim -2.5$ .

### References

- Asplund M. 2005, ARA&A 43, 481  
 Caffau E. et al. 2005, A&A 441, 533  
 Chen Y. Q. et al. 2002, A&A 390, 225  
 Israelian G. and Rebolo R. 2001, ApJ 557, L43  
 Käuffel et al. 2006, The Messenger 126, 32  
 Nissen P. E. et al. 2004, A&A 415, 993  
 Nissen P. E. et al. 2007, A&A 469, 319  
 Takada-Hidai M. et al. 2002, ApJ 573, 614  
 Takeda Y. et al. 2005, PASJ 57, 751

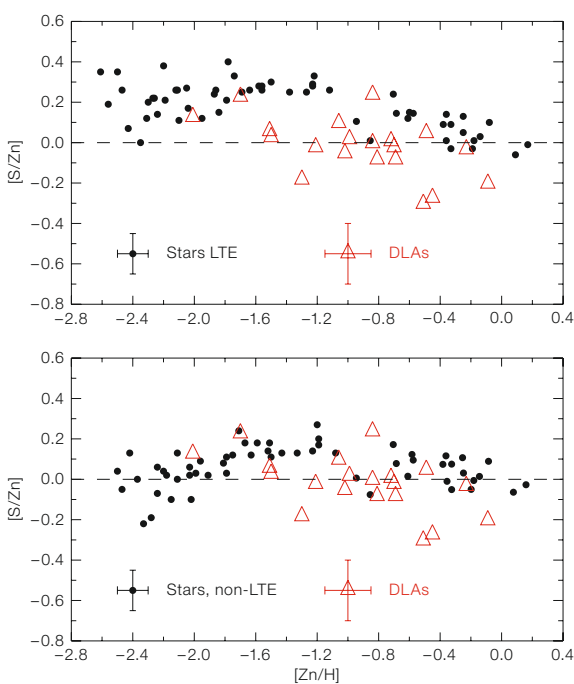


Figure 4:  $[S/Zn]$  versus  $[Zn/H]$  for Galactic stars and damped Lyman-alpha systems. Typical  $1-\sigma$  error bars are shown. In the upper panel the stellar S and Zn abundances have been derived assuming LTE, whereas the lower panel includes non-LTE corrections from Takeda et al. (2005).

# Using Globular Clusters to Test Gravity in the Weak Acceleration Regime

Riccardo Scarpa<sup>1</sup>  
Gianni Marconi<sup>2</sup>  
Roberto Gilmozzi<sup>2</sup>  
Giovanni Carraro<sup>3</sup>

<sup>1</sup> Instituto de Astrofísica de Canarias,  
La Laguna, Tenerife, Spain

<sup>2</sup> ESO

<sup>3</sup> Università di Padova, Italy

We report on the results from an ongoing programme aimed at testing Newton's law of gravity in the low acceleration regime using globular clusters. We find that all clusters studied so far behave like galaxies, that is, their velocity dispersion profiles flatten out at large radii where the acceleration of gravity goes below  $10^{-8}$  cm s<sup>-2</sup>, instead of following the expected Keplerian fall-off. In galaxies this behaviour is ascribed to the existence of a dark-matter halo. Globular clusters, however, are not supposed to contain dark matter, hence this result might indicate that our present understanding of gravity in the weak regime of accelerations is incomplete and possibly incorrect.

## Newtonian dynamics and globular clusters

Stars within galaxies, and galaxies within clusters of galaxies, are very far apart from each other. As a consequence, the typical accelerations governing the dynamics of galaxies are orders of magnitude smaller than the ones probed in our earth-based laboratories or in the Solar System. Thus, any time Newton's law is applied to galaxies (e.g., to infer the existence of dark matter), its validity is severely extrapolated. Although there are in principle no reasons to distrust Newton's law in the weak acceleration regime, agreement has been reached (e.g., Binney 2004) that galaxies start to deviate from Newtonian dynamics, and that dark matter is needed to reconcile observations with predictions, always for the same value of the internal acceleration of gravity of  $a_0 \sim 10^{-8}$  cm s<sup>-2</sup>. This systematic property, more than anything else, raises the possibility that we may

be facing a breakdown of Newton's law, rather than the effects of dark matter.

Since globular clusters are free falling toward the Milky Way, their internal dynamics are only affected by tidal stress, which is in most cases well below  $a_0$ . Therefore the internal dynamics of globular clusters can be used to probe the same range of accelerations typical of galaxies, without the complication of dark matter. Following this idea, we have studied the dynamics of the external regions of  $\omega$  Centauri (Scarpa, Marconi and Gilmozzi 2003). This massive cluster was selected because proper motions for several thousand stars were available in the literature. Combining proper motions with radial velocity information allows all three components of the velocity vector to be obtained, thus fully addressing the possible effects of anisotropy. The result is clearly shown by Figure 1. The velocity dispersion profiles, as derived for the three components of motion, are very similar, showing that the cluster is isotropic (as is also indicated, by the way, from its very nearly circular shape). Moreover, the dispersion is found to be constant at large radii.

Following this initial result, that could be due to some other effect like tidal heating, we collected data for three more globular clusters: NGC 7078 (M15) and NGC 6171 (Scarpa, Marconi, and Gilmozzi 2004A,B), and NGC 7099 (Scarpa et al. 2006). Data for a fourth cluster, NGC 6341 (M92), appeared recently in the literature (Drukier et al. 2006) and this cluster is also presented here. In all cases (see Figure 2) the

velocity dispersion profile mimics what is observed in high surface brightness elliptical galaxies. That is, the dispersion is maximal at the centre, then decreases toward a constant value at large radii, where the acceleration goes below  $a_0$ . With data for five globular clusters, one can start comparing results and, interestingly, we found that in all cases the flattening of the dispersion profile occurs for very similar values of the internal acceleration of gravity. Values are collected in Table 1, where we present, for each cluster, its absolute V magnitude, the radius where the flattening occurs, and the corresponding acceleration derived assuming a mass-to-light ratio of one. Within errors all profiles flatten out at  $a_0$ . It is worth pointing out that these five clusters are different in size, mass, position in the halo of the Milky Way and dynamical history. Therefore there is no obvious reason why they should conspire to have a similar velocity dispersion profile at large radii.

Galaxies provide us with another powerful tool to further disentangle non-Newtonian effects from other more classical phenomena like tidal heating, or a combination of effects like the distribution of dark remnants plus tidal heating plus cluster evaporation and so on, that might be responsible for increasing the velocity dispersion in the outskirts. High surface brightness galaxies (HSB) and low surface brightness galaxies (LSB) are known to behave differently. The latter have a remarkably flat velocity dispersion profile (e.g., Mateo 1997; Wilkinson 2006), allegedly due to LSB galaxies being dark matter dominated all the way to their centre, while HSB galax-

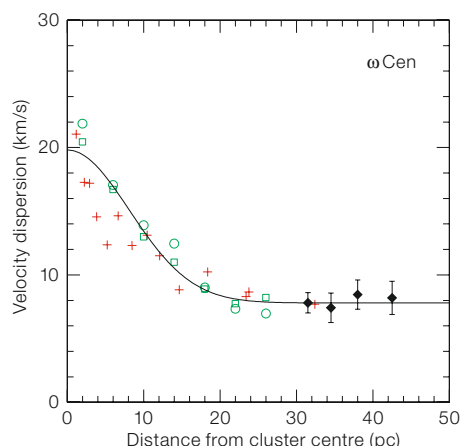


**Figure 1:** The velocity dispersion profile of  $\omega$  Centauri. Circles and squares represent the dispersion as derived from proper motion data. Crosses are radial velocity dispersions from the literature, to which we added data for 75 stars (the four last points with error bars). The solid line is not a fit to the data. It is a Gaussian plus a constant drawn to emphasise the flattening of the dispersion at large radii.

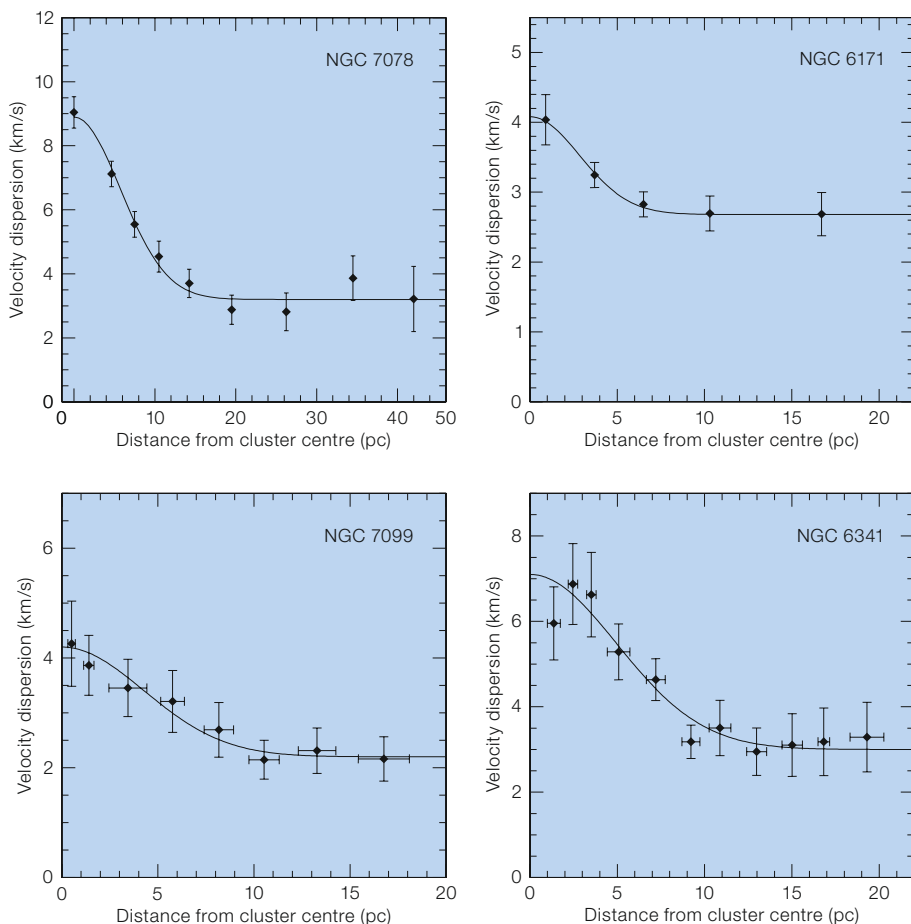


**Figure 2:** Velocity dispersion profiles of the other four clusters studied so far. In all cases the velocity dispersion is maximal at the centre, then decreases to converge toward a constant value at large radii. This is similar to the case of high surface brightness elliptical galaxies. Note that the profiles of NGC 6171 and NGC 7099 were derived from our own data, while the profiles of NGC 7078 and NGC 6341 were derived from data in the literature (Drukier et al. 2006 and references therein). The solid line has the same meaning as in Figure 1.

ies are baryon-dominated at the centre. In view of what we have found for dense globular clusters that probe the same accelerations as HSB galaxies, it is natural to wonder whether low-concentration globular clusters behave like LSB galaxies. That is, do low-concentration globular clusters have constant velocity dispersion?

### The case of NGC 288

In an attempt to answer this question we studied NGC 288, a low-concentration cluster located at 8.3 kpc from the Sun and 11.6 kpc from the Galactic Centre, that has internal acceleration of gravity everywhere below  $a_0$ , as is the case for LSB galaxies. The initial selection of targets around NGC 288 was based on colour, as derived from the analysis of ESO Imaging Survey frames. A catalogue of targets was prepared including mostly stars from the sub-giant branch down

to the turn off, between 15 and 18 apparent V mag. Observations were then obtained with FLAMES at the ESO VLT telescope. FLAMES is a fibre multi-object spectrograph, allowing the simultaneous observation of up to 130 objects. We selected the HR9B set-up that includes the magnesium triplet covering the wavelength range  $5143 < \lambda < 5346 \text{ \AA}$  at resolution  $R = 25900$ . Stellar astrometry was derived cross correlating the stellar positions on the EIS frames with coordinates from the US Naval Observatory (USNO) catalogue, which proved to have the required accuracy (0.3 arcsec) for FLAMES observations. Two different fibre configurations were necessary to observe all the selected stars (Figure 3). For each con-

figuration three 2700 s exposures were obtained under good atmospheric condition (clear sky and seeing  $\sim 1$  arcsec) on 29 and 30 August 2005.

Radial velocities were derived by cross-correlating the spectra of each target with a template (the target with the best spectrum). The two configurations shared a small number of stars, to evaluate and eliminate possible offsets in the velocity zero point. A posteriori, we verified that no correction was necessary down to a level of accuracy of  $250 \text{ m s}^{-1}$ , well below the accuracy required for our study. Finally, keeping in mind that we are interested only in the velocity dispersion, the global velocity zero point was derived by identifying a few lines in the spectrum of the template. Altogether 126 radial velocities with accuracy better than  $1 \text{ km s}^{-1}$  were derived. Of these, all but two were found to be cluster members, consistent with the very low contamination expected at the high Galactic latitude ( $b = -89$  degrees) of this cluster.

To better constrain the velocity dispersion close to the cluster centre, we combined our data with data for 24 additional stars, mostly within 6 pc from the cluster centre, and radial velocity accuracy better than  $1 \text{ km/s}$  (from Pryor et al. 1991). After applying an offset of  $2.9 \text{ km/s}$  to match our radial velocity zero point, these

Cluster Name	$M_v$	R (pc)	$a$ ( $\text{cm s}^{-2}$ )
NGC 5139 ( $\omega$ Centauri)	-10.29	$27 \pm 3$	$2.1 \pm 0.5 \times 10^{-8}$
NGC 6171 (M107)	-7.13	$8 \pm 2$	$1.3 \pm 0.6 \times 10^{-8}$
NGC 6341 (M92)	-8.20	$12 \pm 2$	$1.5 \pm 0.6 \times 10^{-8}$
NGC 7078 (M15)	-9.17	$20 \pm 2$	$1.4 \pm 0.4 \times 10^{-8}$
NGC 7099 (M30)	-7.43	$10 \pm 2$	$1.1 \pm 0.4 \times 10^{-8}$

**Table 1:** For each globular cluster studied, the absolute magnitude, radius at which the velocity dispersion flattens and the corresponding acceleration due to gravity for a mass-to-light ratio of 1, are listed.

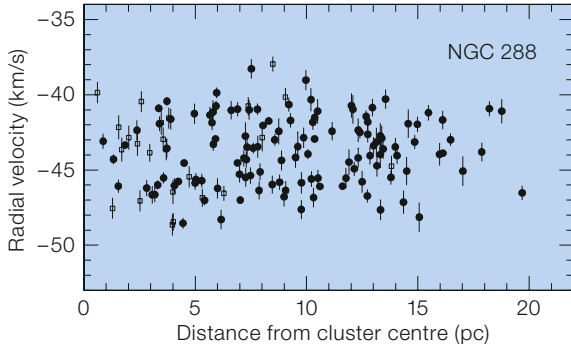


**Figure 3:** Radial velocity distribution for the low-concentration cluster NGC 288. The 124 stars studied as part of this work are shown as solid circles, while 24 velocities from Pryor et al. 1991 are shown as open squares. The data distributes uniformly from the centre to 20 pc, showing no indication of a decrease of the dispersion.

data smoothly merge with ours in the region of overlap, showing basically the same velocity dispersion (Figure 3). This combined sample was used to search for ordered rotation in NGC 288 that might contribute to sustain the cluster, finding no evidence for rotation down to the level of 0.5 km/s.

Velocities from this combined data set allowed us to build a well-sampled velocity dispersion profile from the centre to almost 18 pc (Figure 4). In Table 2 we report the velocity dispersion in km/s with  $1\sigma$  uncertainties, together with the limits of the bins, the number of stars in each bin, and the bin centre, defined as the mean of the radii of the stars in the bin.

Looking at both Figures 3 and 4, we see no indications of a vanishing velocity dispersion at large radii, rather, the dispersion remains constant with an average value of  $2.3 \pm 0.15$  km/s over the full range of radii covered by the data.

The five clusters  $\omega$  cen, NGC 7078, NGC 6171, NGC 7099, and NGC 6341, while having different sizes, different masses, and different dynamical histories, have the common property of being highly concentrated, thus the acceleration of gravity in their central regions is above  $a_0$ . Only in the outskirts is the acceleration below this value. All these clusters are found to behave like HSB elliptical galaxies, i.e. to have a constant velocity dispersion at large radii. By contrast, NGC 288 has the peculiar prop-

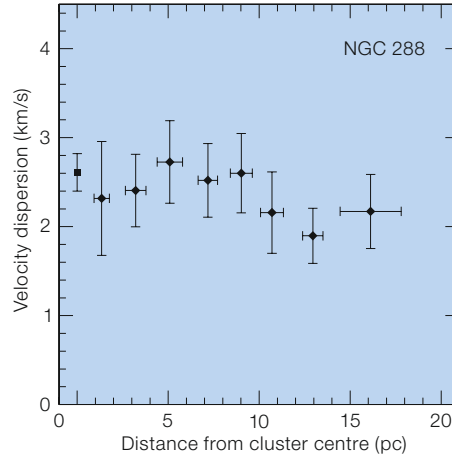


**Figure 4:** The velocity dispersion profile of the low-concentration cluster NGC 288. From the point of view of the internal acceleration of gravity, this cluster is the equivalent of a low surface brightness galaxy and, similarly to what is found in these galaxies, the dispersion profile is remarkably flat.

Bin limits (pc)	Stars/bin	bin centre (pc)	$\sigma$ (km s <sup>-1</sup> )
0–2	8	1.34	$2.32 \pm 0.64$
2–4	21	3.21	$2.41 \pm 0.41$
4–6	20	5.09	$2.73 \pm 0.46$
6–8	22	7.18	$2.52 \pm 0.41$
8–10	20	9.02	$2.60 \pm 0.45$
10–12	14	10.71	$2.16 \pm 0.46$
12–14	25	12.95	$1.90 \pm 0.31$
14–20	17	16.12	$2.17 \pm 0.42$

**Table 2:** Data on the binned radial velocity dispersion for NGC 288.

erty of being rather diffuse, with a central surface brightness of  $\sim 20$  mag arcsec<sup>-2</sup> in the V band. This has the important consequence that the internal acceleration of gravity is extremely small. Indeed it can be shown to be everywhere below  $a_0$  for any of the typical mass-to-light ratios assumed for globular clusters.

It is well known that LSB galaxies have velocity dispersion profiles which are remarkably flat, with no central maximum (Mateo 1997; Wilkinson et al. 2006). If this property is due to a breakdown of Newtonian dynamics below  $a_0$  (and not because of dark matter), then the velocity dispersion of NGC 288 should mimic what is observed in these galaxies. Within the errors, this is certainly the case (Figure 4). The similarity between NGC 288 and LSB galaxies is striking. The canonical explanation for the constant velocity dispersion in LSB galaxies is that these objects are dark matter dominated all the way to their centres. In the case of a globular cluster, this explanation is quite unpalatable. Thus, in view of these results for globular clusters and also of the amazing ability of a particular modification of the Newtonian Dynamics

known as MOND (Milgrom 1983) to describe successfully the properties of a large number of stellar systems without invoking the existence of non-baryonic dark matter, we see here evidence for a failure of Newtonian Dynamics for accelerations below  $a_0$ . Given the potential impact of this claim, we urge the astronomical community to disprove or generalise our results.

## References

- Binney J. 2004, in "Dark Matter in Galaxies", ed. S. D. Ryder et al., IAU 220, 3
- Drukier G. A. et al. 2007, AJ 133, 1041
- Mateo M. 1997, in "The nature of Elliptical Galaxies", ed. M. Arnaboldi, ASPC 116, 259
- Milgrom M. 1983, ApJ 270, 365
- Pryor C. et al. 1991, AJ 102, 1026
- Scarpa R., Marconi G. and Gilmozzi R. 2003, A&AL 405, 15
- Scarpa R., Marconi G. and Gilmozzi R. 2004a, IAU 220E, 215
- Scarpa R., Marconi G. and Gilmozzi R. 2004b, in "Baryons in Dark Matter Halos", eds. R. Dettmar et al., SISSA, Proceedings of Science, 55.1, <http://pos.sissa.it>
- Scarpa R. et al. 2007, A&AL 462, 9
- Wilkinson M. I. et al. 2006, The Messenger 124, 25

# Dissecting the Nuclear Environment of Mrk 609 with SINFONI – the Starburst-AGN Connection

Jens Zuther<sup>1</sup>  
 Sebastian Fischer<sup>1</sup>  
 Jörg-Uwe Pott<sup>1,2</sup>  
 Thomas Bertram<sup>1</sup>  
 Andreas Eckart<sup>1</sup>  
 Christian Straubmeier<sup>1</sup>  
 Christof Iserlohe<sup>1</sup>  
 Wolfgang Voges<sup>3</sup>  
 Günther Hasinger<sup>3</sup>

<sup>1</sup> I. Physikalisches Institut, Universität zu Köln, Germany

<sup>2</sup> ESO

<sup>3</sup> Max-Planck-Institut für Extraterrestrische Physik, Garching, Germany

The new VLT instrument SINFONI gives us a view onto the circumnuclear properties of AGN in unprecedented detail, even beyond our local Universe. As a science verification target, the showcase object Mrk 609 demonstrates impressively the necessity of adaptive optics assisted integral-field spectroscopy in order to distinguish between Seyfert and starburst characteristics on nuclear scales.

## Fuelling of nuclear activity

The presence of the Seyfert phenomenon is supposed to originate in the accretion of matter onto a super-massive black hole (SMBH) in the centre of a galaxy. Nuclear activity is composed of nuclear starbursts and Seyfert-like emission. The fuel necessary for driving this activity has to be transported from galactic scales ( $\sim 10$  kpc) down to nuclear scales of  $\sim 10$  pc. We are still far from understanding the detailed processes that create non-axisymmetric potentials leading to the dissipation of angular momentum. Such instabilities are needed for the gas and stars to fall towards the nuclear region. However, considerable theoretical as well as observational effort has been made to understand these processes (e.g. Shlosman et al. 1990; Knapen 2005). We can distinguish external and internal triggers of the fuelling process:

*External triggers* are related to the environment of galaxies and gravitational interaction. Non-axisymmetry, which can lead to loss of angular momentum, can

result from galaxy interactions. For Ultra Luminous Infra-red Galaxies (ULIRGs), which show the most extreme cases of infrared nuclear activity, there is intriguing evidence for a connection between galaxy interaction and nuclear activity.

*Internal triggers* are based on instabilities generated from within the host. For example a two-step process has been proposed that is able to sweep the interstellar medium (ISM), via a stellar bar, from large scales into a disk of several hundred pc in radius. In the second step, further instabilities (bar-within-bar) drive the material close to the nucleus, until viscous processes take over the angular momentum transport.

While in quiescent galaxies, extensive star formation appears to be related to large-scale bars, the observational evidence for non-axisymmetry-related nuclear activity is not as clear for Seyfert galaxies. A slight but significant increase in the galactic-bar fraction of active galaxies has been found when compared to non-active galaxies. This does not appear to be the case for nuclear bars. Furthermore, there are a considerable number of AGN that show no signs of the presence of a bar, as well as of non-active galaxies that do possess bars.

## Mrk 609: a starburst/Seyfert composite galaxy

Mrk 609 is classified as a *starburst/Seyfert composite* galaxy. This class of AGN appears to be best suited to study the starburst-AGN connection, since the AGN and starburst components present themselves at the same level of activity (Moran et al. 1996). Composite galaxies can be characterised by optical spectra which are dominated by starburst features, while the X-ray luminosity and its variability are typical for Seyfert galaxies. The former property is based on the emission-line diagnostic diagrams by Baldwin, Phillips and Terlevich (BPT 1981). Close inspection of the optical spectra often reveals some weak Seyfert-like features, e.g. [O III] being significantly broader than all other narrow lines, or a weak broad H $\alpha$  component. There is a resemblance to narrow-line X-ray galaxies, which also show spectra of compos-

ite nature. Their soft X-ray spectra are flat, but it is still not clear how this strong and hard X-ray emission can be reconciled with the weak optical Seyfert characteristics. The faintness of these objects in the X-ray, as well as in the optical domain, has prevented them from being studied in detail so far.

## The SINFONI observations

Near-infrared imaging spectroscopy (cf. Gillessen et al. 2006) has considerable advantages over visible wavelength spectroscopy. Besides the much smaller dust extinction, there are a number of NIR diagnostic lines that probe the stellar and non-stellar content in Mrk 609. Among these are hydrogen recombination lines, ro-vibrational transitions of H<sub>2</sub>, stellar features like the CO(2–0) and CO(6–3) absorption band heads, as well as forbidden lines like [Fe II] and [Si VI].

The data (Zuther et al. 2007) have been acquired during the science verification phase of SINFONI in August/October 2004. For the first time we have spatially resolved the circumnuclear environment on the scale of 270 pc in the *J* and *H + K* bands (Figure 1). The morphology is complex, and the continuum image reveals a stellar bar-like structure superposed on the point-like Seyfert nucleus (Figure 1a). The distribution of hydrogen recombination emission (Pa $\alpha$ ) is clumpy and peaks at the tip where the potential bar meets the spiral arms and in regions along the minor axis (Figure 1b). The presence of nuclear broad Pa $\alpha$  and [Si VI] are clear indicators of the accretion of matter onto a nuclear supermassive black hole. The distribution of molecular hydrogen follows the continuum shape, while that of [Fe II] is aligned with the minor axis of the continuum and with the H-recombination emission (Figure 1c and 1d).

The well established BPT emission line diagnostics at visual wavelengths fail for regions with considerable extinction. Recently it was found that an analogous NIR line diagnostic diagram, using [Fe II]/Pa $\beta$  and H<sub>2</sub>/Br $\gamma$  line ratios, allows us to distinguish between starbursts (photoionisation excitation), AGN (mixed excitation), and LINERs (shock excitation). In this diagram, the nucleus of Mrk 609 shows

signs of LINER activity (Figure 2). Shock-driven excitation can be recognised by its high  $[\text{FeII}]/\text{Pa}\beta$  and  $\text{H}_2/\text{Br}\gamma$  values. Our integral-field data clearly resolve the nuclear and starburst activity in the central kiloparsec. Extinction appears to play no crucial role in this region, since the H-recombination line ratios are consistent with unreddened case-B values. This is furthermore supported by the strong Ly $\alpha$  emission in the ultraviolet.

The different regions characterised by clumpy Pa $\alpha$  emission (Figure 1b) clearly follow a trend from a LINER-like value at the nucleus to a starburst-like value in the most distant North-eastern region (data point 5 in Figure 2). The circumnuclear regions (data points 2, 3, and 4) fall in the domain of mixed excitation. In contrast to our nuclear classification, the line ratios extracted from the total field of view resemble those of a typical Seyfert galaxy. The same Seyfert characteristics are obtained from the large aperture Sloan Digital Sky Survey visual spectrum. This demonstrates how the choice of spatial scales to be studied can influence the resulting classification. Our LINER classification of Mrk 609, together with published data on variability of its non-stellar NIR emission, might be explained with the duty-cycle hypothesis, in which short-lived accretion events occur periodically and lead to the appearance of Seyfert features in the high state and low ionisation (shock-driven) emission features in the low state. In order to verify this possible scenario, multi-epoch SINFONI observations are needed.

The small spatial scales which SINFONI resolves on Mrk 609 allow for an investigation of the transport of matter within the central one kiloparsec. Obviously, Mrk 609 shows no signs of external triggers (i.e. interaction with companion galaxies). The presence of a nuclear bar-like stellar structure, as well as the clumpy morphology of the emission line gas, fits into the picture of internal triggers, feeding the AGN and circumnuclear star formation. However the chicken-and-egg problem – whether the star formation activates the accretion onto the SMBH or AGN feed-back initiates nearby starburst activity – remains open.

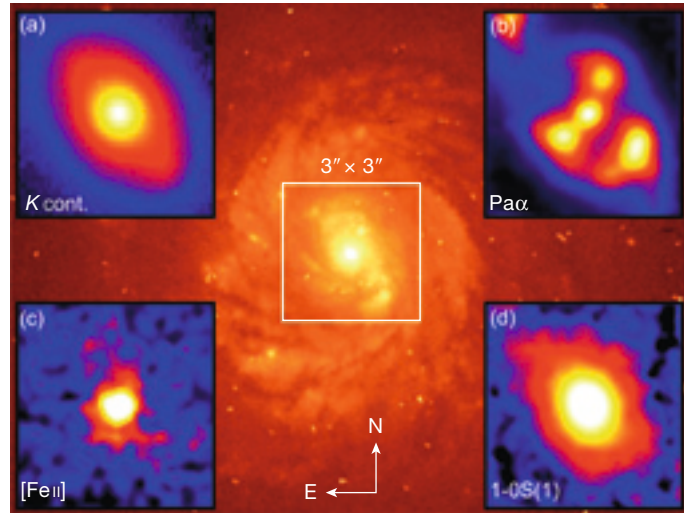


Figure 1: Hubble Space Telescope (HST) F606W-band image of Mrk 609 (centre, from Malkan et al. 1998) overlaid with SINFONI maps of various spectral features: (a) K-band continuum map, (b) Pa $\alpha$  map, (c) [FeII] 1.275  $\mu\text{m}$ , and (d) 1-0S(1) molecular hydrogen. The SINFONI field of view is indicated by the white box in the HST image.

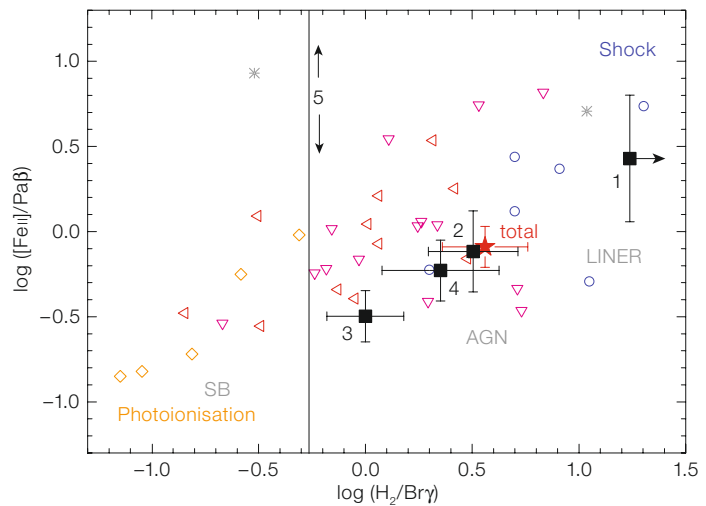


Figure 2: Line ratios of  $[\text{FeII}] 1.257 \mu\text{m}/\text{Pa}\beta$  and  $1-0\text{S}(1) 2.121 \mu\text{m}/\text{Br}\gamma$ . Activity types (starburst (SB), AGN and LINER) are indicated. Filled symbols represent our SINFONI measurements of five distinct regions of Mrk 609, as well as of the total field-of-view (red star). On account of missing J-band data, region 5 is only accurately located along  $\text{H}_2/\text{Br}\gamma$ . Open symbols correspond to literature values; orange diamonds represent starburst galaxies; red left triangles Seyfert 1 galaxies; magenta headlong triangles Seyfert 2s; blue circles LINERs; and grey asterisks supernovae. The diagram is interpreted as displaying the transition from pure photoionisation (lower left corner) to pure shock driven emission (upper right).

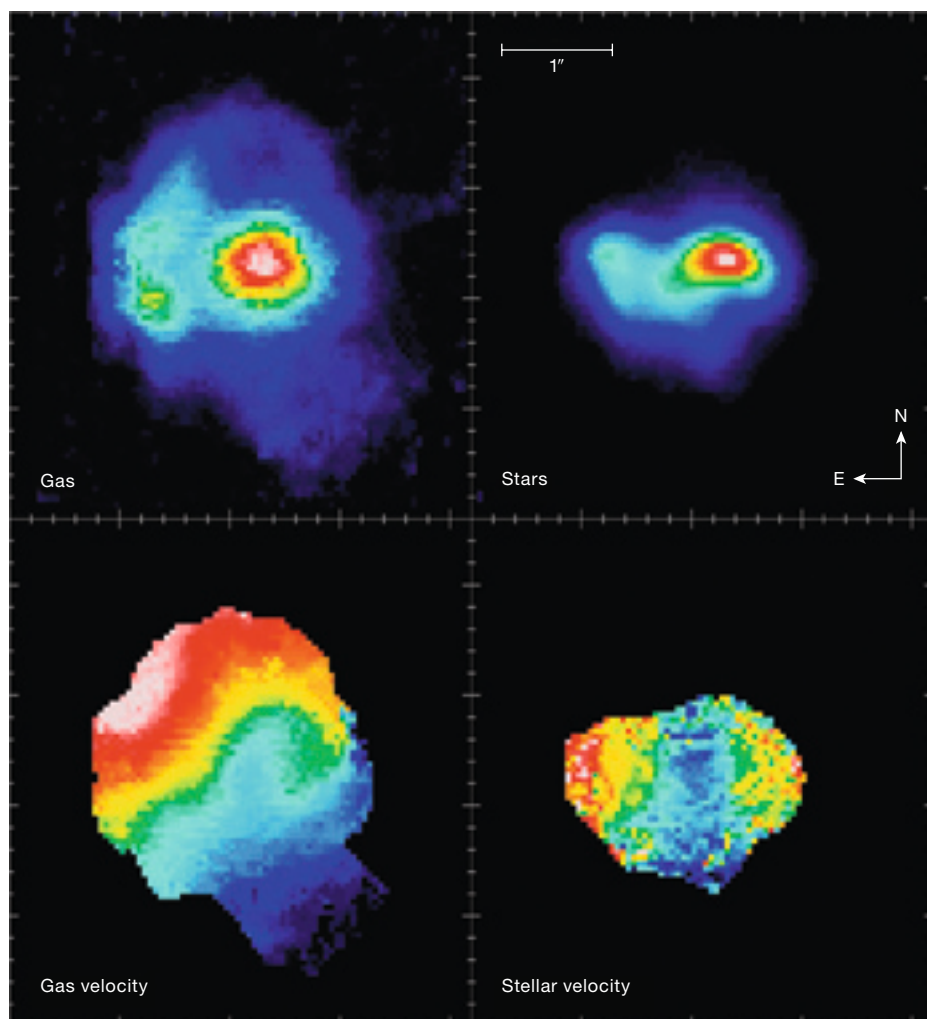
Outlook

The starburst/Seyfert composite nature of Mrk 609 can be disentangled into distinct regions of star formation and strong nuclear activity. Probably, this is true for most composite galaxies. Whether relationships between the occurrence of dynamical instabilities, star formation, and AGN activity are causally linked can only be determined with AO-assisted imaging spectroscopy (e.g. SINFONI) observations on a larger sample of this class of objects. Moving beyond the

backyard of our Milky Way towards larger look-back times and stronger nuclear activity, allows for a comparison with local AGN on the same physical scales. Then we are able to study scenarios such as whether circumnuclear starburst features generally accompany the cores of galaxies with even stronger nuclear activity, i.e. pure Seyferts and/or QSOs, or if enhanced star formation is a distinct phase in the evolution of AGN (e.g. Lípári and Terlevich 2006). However, resolving the central region of these objects on the 100 pc scale is fundamental for these studies.

References

Baldwin J. A., Phillips M. M. and Terlevich R. 1981, PASP 93, 5  
 Gillessen S. et al. 2006, The Messenger 120, 26  
 Knapen J. H. 2005, Ap&SS 295, 85  
 Malkan M. A. et al. 1998, ApJS 117, 25  
 Moran E. C. et al. 1996, ApJS 106, 341  
 Rodríguez-Ardila A. et al. 2005, MNRAS 364, 1041  
 Shlosman I., Begelman M. C. and Frank J. 1990, Nature 345, 679  
 Lípári S. L. and Terlevich R. J. 2006, MNRAS 368, 1001  
 Zuther J. et al. 2007, A&A 466, 451



The famous luminous infra red galaxy merger Arp 220 is shown here in more results from VLT SINFONI, this time used in tandem with the Laser Guide Star System (LGS). The LGS provides real-time adaptive optics correction using an artificial, laser-fed star to correct the distortions of the atmosphere. The two nuclei of Arp 220, separated by 1.0 arcsec, were resolved, the brighter to the west (right) and the more diffuse to the east. The upper images (where the brightness is colour-coded) show the appearance in molecular gas (left) and stellar light (right). The two lower images show the behaviour of the velocities of the gas (left) and the stars (right); the colour-coded images here depict matter moving towards the observer (in blue) and moving away (red). It is apparent that the stars and the gas move differently: the stars in two counter-rotating discs and the gas in a larger-scale disc. The image is taken from ESO PR 27/07, which provides more details.

# GHostS – Gamma-Ray Burst Host Studies

Sandra Savaglio<sup>1</sup>  
 Tamás Budavári<sup>2</sup>  
 Karl Glazebrook<sup>3</sup>  
 Damien Le Borgne<sup>4</sup>  
 Emeric Le Floch<sup>5</sup>  
 Hsiao-Wen Chen<sup>6</sup>  
 Jochen Greiner<sup>1</sup>  
 Aybuk Küpcü Yoldaş<sup>1</sup>

<sup>1</sup> Max-Planck Institute for Extraterrestrial Physics, Garching, Germany

<sup>2</sup> Johns Hopkins University, Baltimore, USA

<sup>3</sup> Swinburne University, Melbourne, Australia

<sup>4</sup> CEA-Saclay, Gif-sur-Yvette Cedex, France

<sup>5</sup> Institute for Astronomy, Honolulu, Hawaii

<sup>6</sup> University of Chicago, USA

GHostS is the largest public data-base on gamma-ray burst (GRB) host galaxies and is accessible at the URL <http://www.grbhosts.org>. Started in 2005, it currently contains photometric and spectroscopic information on 39 GRB hosts, almost 2/5 of the total number of GRBs with measured redshift. It will continue to grow, together with the unstoppable data flow from the observatories all over the world, every time a new event is discovered. Among other features, GHostS uses the Virtual Observatory resources.

## The Gamma-Ray Burst phenomenon

Gamma-ray bursts (GRBs) are the most energetic events in the Universe, and also among the fastest. They are associated with the death of massive stars (core collapse supernovae) or the merging of compact objects, such as neutron stars and black holes. During the explosive phase, they emit most of their energy as a collimated flux of gamma-ray photons from neutrino-antineutrino annihilations, and as gravitational waves. The gamma emission lasts from a few milliseconds to a few minutes.

The first GRB was discovered in 1967, by the US military satellite Vela, but it took six years, until 1973, for the first paper to appear in a scientific journal. The first red-

shift was measured in 1997, when GRBs were finally confirmed to be cosmological sources. Today there are 108 GRBs with measured redshift, the highest being GRB 050904, at  $z = 6.3$ . The typical energy emitted by a GRB, in a couple of minutes, is  $10^{51}$  ergs, equivalent to the energy emitted by the sun in 10 billion years.

Today GRBs are primarily discovered by the satellite *Swift* (<http://swift.gsfc.nasa.gov>), the dedicated NASA mission which in two years of operation helped to double the number of measured redshifts. With the growing data collected from space and ground telescopes, and the advent of *Swift*, our group decided to create a database, available to scientists, which collects observational results on the galaxies hosting GRB events. We called it GHostS, or GRB Host Studies. Our focus is to explore and unveil the nature of galaxies in which GRBs occur. Our goal is to answer fundamental questions, such as: are these galaxies different from the general galaxy population; are they special in any way; can we use them to understand galaxy formation under extreme conditions?

Today the GHostS database includes results for 39 GRB host galaxies. This is a large number, considering that only 108 GRBs have known redshift (see Figure 1).

## The GRB host galaxy population

There is no doubt that studies of GRB host galaxies are entering into a realm of galaxy formation that was hardly known before. The reason is that GRB hosts are generally faint and detected at high redshifts. Similar galaxies are very hard to find using conventional techniques, because they would require very long integration times, even for the largest and most efficient telescopes.

GRB events offer a shortcut to the quest for faint and distant galaxies. They are detected as short and energetic events. The localisation (and for a fraction of them the redshift) is measured from the bright X-ray and optical afterglow. We know that long-duration GRBs occur in regions of star formation, therefore, they are associated with galaxies. Dedicated programmes can observationally complete the investigation.

In our GHostS search, we want to explore many of the most interesting galaxy parameters, such as metallicity, star-formation rate, stellar mass, age of the stellar population and dust extinction. Each of these parameters are very difficult to derive. One difficulty is the faintness of the typical GRB host. Moreover, the data obtained by the community are often not homogeneous. To complicate the picture, the tools often used to derive the physical quantities are affected by systematic uncertainties which are sometimes greater than the relations being derived.

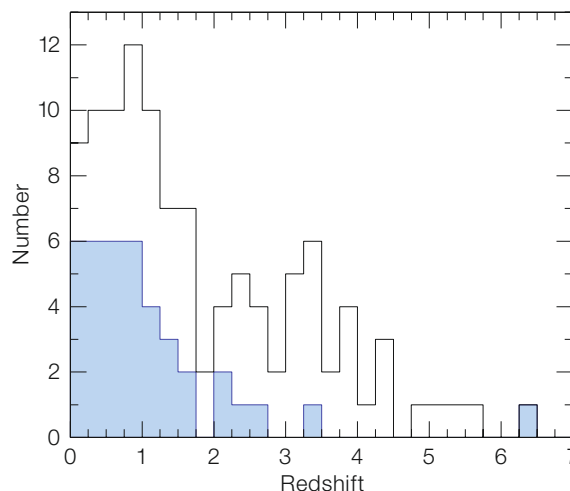


Figure 1: Redshift distribution of all GRBs (empty histogram) and the subsample of GRBs included in the GHostS database (blue histogram).

The typical GRB host is a star-forming, low-mass and low-metallicity galaxy, detected at redshift below  $z = 2$ . The mean stellar mass we derived in our sample is similar to the stellar mass of the Large Magellanic Cloud (Figure 2). Observational limitations prevent us from fully exploring the same parameters in GRBs at larger redshift, but in exceptional cases. The detection of the cold interstellar medium in high-redshift hosts indicates that there the population is different, with larger stellar masses, higher star-formation rates and higher metallicities (Berger et al. 2005, Fynbo et al. 2006, Savaglio 2006). It is still unclear if this means a different population, or different observational biases. Such issues will be faced and fully exploited by the future generation of telescopes and instruments.

In general, we know that GRB hosts are very peculiar galaxies. We still do not know whether this is because our traditional observational technique cannot reach the extreme limits attained by GRB detections, or because GRB hosts are intrinsically different. The main limitation is the small number of galaxies discovered so far. This number is still below 100, while the number of galaxies in today's surveys exceed  $10^5$ .

The GHostS database

GHostS includes GRB hosts for which photometric and spectroscopic information is available from the literature (Figure 3). In total 39 galaxies, out of a total of 108 GRBs whose redshift is known, have been gathered from 81 different papers and sources.

One of the spectra in the GHostS database is shown in Figure 4. The galaxy hosting GRB 990712 at redshift  $z = 0.433$  was observed at the Very Large Telescope (Küpcü Yoldaş, Greiner, Perna, 2006). It has very strong emission lines, originating in regions of the galaxy where star formation is very active. We derived a stellar mass of the galaxy of a few times  $10^9 M_{\odot}$ , similar to the stellar mass of the Large Magellanic Cloud, but it forms stars at a rate that is ten times higher, about  $6 M_{\odot} \text{ yr}^{-1}$ . This gives a specific star formation (the SFR per unit stellar mass) of 100 times that in the Milky Way. Similar

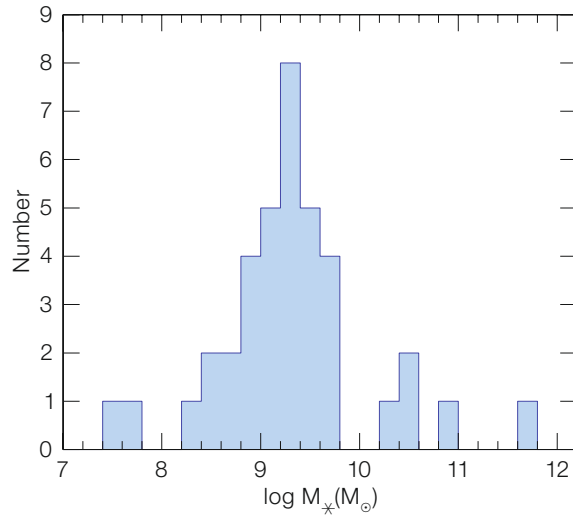


Figure 2: Histogram of the stellar mass of GRB host galaxies in the redshift interval  $0 < z < 6.3$ , from the GHostS sample. The mean stellar mass is of the order of the stellar mass of the Large Magellanic Cloud. This is ten times smaller than the stellar-mass limit reached by the deepest high-redshift galaxy surveys, performed by today's largest telescopes.

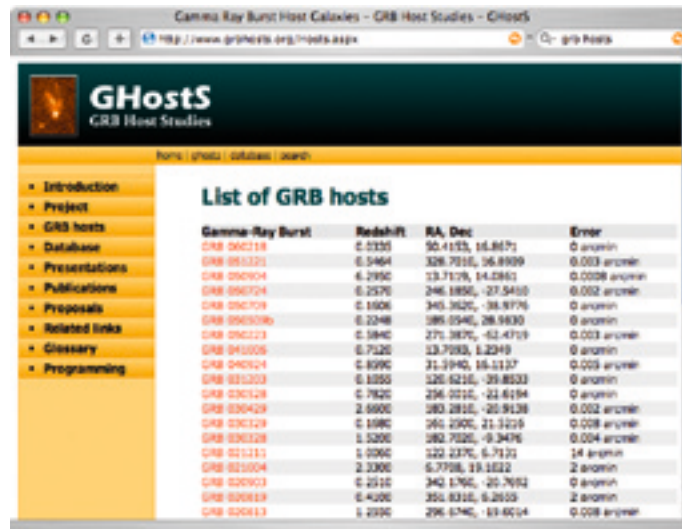


Figure 3: Example of the GHostS database web pages. Each GRB entry includes basic information on the event, together with access to relevant papers available in the literature. It reports multi-band photometry, fluxes of emission lines and images of the field.

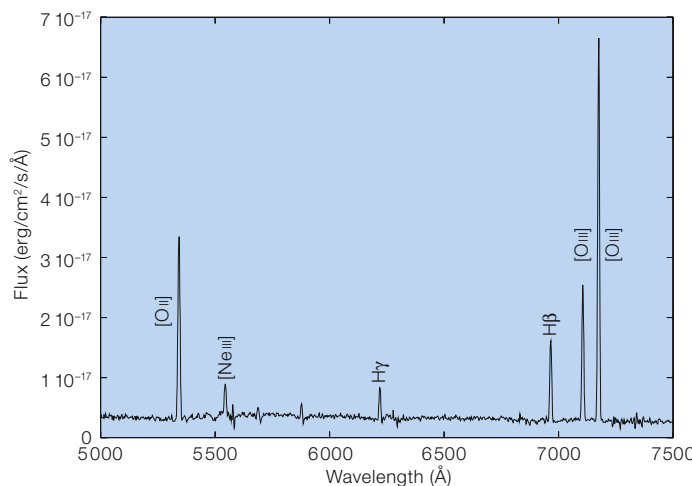


Figure 4: Very Large Telescope spectrum of the galaxy hosting GRB 990712 at redshift  $z = 0.433$  (Küpcü Yoldaş et al. 2006).

galaxies hosting GRBs are detected up to a distance when the Universe was less than 1 Gyr old. They are very hard to find using normal tools of investigation. Most surveys, probing the high-redshift Universe today, can reach, in terms of stellar mass, galaxies similar to or larger than the Milky Way.

It is generally not easy to collect results published by the GRB community, because the number of papers available for each event can be large. One extreme case was GRB 060218, which occurred in February 2006, at redshift  $z = 0.0335$ , associated with a supernova, detected three days after the alert (Masetti et al. 2006). In about a year and a half, more than 20 articles dedicated to this event have been published (or are in the process of being published) in refereed journals, four of which appeared in *Nature*.

This proliferation of material is one of the main motivations for the existence of GHostS. Observational results are searched, collected, homogenised and made easily accessible for the whole community. The database is constantly growing in terms of total number of objects, and in terms of tools offered. We plan to eventually include all host galaxies discovered in the past and in the future for the years of operation of Swift, and it will likely contain a final sample of a few hundred galaxies.

### The Virtual Observatory

The Virtual Observatory (VO) is one of the features offered in our database. The VO is one of the newest and most promising tools introduced in the astronomy world, allowing scientists to easily access data from multiple astronomical observatories, both ground- and space-based facilities, through one portal (see for instance <http://www.us-vo.org/>). Its components have been added to the GHostS web portal (Figure 5). Using information about the GRBs and their hosts stored inside our SQL database, one can automatically enhance the view of the catalogued hosts by using various VO resources. The details pages currently show images of the relevant pieces of the sky as seen by the Sloan Digital Sky Survey (SDSS) and the legacy Digitized Sky Sur-

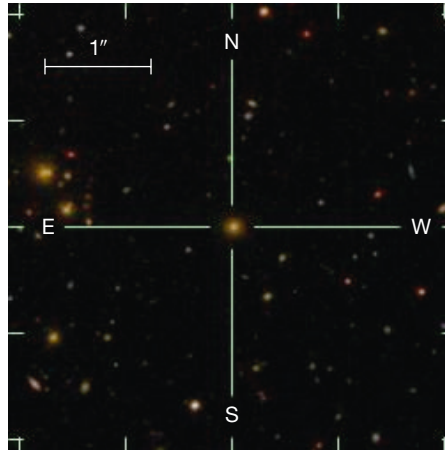


Figure 5: One example of the tools offered by GHostS. The images show the field of GRB 050509b, at redshift  $z = 0.2248$  (Gehrels et al. 2005), obtained from the Sloan Digital Sky Survey (left) and Digitalized Sky Survey (right) archives, through the Virtual Observatory.

vey (POSS, SERC). Other types of automated searches are also in the works, e.g., for finding spectra at the given position. These VO additions, the efficient database, and the presentation of the scientific data, make the website not only an invaluable research tool for GRB host studies, but also very enjoyable to navigate. GHostS will feature in the future advanced search capabilities for the community, fine-tuned for astronomical data and will eventually dynamically search VO resources for relevant observations, such as images and spectra.

### The future

The future of GRB science fully depends on the life of GRB hunting machines, i.e. gamma-ray detectors. Today it almost exclusively relies on the existence of Swift, which has been funded for an additional four years.

Among the many unexplored territories, we mention the discovery of the very high redshift GRBs, at  $z > 6$ . We know that there are collapsed objects at those times. We do not know under which physical conditions these objects formed: are they stars, galaxies or massive black holes? At  $z > 6$ , QSO searching has failed in providing a satisfactory picture, and galaxies are incredibly hard to find. GRBs on the other hand have shown some very promising results. In the first two years of operations, Swift has discovered 8 GRBs at redshift larger than 4, and 4 at redshift larger than 5. This is 7% and 3.5% of the total GRB population with measured redshift, and probably the num-

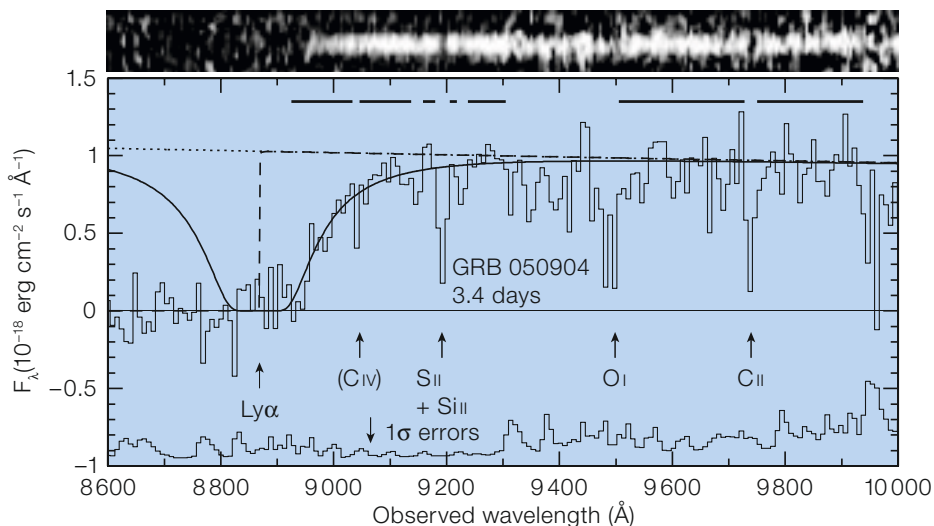
bers would be larger if we were able to observe all GRB afterglows early on. In fact, 2/3, of the Swift GRBs have no measured redshift. The fractions of  $z > 4$  and  $z > 5$  known QSOs are 0.8% and 0.03% of the total, with only 17 QSOs known with redshift larger than 5.

Particularly impressive was GRB 050904, the record holder at  $z = 6.3$  (Kawai et al. 2005). This GRB was observed with the Japanese telescope Subaru more than three days after the Swift alert, when it had already faded 11 magnitudes from its initial brightness. Fortunately at high redshifts the brightness of a fading object is helped by time dilation, the effect described in Einstein's theory of General Relativity. If this GRB had occurred in the local Universe, it would have faded at a rate more than seven times faster. The spectrum of this spectacular event is shown in Figure 6 (from Totani et al. 2006). The host galaxy is barely detected by the Hubble Space Telescope and Spitzer Space Telescope (Berger et al. 2006). We estimate a stellar mass which is half that of the Large Magellanic Cloud, and a rate of star formation ten times higher. Although this event happened less than 900 million years after the Big Bang, the absorption lines detected in its spectrum indicate a surprisingly high pollution of heavy elements in the interstellar medium in the host galaxy, of the order of 1/10 that of the solar vicinity (Totani et al. 2006;

**Figure 6:** Subaru spectrum of the most distant GRB ever discovered, GRB 050904 at  $z = 6.3$  (Totani et al. 2006). It was observed more than three days after the alert given by the gamma-ray burst finder Swift, when it had already faded 11 magnitudes from its initial brightness.

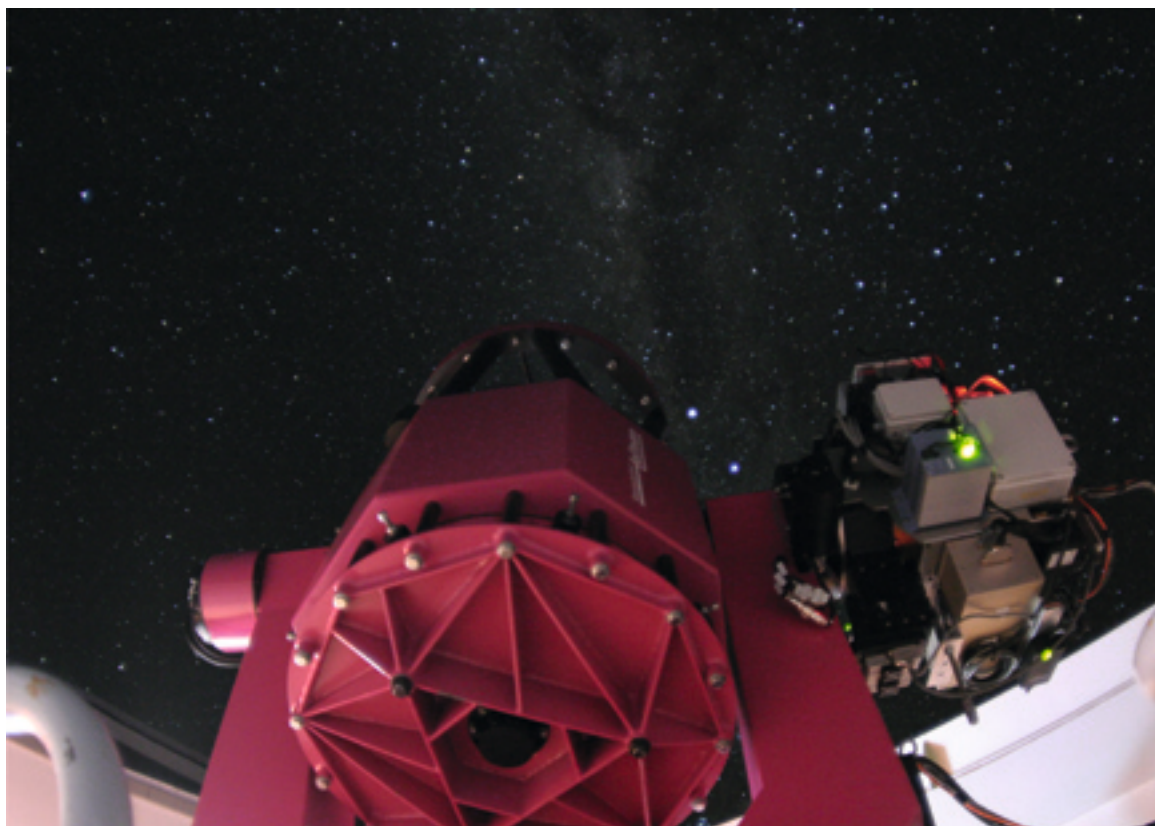
Savaglio 2006). This is hardly explained by most theories of chemical enrichment in the primordial Universe. Galaxies like these are very likely faint and dormant today, because they would have consumed their gas reservoir for star formation in less than one Gyr, i.e. by redshift  $z = 3$ .

If GRB 050904 were observed two hours after the Swift alert, its spectrum would have been much more spectacular, with a signal-to-noise ratio ten times better than that of the Subaru spectrum. Nothing like this has ever been achieved in the remote Universe with normal galaxies or QSOs. It is only a matter of time that, sooner or later, Swift will trigger similar events at higher redshift. Then telescopes from the ground will be ready to catch the fading sources and deliver a unique data set to the scientific community, for new exciting discoveries. We will be there to continue our service to the community with GHostS, in the attempt to fully characterize those galaxies parenting one of the most extraordinary objects in the Universe.



**References**

Berger E. et al. 2005, ApJ 642, 979	Kawai N. et al. 2005, GRB Coordinates Network 3937, 1
Berger E. et al. 2006, ArXiv Astrophysics e-prints, arXiv: astro-ph/0603689	Küpcü Yoldaş A., Greiner J. and Perna R. 2006, A&A 457, 115
Fynbo J. P. U. et al. 2006, A&A 451, L47	Masetti N. et al. 2006, GRB Coordinates Network 4803, 1
Gehrels N. et al. 2005, Nature 437, 851	Savaglio S. 2006, New Journal of Physics 8, 195
	Totani T. et al. 2006, PASJ 58, 485



The Rapid-Eye Mount (REM) 0.6-m telescope at the ESO La Silla Observatory, which is dedicated to the follow-up of gamma-ray bursts, is shown in operation. ESO PR 26/07 provides details of the telescope and some science results.

# The Puzzle of the Ly $\alpha$ Galaxies: New Results from the VLT

Christian Tapken<sup>1</sup>  
 Immo Appenzeller<sup>2</sup>  
 Armin Gabasch<sup>3,4,5</sup>  
 Jochen Heidt<sup>2</sup>  
 Ulrich Hopp<sup>3,4</sup>  
 Ralf Bender<sup>3,4</sup>  
 Stefan Noll<sup>3,4</sup>  
 Stella Seitz<sup>3,4</sup>  
 Sabine Richling<sup>6</sup>

<sup>1</sup> Max-Planck-Institut für Astronomie,  
 Heidelberg, Germany

<sup>2</sup> Landessternwarte Heidelberg-König-  
 stuhl, Heidelberg, Germany

<sup>3</sup> Universitäts-Sternwarte München,  
 Germany

<sup>4</sup> Max-Planck-Institut für Extraterres-  
 trische Physik, Garching, Germany

<sup>5</sup> ESO

<sup>6</sup> Institut d'Astrophysique de Paris, France

Observations of high-redshift galaxies show that at early cosmic epochs the cosmic UV radiation field appears to be dominated by small galaxies with strong Ly-alpha emission. Although usually small and of relatively low luminosity, these galaxies are easily identified from their line emission. Observations with the VLT resulted in significant progress in the understanding of the nature of these distant galaxies and of their role in the early Universe.

The pioneers: R. B. Partridge and  
 P. J. E. Peebles

The history of the Ly $\alpha$  galaxies began in 1967 with a pioneering paper by R. B. Partridge and P. J. E. Peebles. In this article, published in the *Astrophysical Journal*, the two Princeton University astrophysicists discussed the formation of the first galaxies in the Universe. They concluded that the first galaxies probably began their lives with strong initial bursts of star formation at cosmic epochs corresponding to redshifts between 10 and 30. Because of the presence of many massive, hot, and luminous stars in these starbursts, Partridge and Peebles predicted very high ultra-violet (UV) luminosities of the newly formed galaxies, and they estimated that the light emitted by such objects during the first few hundred million years should actually be observ-

able. Because of the large distance, the light emitted by the young galaxies as far-UV radiation is redshifted to the red and near-infrared spectral range. Hence, the detection of such objects requires observations at these wavelengths.

As the most promising way to find these objects, Partridge and Peebles proposed to search for their Lyman- $\alpha$  (Ly $\alpha$ ) line emission. This spectral line, due to transitions from the first excited energy level to the ground state of hydrogen atoms, is important in many astrophysical processes. In normal galaxies Ly $\alpha$  emission is produced during the recombination of interstellar hydrogen gas, which has been ionised by hot stars. Simple estimates show that up to about 2/3 of the Lyman continuum photons (and up to about 6% of the total luminosity) of hot stars can be converted into Ly $\alpha$  photons. This also means that, in principle, Ly $\alpha$  emission equivalent widths of the order 100 to 200 Å can be expected in the spectra of such galaxies.

Of course 6% is still only a minor fraction of the total emitted luminosity. However, as noted by Partridge and Peebles, in the small wavelength range covered by the Ly $\alpha$  line, the expected spectral flux density is much higher than in the adjacent continuum. Therefore, detecting the line emission against the strong sky background in the red spectral range appeared much easier than looking for the continuum emission.

In 1967 sensitive astronomical detectors were limited to wavelengths  $\leq 1 \mu\text{m}$ . Thus, observations of the redshifted Ly $\alpha$  line appeared feasible only up to redshifts where the observed wavelength of Ly $\alpha$  does not exceed  $1 \mu\text{m}$ , which means redshifts  $z = \Delta\lambda/\lambda \leq 7$ . In view of this limitation, Partridge and Peebles calculated the emitted luminosity and the expected observed Ly $\alpha$  flux emitted at an epoch corresponding to  $z \approx 7$ .

To appreciate the courage and foresight of taking up this topic in 1966, when the paper was submitted, we have to recall that the Cosmic Microwave Background, confirming the present cosmological concepts, had been discovered just one year before, that the most distant galaxy known at that time had a redshift of

about 0.5, that neither galaxy formation nor star formation was well understood, that the most advanced astronomical detectors were image tubes followed by photographic plates, and that there existed only two astronomical telescopes with apertures exceeding 2.5 m. Since in 1966 getting time at the largest existing telescopes was probably as difficult as today, Partridge and Peebles assumed for their feasibility estimates a more modest (and more typical) 90-cm telescope, equipped with an image tube with an S1 cathode. With these assumptions Partridge and Peebles predicted that the Ly $\alpha$  emission of very young galaxies at  $z \approx 7$  should be detectable with an exposure time as short as five minutes(!).

The search for the Ly $\alpha$  emitting galaxies

Prompted by the 1967 paper, many different groups started searching for redshifted Ly $\alpha$  (and UV continuum) emission of high-redshift galaxies. However, although a large amount of observing time was invested, and although the surveys soon reached much fainter magnitudes than those predicted by Partridge and Peebles, for many years no redshifted Ly $\alpha$  emitting galaxy was found. Some Ly $\alpha$  emission was detected from distant radio galaxies and from some galaxies associated with distant QSOs. However, it was not clear whether starbursts or non-thermal ionising sources were responsible for the Ly $\alpha$  emission from these objects.

Starting about 1995, many galaxies with redshifts of  $z \approx 3$  were discovered using the Lyman-break technique. Practically all the distant galaxies found with this technique showed clear spectroscopic signatures of strong starbursts. However, in most cases the Ly $\alpha$  line occurred either in absorption or as a relatively weak emission feature. Similar results were found for samples of high-redshift galaxies selected on the basis of photometric redshifts (see Figure 1).

More detailed models of starburst galaxies soon provided a plausible explanation for the weakness of the Ly $\alpha$  emission of the young  $z \approx 3$  galaxies. Partridge and Peebles were certainly correct, noting that in young starbursts copious

numbers of Ly $\alpha$  photons are produced. However, because of the high absorption cross-section of hydrogen atoms for Ly $\alpha$  photons, even a small amount of neutral hydrogen can make a galaxy completely opaque for Ly $\alpha$ .

Normally the absorption of Ly $\alpha$  by an interstellar hydrogen atom will be followed by a re-emission at the same frequency. Thus, hydrogen atoms essentially scatter the Ly $\alpha$  photons, which in principle can still escape after some random walk through the neutral hydrogen layer. However, the resonance scattering greatly increases the effective light path of these photons. Therefore, even a small amount of truly absorbing material embedded in the scattering layer will result in the eventual absorption of the Ly $\alpha$  photons. A most efficient UV absorber is interstellar dust, which is normally abundant in star-forming regions. Thus, the combination of resonance scattering by neutral hydrogen and dust absorption provides a highly plausible explanation for the absence of strong Ly $\alpha$  emission in most known young galaxies. It also seemed to explain why more than two decades of searches for high-redshift Ly $\alpha$  galaxies were not successful.

Soon after the above explanation for the absence of strong Ly $\alpha$  emission in distant starburst galaxies, and the reason for the futility of the earlier searches had been more or less accepted, the history of the Ly $\alpha$  galaxies took an unexpected turn in the mid-1990's. The first Ly $\alpha$  galaxies were detected on the basis of their strong emission line. In an ApJ letter of 1998 Ester Hu, Lennox Cowie, and Richard McMahon reported the discovery of the elusive high-redshift Ly $\alpha$  galaxies during observations with the new 10-m Keck II telescope. The objects discovered by these authors had redshifts of  $z \approx 3.4$  and  $z \approx 4.5$  and Ly $\alpha$  emission equivalent widths  $> 100 \text{ \AA}$ . However, their luminosities were only about one hundredth of that predicted by Partridge and Peebles. This obviously explains why it took a telescope of 10 m (instead of 1 m) aperture to find them.

From the large Ly $\alpha$  equivalent widths, it was clear that the faintness of these objects was not due to dust absorption. Obviously, these galaxies were intrinsi-

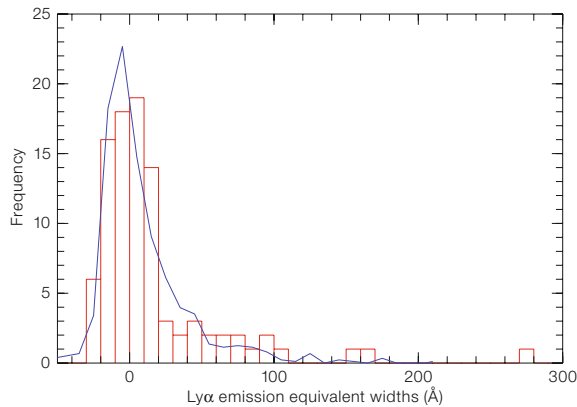


**Figure 1:** Distribution of the Ly $\alpha$  emission equivalent widths in samples of high-redshift galaxies selected using broadband photometry. The histogram is based on the FDF spectroscopic survey (Noll et al. 2004), selected on the basis of photometric redshifts. The blue line shows the distribution derived by Shapley et al. (2003) for Lyman-break-selected galaxies.

cally faint and small (see Figure 2). On the other hand, the relatively high space density of the distant Ly $\alpha$  galaxies derived by Hu et al. indicated that the Ly $\alpha$  galaxies provided a major contribution to the star formation and to the cosmic radiation field at the corresponding epochs. Nevertheless a reliable assessment of the effects and the importance of the Ly $\alpha$  galaxies required more information on their detailed properties and their density as a function of redshift. Therefore, the first results immediately started a new wave of searches for high redshift Ly $\alpha$  galaxies. In addition, new studies of the physics of these objects were triggered. Some of this new work was carried out at ESO using the VLT. In the following we describe new results on the nature and the space density of these distant galaxies which resulted from these VLT observations.

#### The mystery of the strong line emission

As described above, for many years astronomers were puzzled by the fact that no Ly $\alpha$  galaxies could be observed. That they were finally discovered in the mid-1990's resulted in a new big mystery. The question now was, why these galaxies could emit such a strong Ly $\alpha$  flux in spite of the expected quenching of the Ly $\alpha$  photons by the combination of resonance scattering and dust absorption. As a possible answer to this question it was suggested in the literature that the Ly $\alpha$  galaxies were too young to have formed heavy chemical elements, which are needed to form dust. This explanation appeared plausible, since the first galaxies are expected to form from primordial matter produced by the Big Bang, which (apart from tiny amounts of deuterium and

lithium) is composed of hydrogen and helium. Under astrophysical conditions neither hydrogen nor helium can form solids. Thus, dust particles can form only after heavier chemical elements have been produced by the nuclear processes in stars. A very important first result of the VLT observations was high-quality FORS spectra of Ly $\alpha$  galaxies showing conspicuous lines of heavy elements (Figure 3). In particular, these spectra contained lines of carbon and silicon, which are among the main constituents of interstellar dust particles.

If dust is present in young galaxies, Ly $\alpha$  photons can still escape, if the dust and (or) the neutral hydrogen are distributed inhomogeneously and if, by chance, no such material is present along the line of sight between us and the starburst. That the amount of dust and cool material along the line of sight plays a role for the observed Ly $\alpha$  flux is supported by the finding that the Ly $\alpha$  emission strength of high-redshift galaxies decreases with increasing dust reddening and that the Ly $\alpha$  emission is lower in galaxies with strong interstellar absorption lines, typical for cool interstellar gas (Shapley et al. 2003, Noll et al. 2004). However, for a given reddening, the Ly $\alpha$  emission strength tends to vary considerably and there exist Ly $\alpha$  galaxies with high Ly $\alpha$  equivalent widths and a modest amount of reddening. Thus, missing dust and/or missing neutral hydrogen along the line of sight cannot fully explain the observed strong line emission.

Another mechanism, which can avoid the quenching of the Ly $\alpha$  emission, is the presence of sufficiently large velocity gradients in the neutral gas. If a hydrogen

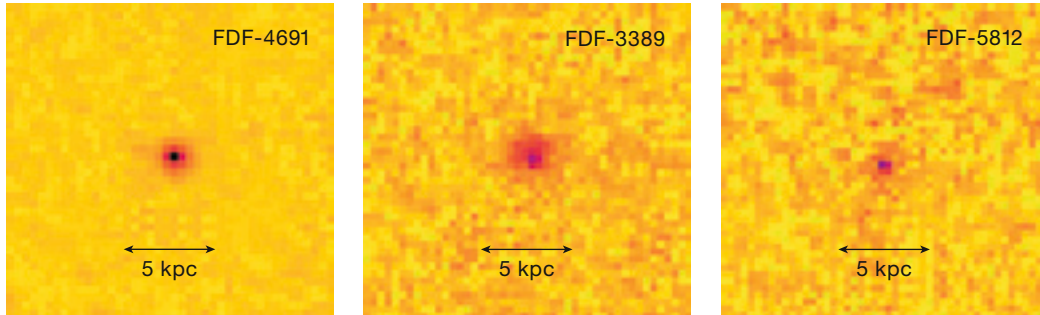


Figure 2: Examples of HST/ACS F814W images of three Ly $\alpha$  galaxies.

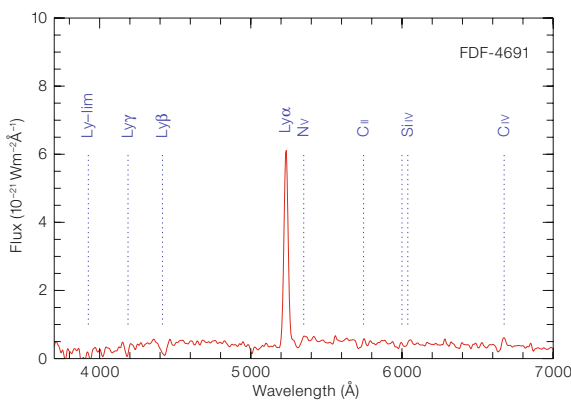


Figure 3: FORS spectrum of the Ly $\alpha$  galaxy FDF-4691 (from Tapken et al. 2004).

atom is moving relative to the volume emitting the Ly $\alpha$  line with a velocity larger than the line widths, the atom cannot absorb or scatter the Ly $\alpha$  photons. In this case the Ly $\alpha$  photons can penetrate the neutral hydrogen layer and escape. Such velocity differences are not unexpected since the velocity of sound is much higher in the hot Ly $\alpha$  emitting gas than in the cool neutral hydrogen layers. Thus, assuming turbulent media with subsonic turbulence, the Ly $\alpha$  lines emitted by the hot ionised gas are expected to have profiles which are significantly broader than the velocity dispersion of the scattering layers. However, because of the very high absorption cross-section of neutral hydrogen, even the outer wings of the absorption profiles can prevent the escape of the Ly $\alpha$  photons. On the other hand, it can be shown that the probability for an escape of the Ly $\alpha$  photons can increase strongly if large-scale velocity fields are present in the scattering layers. Mechanisms producing such large-scale velocity fields can be mass infall, or mass outflows from the galaxies powered by stellar winds or radiation pressure from the central stars. Since such velocity fields also affect the profiles of the Ly $\alpha$  lines, line profile observations provide a critical test of this hypothesis.

We have used the VPH grisms available on the FORS instruments to obtain medium-resolution spectra of a sample of Ly $\alpha$  emitting high-redshift galaxies in the FORS Deep Field (Appenzeller et al. 2004). The observed Ly $\alpha$  profiles were compared to model profiles, which were computed using the radiative transfer code of Meinköhn and Richling (2002), which is particularly well suited for modelling resonance scattering in moving media. Examples of the observed profiles and model fits are presented in Figure 4. For these computations (described in detail in Tapken et al. 2007) we assumed a central volume of turbulent, ionised hydrogen, emitting the Ly $\alpha$  radiation. This region was assumed to be surrounded by a shell of dusty neutral hydrogen.

The calculations showed that the observed profiles could be reproduced reasonably well with this model, if a modest (10–200 km s $^{-1}$ ) expansion velocity of the neutral hydrogen shell was assumed. From the observed line wings (which are not much affected by the neutral hydrogen shell) high velocities (> 600 km s $^{-1}$ ) of the ionised gas could be derived. These high velocities can be explained by supersonic turbulence caused by supernova shocks and strong stellar winds in the

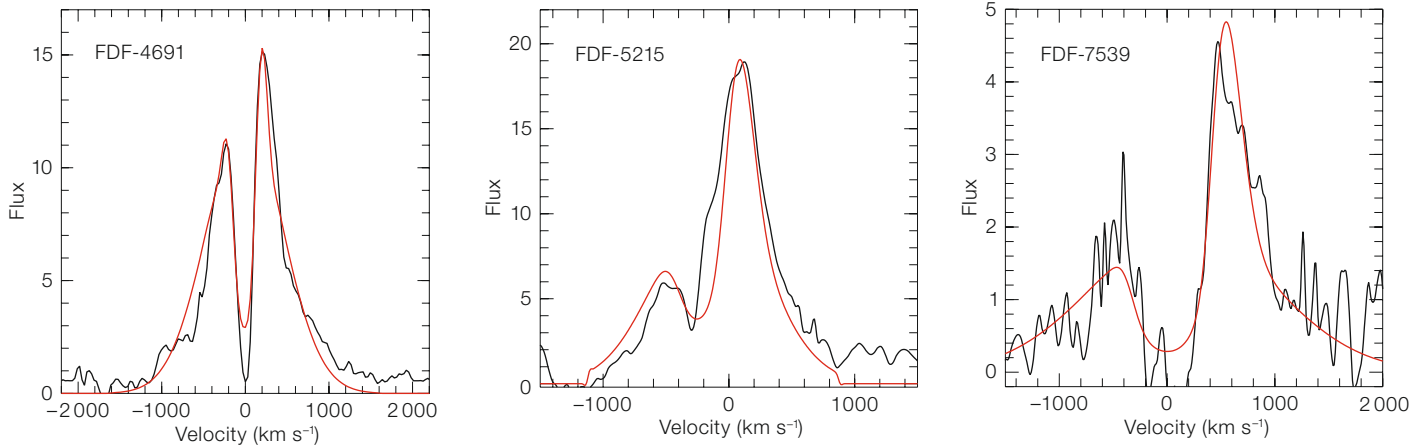
compact, strong starbursts. The combination of the relatively broad intrinsic Ly $\alpha$  profiles and the expansion of a neutral hydrogen shell readily explains the fact that a major fraction of the Ly $\alpha$  photons can escape, in spite of the presence of a dusty neutral hydrogen shell in front of the emitting region.

From our results, we conclude that, although a relatively small amount of neutral matter along the line of sight certainly plays a role, the high intrinsic velocity dispersion of the emitting ionised gas and large-scale outflows of the neutral hydrogen are the main reasons for the escape of a large fraction of the Ly $\alpha$  photons from the observed galaxies. The small continuum flux (relative to other high-redshift galaxies) indicates a low total mass of the hot stars of Ly $\alpha$  galaxies. If the mass of the hot stars is a measure of the total mass of these objects, Ly $\alpha$  galaxies are probably of lower (and more normal) mass than other known high-redshift galaxies. Therefore, they probably have lower gravitational potentials, which may explain the observed strong outflows.

#### The space density of Ly $\alpha$ galaxies and their role in cosmic evolution

As noted above, most known Ly $\alpha$  galaxies are small and have intrinsically faint UV continua. However, already Hu et al. (1998) found for the redshift range  $3.4 < z < 4.5$  a total star-formation density due to the Ly $\alpha$  galaxies which is comparable to that due to all other known high-redshift galaxies. Since Ly $\alpha$  galaxies tend to be less affected by reddening than other high-redshift galaxies, they are expected to dominate the UV radiation field at these redshifts. Moreover, studies of high-redshift galaxy samples based on photomet-

Figure 4: Examples of observed (black) and computed (red) Ly $\alpha$  emission line profiles of Ly $\alpha$  emitting galaxies.



ric redshifts (and, therefore, relatively free of selection effects) show that the fraction of Ly $\alpha$  emitting galaxies is increasing with redshift (Noll et al. 2004). According to Shimasaku et al. (2006) at  $z = 6$  about 80% of all high-redshift galaxies are Ly $\alpha$  galaxies with intrinsic Ly $\alpha$  emission equivalent widths  $> 100 \text{ \AA}$ . Hence, at very high redshifts these objects are expected to strongly dominate the cosmic UV radiation field and the cosmic ionisation.

For a more quantitative assessment of the role of the Ly $\alpha$  galaxies in the early Universe obviously a reliable knowledge of their space density as a function of luminosity and redshift is needed. Therefore, during the past years, various different groups have invested much work to derive this so-called 'luminosity function' of the Ly $\alpha$  galaxies at different redshifts. There were basically two types of such programmes: firstly, large-area surveys were used to improve the number statistics of these objects; secondly, very deep observations in smaller fields were used to reach fainter Ly $\alpha$  galaxies and to derive the faint part of the luminosity function for these objects. This faint part is important, since, within the observational limits, faint galaxies are always more numerous than the bright ones.

Particularly successful among the large-area surveys were studies carried out with the wide-field SUPRIME camera of the Japanese national telescope Subaru (see, e.g., Shimasaku et al. 2006). These surveys resulted in important information on the space density of luminous Ly $\alpha$  galaxies and on the cosmic variance of this quantity. Our contribution to the topic

was an extension of the luminosity function to lower luminosities, which was possible as a result of the superior sensitivity of the FORS2 instrument and a specially developed set of narrowband filters (Tapken et al. 2006).

Like all current searches for Ly $\alpha$  galaxies, the survey carried out with the VLT used sky images obtained through a combination of broadband and narrowband filters. Normal galaxies, where the light is dominated by the stellar continua, tend to be visible with a similar brightness in many different filter bands. Emission-line objects are characterised by an excess emission in one or, if the emission line coincides with the overlap region of two filters, in at most two adjacent filter bands (see Figure 5). Filter photometry allows a reliable detection of galaxies which have emission lines in their spectra. More difficult and more complex is the unambiguous identification of the observed emission lines as Ly $\alpha$ . For this purpose one needs reliable photometric redshifts and low-resolution spectra of the candidate galaxies, which rule out other identifications of the observed lines.

In order to reach an optimal signal-to-noise ratio, the passbands of the narrowband filters used for searches of Ly $\alpha$  galaxies are designed to coincide with wavelength regions of particularly low night sky background. Since most of the night sky background in the red and near-infrared is due to airglow produced by OH molecules in the high atmosphere, the spectral regions of low sky background are the gaps or 'windows' in the OH line spectrum. One of these 'OH win-

dows' covers about 20 nm wavelength interval near  $\lambda = 815 \text{ nm}$  (corresponding to a Ly $\alpha$  redshift of  $z \approx 5.7$ ). This window is particularly important since, at this wavelength, photometric and spectroscopic follow-up observations are still relatively easy. Therefore, this window was also used for our VLT observations. To reach an optimal sensitivity, the wavelength interval of the 815-nm OH window was covered by a set of three filters (Figure 6). In this way it is possible not only to avoid the strong OH lines outside the window, but also to partially suppress the weaker lines still present inside the 815-nm OH gap. Because of the resulting lower background, the VLT observations allowed us to reach significantly lower Ly $\alpha$  luminosities than had been possible before.

Figure 7 shows the results together with luminosity function data from another recent survey. The new data confirm the high space density of faint Ly $\alpha$  galaxies at high redshift. In particular up to  $z \approx 6$  the space density seems not to decrease with redshift. On the other hand, the observed luminosity range and the number of observed objects are still too small, to constrain the luminosity function well. Although much progress has been made, obviously more work is needed to derive the radiation field produced by the Ly $\alpha$  galaxies with an adequate accuracy.

#### Future work and outlook

Several ambitious large-area searches for Ly $\alpha$  galaxies are underway which will further improve the statistics of these ob-

jects. Of particular interest will be the results of the DAzLE survey, which, using infrared imaging, aims at finding Ly $\alpha$  galaxies at redshifts  $z > 7$ . Hence, during the next few years we will certainly see much more and better statistical data on the bright part of the luminosity function of the Ly $\alpha$  galaxies. Less clear is the outlook for more information on the important faint part of the luminosity function of these objects. Reaching significantly fainter galaxies with normal deep-field observations would require very long exposures times, which appear not realistic for such programmes. More promising may be the ‘gravitational telescope’ technique, i.e., making use of the flux amplification of distant objects by strong gravitational lensing. Because of their relatively high surface density, Ly $\alpha$  galaxies are well suited for such programmes. Estimates have shown that, with presently available instruments, observations of lensed Ly $\alpha$  galaxies in the field of a single galaxy cluster with a high lensing strength (such as the ROSAT source RX J1347-1145) could provide a significant sample of Ly $\alpha$  galaxies with intrinsic luminosities one to several magnitudes fainter than those known at present. These data could be obtained with a rather modest amount of observing time. Thus, progress concerning the luminosity functions also seems to be possible, provided observing time for such programmes can be obtained.

#### Acknowledgements

Our research has been supported by the German Science Foundation DFG (SFB 439). We would like to thank the staff of the Paranal Observatory for carrying out the service mode observations. We also thank Dörte Mehlert and Erik Meinköhn for discussions and valuable comments.

#### References

- Appenzeller I. et al. 2000, *The Messenger* 116, 18  
 Hu E. M., Cowie L. L. and McMahon R. G. 1998, *ApJL* 502, L99  
 Meinköhn E. and Richling S. 2002, *A&A* 392, 827  
 Noll S. et al. 2004, *A&A* 418, 885  
 Partridge R. B. and Peebles P. J. E. 1967, *ApJ* 147, 868  
 Shapley A. E. et al. 2003, *ApJ* 588, 65  
 Shimasaku K. et al. 2006, *PASJ* 58, 313  
 Tapken C. et al. 2004, *A&A* 416, L1  
 Tapken C. et al. 2006, *A&A* 455, 145  
 Tapken C. et al. 2007, *A&A* 467, 63

Figure 5: Bessell-R and broadband images and narrowband images of four galaxies in the FORS Deep Field. The upper two panels show  $z \approx 5.7$  Ly $\alpha$  galaxies. The lower two panels show, for comparison, corresponding data for a normal  $z \approx 3.2$  starburst galaxy and for a  $z \approx 1.2$  [OII] emitter.

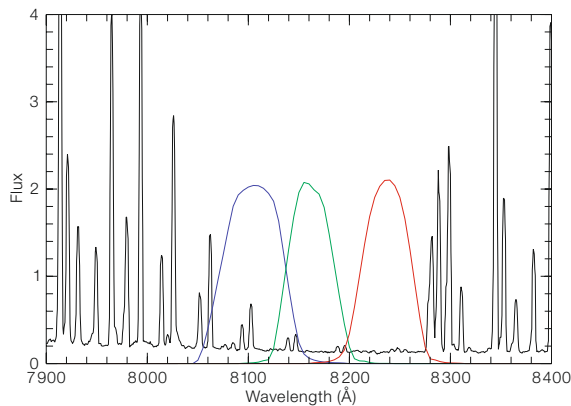
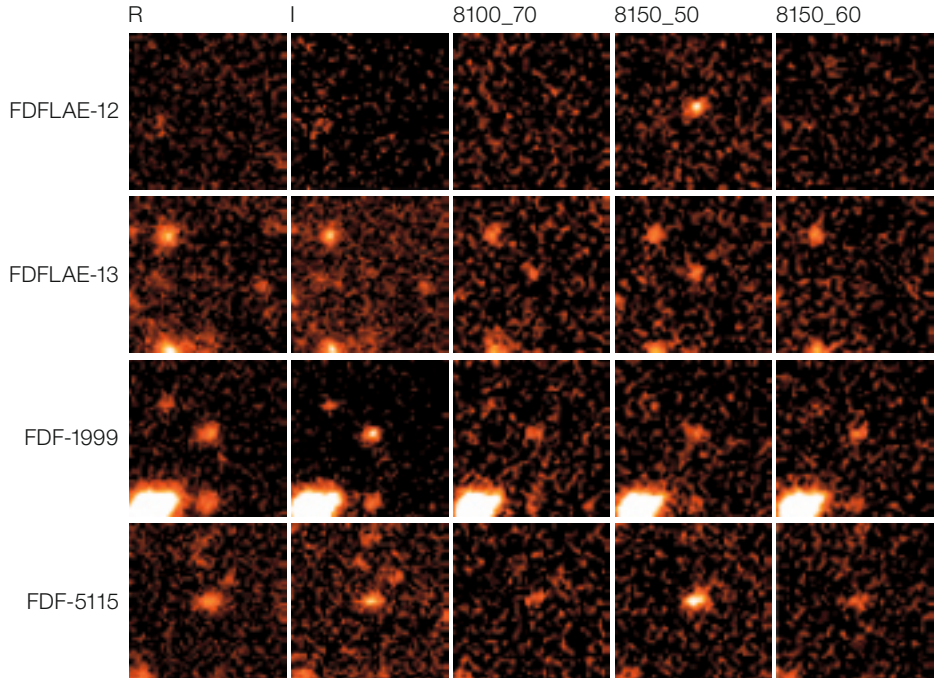


Figure 6: Spectrum of the OH airglow near the 815 nm window. Overplotted are the transmission curves of the special FORS2 narrowband filter set for detecting Ly $\alpha$  galaxies at redshifts  $\approx 5.7$ .

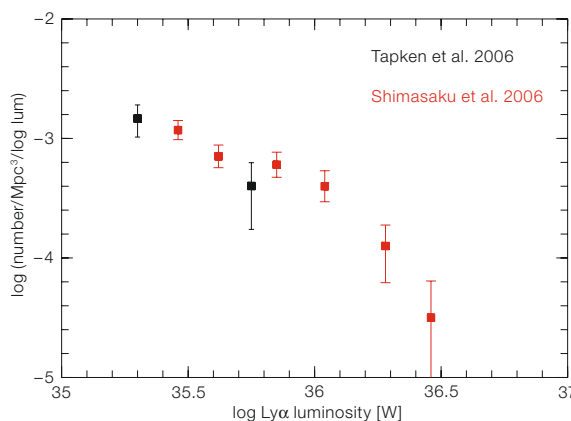


Figure 7: The luminosity function of Ly $\alpha$  galaxies at  $z = 5.7$ .



Atacama landscape  
view near the  
ALMA Site Museum at  
3 200 m.

Photo: H. H. Heyer, ESO

## Nature Around the ALMA Site – Part 2

Michel Grenon  
(Geneva Observatory, Switzerland)

The natural environment around the ALMA site, its flora, fauna and landscape morphology, are presented and interpreted in terms of combined geological and climatic evolution with, in parallel, the necessary biological adaptations. This part covers vegetation and animal life.

### The vegetation belts

The vegetation belts contain plant associations adapted to a given range of atmospheric parameters, soil composition and texture. A recent phytosociological survey by Richter (2003) provides vegetation transects in the ALMA area, namely at Sairecabur, Toco Toco and Miñiques (Figure 1). On the western slopes of Toco Toco, all belts are present, because the rocks are old enough to have been altered into sand and clay, and hence are able to retain water.

At the lowest level, 2900–3350 m, the limiting factors are the scarcity of precipitation, the high evapotranspiration and the salt and nitrate content in the soil. *Atriplex* communities – tall greyish bushes – develop on the shore of the Atacama Salar in salt rich soils. On undisturbed rocky places, the cactus *Maihueniopsis camachoii* forms colonies of spiny pillows (Figure 2), among several other plants. In wind shadow places, the tall cactus *Trichocereus atacamensis*, an invader from Argentina, grows.

At higher altitudes, evapotranspiration becomes the dominant factor. The efficiency of the evaporation increases with the square of the wind velocity. Low humidity and high wind velocity favour high rates of water loss by the plant epiderm. Several techniques are developed by plants to reduce these losses.

In the second vegetation zone, 3350–3850 m, is found *Fabiana bryoides*, with leaves reduced to minute rosettes, forming a compact cover on the stem, mimicking coral branches (Figure 3). In the same zone, *Fabiana denudata* represents an extreme case: its leaves are

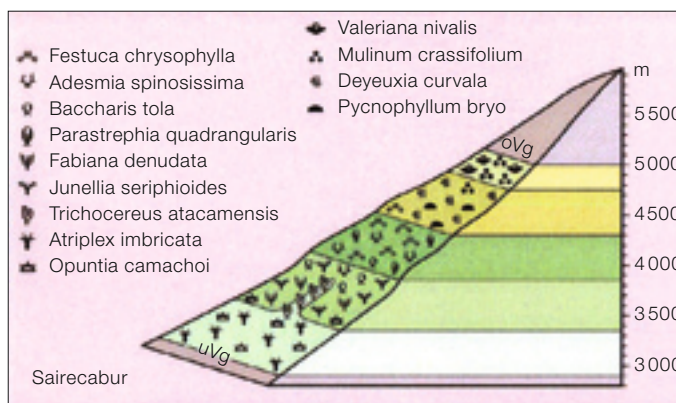


Figure 1: The vegetation belts as described by Richter (2003) on the slopes of Sairecabur volcano, NW of ALMA, with indication of characteristic plants.



Figure 2: The *Maihueniopsis* pillows show the effect of the katabatic winds. The side exposed to the cold flow is redder, an indication of a higher content in anthocyanine, a molecule acting as anti-freeze.



Figure 3: Thanks to the reduction of the leaf size, *Fabiana bryoides* resists desiccating winds and may grow up to 4900 m.

suppressed and photosynthesis takes place at the upper stem surface. The whole plant is varnished with a viscous resin. In other plants, such as some *Senecios*, the water losses are minimised through the development of a white tomentum of dense crispy hairs, reflecting the solar radiation and setting the wind velocity to zero at the epiderm surface.

In the zone 3850–4300 m, the vegetation becomes scarce and the graminaceae herbs are dominant. The golden *Festuca chrysophylla* gives the landscape its colour and specific character (Figure 4). Behind the tufts of *Festuca*, in the wind shadow, several plant species may develop. *Parastrephia quadrangularis* is another typical plant with leaves reduced

to scales, covering the stem as tiles. The association of *Festuca*, *Parastrephia* and *Baccharis* provides the preferred pasture of *guanacos* and *vicuñas* (Figure 5).

The high-altitude vegetation

In the zone 4 350 m to 4 850–5 150 m, the wind intensity, the eolian erosion and the temperature are the limiting factors for vegetation. On flat surfaces, plants have to minimise their cross section with respect to the thermal and zonal winds. To expand horizontally is a frequently encountered adaptation, e.g. by *Pycnophyllum bryoides* (Figure 6) and by the *Calyceras* genus (Figure 7). This strategy is also adopted by some dwarf trees as *Adesmia* sp., which develops an underground stem and branch systems extending well below the surface. Leaves are covered with hygrosopic glanduliferous hairs able to absorb directly the humidity from the air.

In rocky places, plants may develop provided the soil is evolved. Fresh lava or lapilli cannot retain water close to the surface and several centuries of weathering are needed before the first plant colony may settle. On older substrates, such as at Toco Toco, plants use rock cracks, at wind shadow, to expand their roots in clay, searching for residual humidity. *Nototriche holosericea* and *Chaetanthera revoluta* (Figure 9), and *Oxalis* sp. (Figure 10), are typical examples of this behaviour.

In small valleys oriented NS, perpendicular to the afternoon and zonal winds, the soil and plant evaporation is noticeably reduced. Snow may accumulate during winter and stay until the next blossoming season. Plant communities requiring less protection against evapotranspiration may develop up to very high altitudes, as the *Werneria-Senecio* association, consisting of a dozen different species. Around ALMA, this association is characterised by the presence of *Werneria poposa* and *Valeriana nivalis* (Figure 11). In these sites, the limiting factor is the temperature, which reduces the duration of the vegetation period to nearly zero above 4 850–4 900 m.



Figure 4: *Festuca chrysophylla* forms large populations giving a golden aspect to the landscape at altitudes where most bushes, except *Parastrephia*, have disappeared.



Figure 5: *Vicuñas* in the altoandine steppe near Maricunga Salar, 3 800 m.

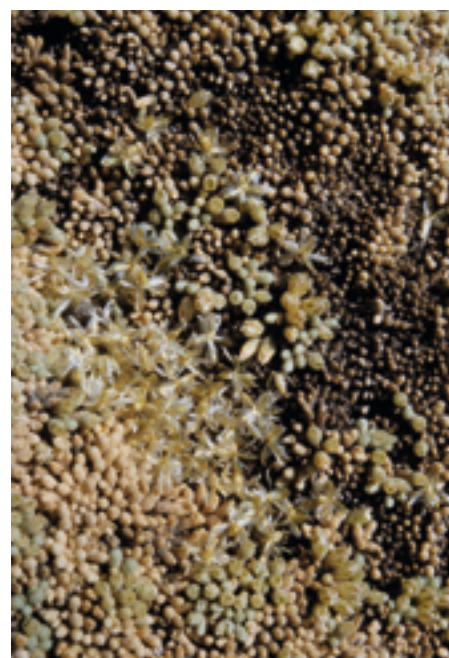


Figure 6 (below): *Pycnophyllum bryoides* expands as rings on flat gravel surfaces (left). Leaves are reduced to ovoid cones (right), petals are translucent, and so the plant offers a minimum surface to desiccating winds.



Figure 7 (above): In *Calyceras* genus, the hemispherical head of green flowers is the only part emerging above ground level (Laguna Miscanti, 4000 m).

Figure 9 (below): In *Nototriche holosericea* (left) leaves are undulated and cerebriform; the surface available for gas exchanges exposed to the wind is manyfold. A white indumentum protects the leaf from transpiration and UV radiation. *Chaetanthera revoluta* flowers (right) open on top of 1 cm long cones, covered by hairy leaves (Llano de Pajonales, 4410 m).



Figure 8: This *Adesmia* sp. is an underground dwarf tree. Strong spines prevent grazing by *viscachas* or *vicuñas* (Toco Toco, 4500 m).



Figure 10: This *Oxalis* sp. expands along narrow cracks, in sunny places, at Toco Toco, 4400 m.

Figure 11: *Werneria poposa* (left) grows in wet and wind-shadow rocky places, close to *Valeriana nivalis* (right), a rather common plant reaching the upper limit of the vegetation; its thick root is strongly aromatic, reminiscent of the Celtic Nard (N of Toco Toco, 4520 m).



Figure 13: *Calceolaria stellariifolia* is a rare plant found between 4000 and 4300 m around ALMA. Its geographical distribution shows a typical area disjunction consequent on the postglacial climate warming.



Figure 12: Four representative plants at the vegetation limit in humid places at Cerro Toco Toco. Top left: *Calandrinia* sp.; top right: *Menonvillea* sp. (4820 m); lower left: *Perezia atacamensis* (4700 m); lower right: *Werneria pinnatifida* (4700 m).

A notable character of the high-altitude flowers is the restriction of their colour range. They look unattractive to the human eye: blue, orange, red colours are no longer present. Most flowers are white, yellowish or at best bright yellow (Figure 12). With a very low ground coverage, plants appear to rely more on petal UV-reflectivity, (increasing the contrast between the flowers and the

ground), than on bright colours, in order to attract hymenopter pollinators whose eyes, or ocelli, are sensitive down to UV-B radiation.

The present geographical distribution of high Andes plants reflects the restriction of areas consequent on the climate warming after the Ice Age. Intermediate altitude plant communities had to move up by about 1 km, migrating towards the altiplano on gentle slopes east of the Atacama Desert core, or towards the top of isolated mountain ranges. Those already growing on the altiplano during the Ice Age are found presently on isolated peaks, close to the upper vegeta-

tion limit. As a result, the areas occupied by high Andian plants are now disjunct. An example of severe area restriction is that of *Calceolaria stellariifolia* (Figure 13), found in only half a dozen sites, spread over 1500 km in the high Andes. When isolated, plants may follow divergent genetic evolution, they have no chance to merge their genes again before the next glaciation.

Plants reaching the maximum altitude around ALMA belong to the *Senecio* genus. *Senecio Puchii* is frequently seen up to 4750 m. *Senecio aff. algens* (Figure 14), replaces it at higher altitude, in sunny places between 4850 and 5150 m.

### Hot springs and high altitude vegas

Wet biotopes are due either to hot springs in hydrothermal fields as at El Tatio, or to the development of high altitude vegas, the southern counterpart of peat bog in the Northern Hemisphere. In the Andes, the bog is made up of a very compact plant interlacing, where the Juncaceae *Oxychloe andina* plays a central role (Figure 15). Water pools are resting places for many birds, including the large andine goose, as well as for migrating birds, transporting seeds from one vega to the next. The vega vegetation is hence very uniform along the Andes. Hot springs host highly specialised life forms, adapted both to high soil temperature and high mineral content, such as *Frankenia triandra* (Figure 16), widespread over 1200 km in the Central Andes.

### Many more adaptations

Not only plants, but also wildlife, show surprising adaptations to the extreme arid and cold conditions prevailing in North East Chile. As an example, a group of reptiles from the Iguanidae family, the genus *Liolaemus*, has evolved in parallel to plants, into an incredible number of species and varieties, able to colonise nearly all biotopes from the margin of the absolute desert up to the upper vegetation limit. As insects are often uncommon, they had to become omnivorous, some totally vegetarian. At high altitude, they are adapted to absorb the solar radiation, and hence able to move even if the external temperature is well below 0°C. The specimen shown in Figure 17 is an extreme case of this kind of adaptation.

### ... and final remarks

After this quick overview of the ALMA site natural history and climate, and of some of the adaptations imposed on life – at the cost of massive extinction – we may appreciate even more the apparent paradox that scientists had to put the ALMA complex at the upper limit for evolved terrestrial life, to be in a good position to search for molecules in space, progenitors of terrestrial and extraterrestrial life. We may simply regret that, thanks to ser-



Figure 15: High andine vegas are formed of compact material, strong enough to resist the weight of vicuñas or even llamas (Chungara, 4500 m).

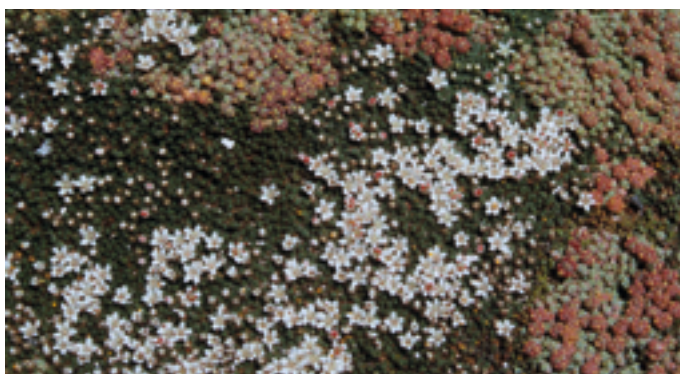


Figure 16: *Frankenia triandra* grows on warm bumps in the immediate vicinity of hot springs (El Tatio geyser, 4350 m).



Figure 17: This *Liolaemus* sp. lizard is perfectly mimetic with the rocky environment. Able to absorb the solar radiation, it may start hunting in the early morning when the air temperature is still -25°C (Laguna Verde, East of Copiapo, 4500 m).

vice observations, very few observers will have the opportunity to visit and enjoy the unique natural surroundings of Chajnantor, even if *Homo sapiens* is still not yet perfectly tuned to activities above 5000 m. A more serious concern is the expected final extinction of a large fraction of the high-altitude species as a result of the global warming during the XXIst century. A local warming by about +3.5°C would increase the vegetation belts altitude by 500 to 600 m.

All meteorological, climatic and biological indicators converge to qualify the Chajnantor site as the best possible for milli-

metre and submillimetre astronomy by the end of the XXth century. Whether its exceptional qualities will be preserved through the XXIst century, depends on the amplitude of the climate change and the evolution of precipitation patterns in the area. Most Global Circulation Models (GCM) predict an aridification of the Atacama area, but an increase of wetness and precipitation on the eastern side of the Andes.

### Reference

Richter M. 2003, *Lyonia* 4(1), 1

# Using the $h$ -index to Explore the Scientific Impact of the VLT

Uta Grothkopf, Claudio Melo,  
Christopher Erdmann, Andreas Kaufer,  
Bruno Leibundgut (all ESO)

The productivity and scientific impact of observatories and individual instruments are one measure of their success. This article presents the results of a study where we have applied the  $h$ -index, previously proposed for individual researchers, to major ground-based observatories (VLT, Keck, Gemini, Subaru) as well as individual VLT instruments. The concept is expanded by exploring the time-dependence of the  $h$ -index  $h(t)$ . Overall, the VLT appears to be among the most successful 8-m-class telescopes. We also show that ESO instruments are making important contributions to progress in astronomy.

## Introduction

In order to examine their return on investment, major observatories around the world have developed metrics to trace their scientific output. Such metrics often focus on the observatories' productivity and impact in the scientific community. These two factors are typically measured through the number of scientific publications based on astronomical data and the citations these publications generate, respectively. The methodologies used to compile the ESO Telescope Bibliography, a database that lists all papers based on ESO data, as well as publication and citation statistics derived from this database have been documented in Leibundgut, Grothkopf and Treumann (2003) and Grothkopf et al. (2005). The Telescope Bibliography is publicly available via the web (<http://www.eso.org/libraries/telbib.html>) as well as through the "Select References In: ESO/Telescopes" filter at the ADS (see Delmotte et al. 2005 for more details).

In a recent paper, Hirsch (2005) proposed a new index to measure research output, the so-called  $h$ -index. While originally meant to analyse the productivity of individual researchers, we recently introduced it into telescope statistics (Grothkopf and Stevens-Rayburn 2007). Based on  $h$ , we developed  $h(t)$  which reflects changes of the  $h$ -index in the course of

time. In this paper, we apply  $h$  and  $h(t)$  to selected observatories as well as to the VLT instruments.

There are several caveats to bibliometric studies, in particular when used for comparison across various institutes. Despite attempts to synchronise the methods applied to compile science bibliographies, criteria for paper selection are still defined by the individual observatories and are therefore not identical. Similarly, methodologies for building telescope bibliographies vary (for instance, retrieval of relevant publications through database (ADS) searches alone, through screening of paper journals, etc.). Even more importantly, comparing telescope statistics is problematic because of the different features and ways of operation of ground-based and space-based telescopes, different apertures and numbers of instruments, different wavelengths of observations, etc. Any comparison has therefore to be interpreted with utmost care in order to avoid unbalanced or wrong conclusions.

## Use of bibliometrics by observatories

In preparation for a presentation given at the IAU General Assembly in Prague, Czech Republic in August 2006, we conducted a survey among large observatories to better understand what kind of telescope statistics are compiled at observatories, at which intervals, and by whom.<sup>1</sup> All respondents regularly gather total and/or average numbers of their refereed publications, the majority also monitor unrefereed publications (e.g. conference proceedings), either regularly or on request. Citation statistics of refereed publications are collected by all respondents, even though only half of them does so on a regular basis, the remaining 50% only on request.

As can be expected, observatories compile statistics tailored to their individual needs, for instance number of publications and citations per instrument, pro-

<sup>1</sup> The following observatories responded to our questionnaire (<http://www.eso.org/libraries/telstats-questionnaire.html>): CFHT, Chandra, Gemini, HST, Isaac Newton Group, Keck, NRAO, Subaru, XMM Newton. For more information, contact Uta Grothkopf at [esolib@eso.org](mailto:esolib@eso.org).

gramme type, observing cycle, observing mode, etc. In addition, almost all respondents investigate their high-impact papers ("most productive instrument, programme, individual authors", etc.) A study of highly cited papers and their distribution among facilities is carried out every year in April at the Space Telescope Science Institute (Madrid and Macchetto 2007).

All methodologies used by observatories have some advantages and some disadvantages: counting publications measures the productivity of facilities, but does not indicate whether or not these publications actually have any influence on the advancement of astronomy. Looking at the numbers of citations does indicate the impact among the astronomical community, but values can easily be inflated by a few extremely highly cited papers. Investigating so-called high-impact papers and their distribution across observatories is less biased, but retrieving such statistics is by far not as straightforward as mere publication and citation counting.

Several in-depth studies have been carried out by Trimble et al. who investigated productivity and impact of optical, space-based, and radio telescopes, respectively (Trimble, Zaich and Bosler, 2005, 2006; Trimble and Zaich 2006). The authors analyse papers, citations and impact factors of articles from 18 journals regarding their distribution among facilities, thus avoiding the bias that typically can be noted in studies from individual observatories.

## The $h$ -index

In order to overcome some of these disadvantages, J. E. Hirsch of the University of California at San Diego suggested a new and surprisingly simple measure which he called the  $h$ -index (Hirsch 2005). While the  $h$ -index originally was meant to be a measure for the research output of individual scientists, we extend it here to observatory publication statistics. In order to determine this value, one needs a list of all relevant papers, ranked by decreasing citation counts;  $h$  can then be found where the citation count is at least as high as the rank. Thus,

the  $h$ -index combines measure of productivity (number of publications) and impact (average number of citations per paper) and is therefore more balanced than most other measures used for bibliometric studies (Figure 1).

Instead of measuring the research output of individual researchers, the concept can also be applied to entire observatories or specific observing facilities – always bearing in mind the caveats described above. In a recent paper, we introduced the  $h$ -index into telescope statistics by computing it for selected publication years of some major observatories (Grothkopf and Stevens-Rayburn 2007).

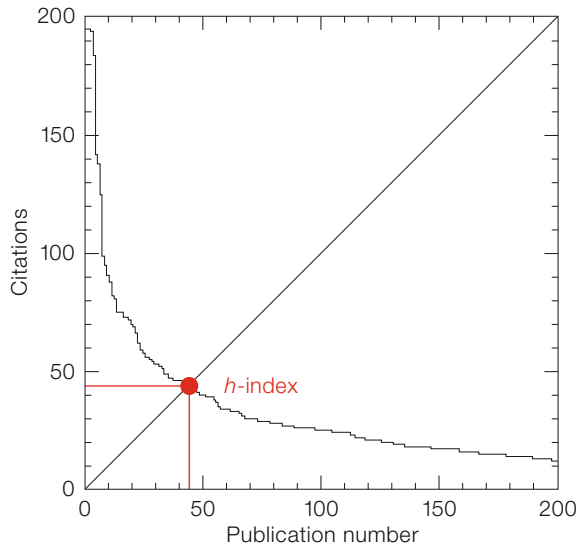


**Figure 1:** The  $h$ -index can be found where the counted publication number equals the number of citations. Neither a large number of publications with low citation rates (right edge of the x-axis) nor individual papers with extraordinarily high numbers of citations (upper edge of the y-axis) will alter  $h$ , therefore this value is more balanced than many other bibliometric measures.

### The $m$ -parameter

It must be noted that, tempting as it may be, comparing  $h$  alone among observatories (or researchers) does not lead to a meaningful result. Facilities that have been operative for many years obviously had much more time to produce publications and accumulate citations, hence their  $h$ -index can be expected to be considerably higher than that of younger facilities. Hirsch therefore introduced the so-called  $m$ -parameter. For individual researchers, this value is computed by dividing  $h$  by the numbers of years since publication of the first paper. Correspondingly, when applied to observatories,  $h$  is divided by the number of years of operation; hence it reflects the various ‘life-times’ of facilities.

### Applying $h$ and $m$ to observatories

We present here  $h$  and  $m$  values for the VLT, Keck, Gemini and Subaru observatories. In order to compute  $h$ , we obtained bibcodes of all papers pertaining to the observatories’ publication lists in the following way: for the VLT, bibcodes are stored in the ESO Telescope Bibliography (<http://www.eso.org/libraries/telbib.html>). References of Keck and Subaru papers were retrieved from the web (Keck Science Bibliography at [http://www2.keck.hawaii.edu/library/keck\\_papers.html](http://www2.keck.hawaii.edu/library/keck_papers.html) and Publishing Results from Subaru, <http://www.naoj.org/Observing/Proposals/Publish/index.html>) and were

Observatory	Range of years of publications	Years since first publication	$h$	$m$
VLT	1999–2006	8	79	9.9
Keck	1996–2005	11	113	10.3
Gemini	2000–2006	7	33	4.7
Subaru	2000–2006	7	41	5.9

**Table 1:** Range of years of publications, number of years since first publication, as well as  $h$  and  $m$  of the observatories included in our study.

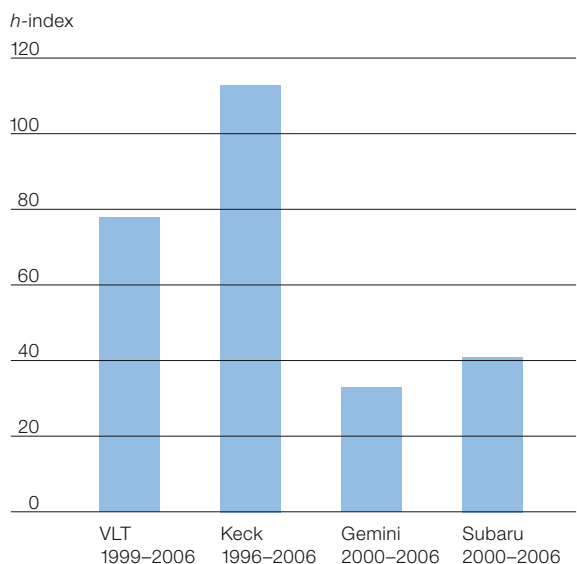


**Figure 2:**  $h$ -index for the VLT, Keck, Gemini, and Subaru observatories as of April 2007. Note that  $h$  correlates with the number of years of operation. Hence, older observatories tend to have higher  $h$  indices.

translated into bibcodes. Papers using Gemini data were found using the “Select References In” filter on the ADS main search screen. These bibliographies include only refereed papers. The respective ranges of publication years are shown in Table 1. For uniformity, we end the range of publication years for all ob-

servatories in 2006. Citation counts for all publications were obtained from the ADS as of April 2007.

For each observatory, citation counts were then ranked in descending order, and  $h$  was computed. Figure 2 shows the  $h$ -indices of the respective observatories.

We also computed the *m*-parameter by dividing *h* by the specific number of years since the first publication (see Table 1). Resulting values are given in Figure 3. This brings the VLT and Keck to the top of the list, and also the young facilities Gemini and Subaru perform well.

One should note that both *h* and *m* depend on the number of telescopes per facility. A facility like the VLT with four telescopes will produce more papers more quickly and hence the *h*-index will increase faster, although it is not obvious exactly how much of an effect this is. For a facility like the VLT, with telescopes becoming operational over some time, it will be difficult to quantify this effect in detail.

The *h*-index versus time

Although the *m*-parameter reflects the total number of years of operation of a facility, both *h* and *m* are integrated values that don't show how these values were achieved in the course of time. We have therefore further developed the *h*-index to analyse its evolution, *h*(*t*).

To compute *h*(*t*), we obtained the citation history for each paper included in our study from the ADS. The citation history shows how many citations a paper generated in a given year. For instance, a paper published in 2002 will generate *x* citations in 2002, *y* citations in 2003, *z* citations in 2004, etc. In order to calculate *h* for a year *Y*, we add up all citations up to the year *Y*, using the citation history of each paper. The papers are then listed in decreasing order, and the *h*-index for that year *Y* is computed.

Figure 4 shows *h* over time applied to the observatories in our study. Trends indicated by *h* and *m* are confirmed. Keck has always been performing extremely well, with a steeply increasing *h*-index right from the start. The VLT started well and has even improved during recent years. Both Subaru and Gemini are now on their way up after a slightly slower start.

In this study, all observatories are treated as entities. This does not accurately reflect their early years. Keck I and II,

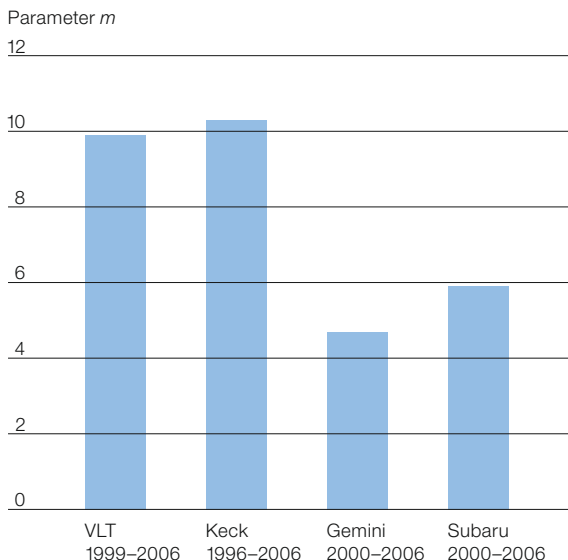


Figure 3: Parameter *m* of the observatories included in this study (as of April 2007).

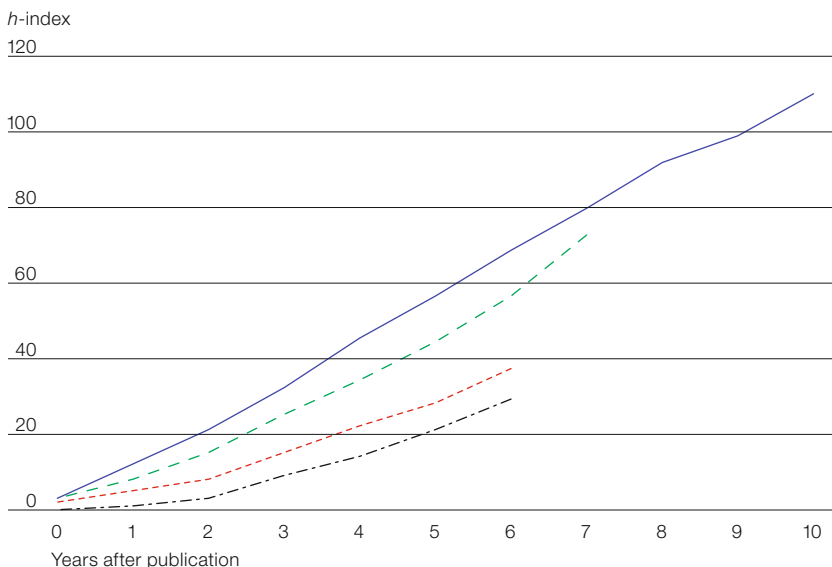


Figure 4: *h*(*t*) of Keck, VLT, Subaru and Gemini by years after first publication (as of April 2007).

— Keck    - - - Subaru  
 - - - VLT    - · - · Gemini

Gemini North and South as well as VLT UT1, 2, 3, and 4 all came online sequentially, increasing the available observing time over the years. A future study may investigate *h*(*t*) based on the actual observing time of each observatory.

Performance of the VLT instruments

In order to investigate the specific performance of the VLT instruments, we applied *h*, *m*, and *h*(*t*) to them. We restrict this analysis to the VLT because instrument-level information for La Silla papers has been systematically recorded only

starting in 2002. The results are presented in Table 2. Although the absolute number of papers and citations differ, the very first instruments of the VLT (FORS1, ISAAC, UVES, FORS2) have a comparable performance. As mentioned above, the number of years in operation is an important factor. Young instruments necessarily have a lower  $h$ -index. This can be partially compensated for by normalising the  $h$ -index by comparing parameter  $m$ .

As done for the observatories, a better glimpse of how the instruments are performing can be achieved by measuring the  $h$ -index versus time. The results of  $h(t)$  as of April 2007 for VLT instruments are shown in Figure 5 relative to the year of the first paper of each instrument. In this graph, we included only VLT instruments that have been operative for two or more years and produced at least ten papers.

An obvious result is that the first-generation VLT instruments (FORS1, UVES, ISAAC, FORS2) are alive and kicking with no sign of changing their slopes. They clearly set a very high standard for future instruments.

With respect to the young instruments, we can say that they are ... young! Their  $h$ -indices are growing at a slow pace. Besides this slow increase of the  $h$ -index for the young instruments, can we predict whether they will look like their older siblings in future?

We see from Figure 5 that most of the young instruments have a much harder time to take off than FORS1 and UVES, but they are not particularly different from the  $h(t)$  curves of FORS2 and ISAAC. But what is behind the plot shown in Figure 5? Does the  $h(t)$  have a practical use in judging instrument performance? Can it help observatories to decide whether a given instrument needs to be upgraded, improved or even decommissioned? The answer is not simple and the reader should take Figure 5 with caution.

As defined above, the  $h$ -index depends on the number of papers and their citation counts. These two quantities are certainly instrument-dependent. For example, detector sensitivity, spectral or spatial resolution, wavelength coverage,

Instrument	$h$ -index	Years since first publication	$m$	Number of papers	Total number of citations	Ratio
<b>VLT</b>						
FORS1	56	8	7.0	525	14 267	27.2
ISAAC	49	8	6.1	413	9 308	22.5
UVES	48	7	6.9	474	9 326	19.7
FORS2	46	7	6.6	342	9 006	26.3
NACO	22	5	4.4	111	1 942	17.5
FLAMES	14	4	3.5	67	877	13.1
VIMOS	14	3	4.7	44	623	14.2
<b>VLTI</b>						
VINCI <sup>2</sup>	14	5	2.8	38	572	15.1
MIDI	7	3	2.3	19	226	11.9

**Table 2:** Performance of VLT and VLTI instruments that have been operative for two or more years and produced at least ten papers.

<sup>2</sup> Note that VINCI was offered to the community only from October 2002 to October 2003.

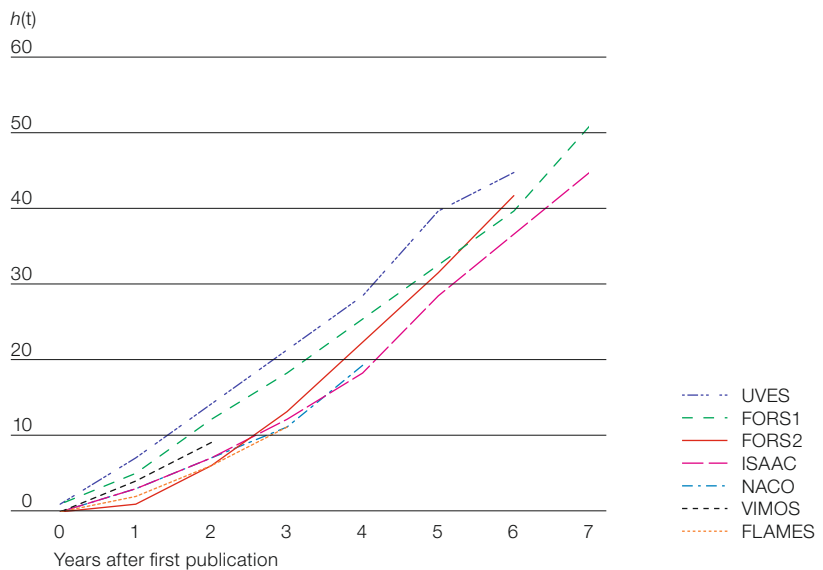


**Figure 5:**  $h(t)$  of selected VLT instruments by years after first publication (as of April 2007).

quality of the documentation and data-reduction software (pipelines). These are all factors that play a role in the way  $h(t)$  evolves.

The intrinsic nature of the instrument itself has an influence on its  $h(t)$ . All instruments have a difficult start with a low

$h$ . As time goes by the community gets used to the modes, pipeline, etc. At this time the number of papers and citations increases fast, and so does the  $h$ . Years later, all possible (hot) applications start to run out and the papers gather fewer citations. New (and hopefully better) instruments come. At this point the  $h$ -index

keeps growing, but at a much slower pace. Thus the  $h(t)$  would have a curve-of-growth shape (similar to those found in chemical abundances studies).

In the case of instruments designed for individual observations, papers can be based on a few observations and the full cycle (from proposal submission to paper acceptance) can be as short as one year. In contrast, papers presenting results based on a large amount of data collected by survey-like instruments (e.g., VIMOS and FLAMES) can take years to be released. But when these papers are finally published, the impact can be immense.

Another bias hidden behind the computation of  $h(t)$  has to do with the complexity of the new instruments, which in some cases are aimed at tackling problems that require the use of cutting-edge technology. Using a complex (new) technology usually implies large overheads. This is the case of AO instruments and even more pronounced in the VLT observations whose complexity is of a higher degree than that of any other VLT instrument.

However, the  $h(t)$  can also be influenced by circumstances not related to the instrument at all. For instance, there is no question that one of the strengths of the first suite of VLT instruments (FORs1, UVES, ISAAC and FORs2) is its versatility, being used from Solar System to cosmological applications. In addition to this versatility, these instruments were favoured by the fact that they were the only ones available to the community during the first years of operation of the VLT. Moreover, they were mounted almost exclusively on each of the UTs. Nowadays, the situation is very different. New instruments have to compete for UT time. For instance, on Kueyen UT2, the time is shared between UVES, FORs1 and FLAMES. Therefore, in order to be fair, the  $h(t)$  curve shown in Figure 5 has to be corrected by the effective fraction of time used by each instrument.

The bottom line is that we should take the results presented in Figure 5 with caution since none of the potential biases discussed above were taken into account and therefore the results presented here are very preliminary. Having said that, it might be interesting to peruse the effort of using the  $h$ -index to measure instrument impact and performance in a deeper and more thoughtful study where all biases are considered.

### Conclusions

The  $h$ -index is a simple, yet powerful indicator that has some important advantages compared to other bibliometric methods:

- it combines productivity and impact;
- it can be relatively easily determined using the ADS;
- it is neither affected by a large number of publications with few or no citations (which usually suggests high productivity, but not necessarily high impact) nor by extraordinarily high citations of only a few papers (which inflates citation counts).

The  $h$ -index is therefore more balanced than other measures if one bears in mind the usual caveats intrinsic to bibliometric comparisons. It is important to note that  $h$  depends on the number of years of operation and therefore needs to be combined with the  $m$ -parameter in order to avoid biased interpretations.

Hirsch (2005) points out that the  $h$ -index is prone to depend on the field of study (Physics, Biology, etc.). This is true even within astronomy. For instance, astronomers in the gamma-ray burst community have higher  $h$ -indices than their colleagues in other areas, partly because of the importance of the field, but also because of the size of the collaborations and the rate of publications.

If this effect is present with regard to instruments, it may indicate that a given instrument is flexible enough to produce papers in a wide range of astronomical fields. The numbers in Table 2 show that the first-generation VLT instruments have similar  $h$ -indices. They constitute an example of such versatility, since they are used for observations ranging from the Solar System to cosmological applications. However, other biases influencing  $h(t)$  need to be carefully corrected before a detailed comparison is made. In this sense, our results concerning the  $h$ -index for instruments are regarded as preliminary.

### Acknowledgements

This research has made extensive use of NASA's Astrophysics Data System Bibliographic Services.

### References

- Delmotte N. et al. 2005, *The Messenger* 119, 50  
 Grothkopf U. et al. 2005, *The Messenger* 119, 45  
 Grothkopf U. and Stevens-Rayburn S. 2007, in "Library and Information Services in Astronomy V", eds. S. Ricketts, C. Birdie and E. Isaksson, ASP Conference Series, astro-ph/0610274  
 Hirsch J. E. 2005, *Proc. Nat. Acad. Sci.* 102, 16569  
 Leibundgut B., Grothkopf U. and Treumann A. 2003, *The Messenger* 114, 46  
 Madrid J. P. and Macchetto F. D. 2007, in "Library and Information Services in Astronomy V", eds. S. Ricketts, C. Birdie and E. Isaksson, ASP Conference Series  
 Trimble V., Zaich P. and Bosler T. 2005, *PASP* 117, 111  
 Trimble V., Zaich P. and Bosler T. 2006, *PASP* 118, 651  
 Trimble V. and Zaich P. 2006, *PASP* 118, 933

# Status of Women at ESO: a Pilot Study on ESO Staff Gender Distribution

Francesca Primas (ESO)

Equal career opportunities require working conditions that make it possible to reconcile family needs and career development. This article describes the goals and main findings of a pilot investigation that has recently been carried out at ESO focusing on gender balance issues.

Over the past decades, several studies in Europe (e.g. within the FP5-FP6 programmes) and the United States have considered gender distribution, and in particular the status of women, in different sciences. Gender equality and dual careers are just two of the many aspects that have been closely scrutinised. In astronomy, the Baltimore Charter and the Pasadena Recommendations are among the main outcomes of these investigations and provide guidelines on how the situation of women in astronomy could be improved. Further, several working groups have been established by international scientific bodies. With ESO as a multi-cultural research organisation, it became clear that a similar, systematic study of its current gender distribution was an important goal to achieve. This article presents the first results of such a study.

## The project and its goals

The “Status of Women at ESO” is a project that, as a start, aimed at evaluating the current gender distribution at ESO, thus providing a snapshot of the status of women at ESO. This task necessitated a systematic and impartial breakdown of the ESO organisational structure in terms of female *versus* male personnel members by division and rank over a given time period. The team was chaired by Francesca Primas and included Roland Block, Mark Casali, Nathalie Kastelyn, Rubina Kotak and Bruno Leibundgut. We focused on the period 1999–2006, which has witnessed a significant expansion in the number of staff members owing to the start of VLT operations, and on the following groups:

a) ESO International Staff Members and Paid Associates by division and by rank;

- b) ESO Faculty members, Fellows and Students;
- c) ESO Governing Bodies and Committees: Council, Observing Programmes Committee, Scientific and Technical Committee, Users Committee, Finance Committee;
- d) ESO Visitors;
- e) invited speakers at ESO Lunch Talks and the Munich Joint Astronomy Colloquia.

## The project and its outcomes

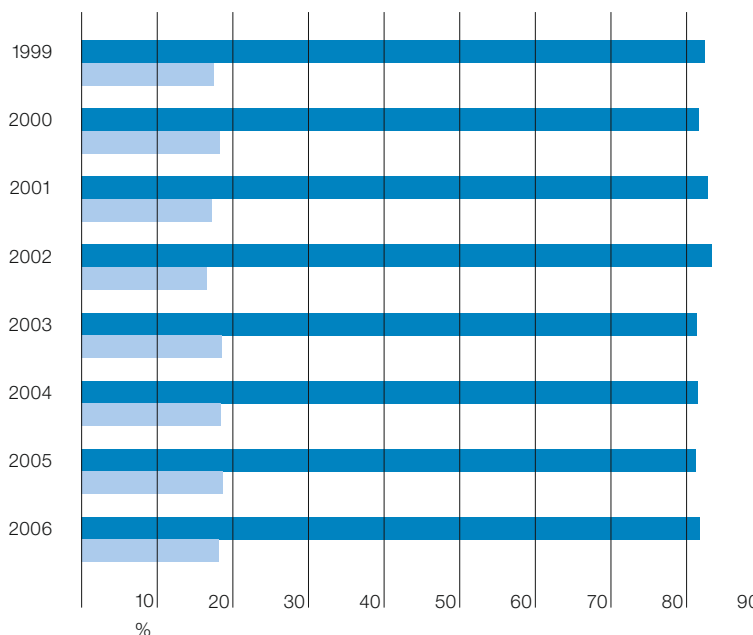
Once all the data were gathered, we compiled and analysed statistics on the distribution of female and male employees by various categories. The numbers reported here cover all international staff of ESO, i.e. at both the ESO Headquarters in Garching and ESO Chile, with the latter including the Vitacura offices and the La Silla Paranal observatory. Where appropriate, we have split the analysis for the two main ESO regions. In the following sections, we will briefly comment on the results obtained for the different categories (a–e) that were scrutinised.

a) ESO staff members

Established members of ESO personnel are identified as International Staff Members (ISM), whereas Paid Associates (PA) belong to the so-called non-established personnel. Typically about 7 to 10 PA are employed at ESO per year and these are included in the overall statistics of ESO staff.

Figure 1 displays the fraction of female ESO staff over the past eight years. During the same time the ESO staff increased from 239 ISM in 1999 to 329 ISM in 2006. This is also reflected in the recruitment statistics: ESO recruited 33 women (17.7%) compared to 153 men (82.3%) between 2000 and 2005. Although the number of women employed as ISM has increased from 44 to 59 over this period, it has clearly lagged behind the pace of male hiring. Among the women hired, nearly half (16 or 48.5%) were scientists, 12 (36.4%) were administrative staff and only 5 women (15.2%) were engineers. When the breakdown is done by ESO division, one finds that while the Office of the Director General and Administration have a nearly even gender balance, the technical divisions have, in general, a very low frac-

Figure 1: Yearly gender distribution of all ESO International Staff Members and Paid Associates (dark blue: male, light blue: female).



tion of women on their staff. The fraction of female Paid Associates is slightly higher than that of ISM; this also holds in the more technically-oriented divisions.

When the grade is taken into account, the difference becomes even more striking: during the past three years, the percentage of female staff (ISM + PA) has remained rather stable, around 50–60% for salary grades 5–7, but only around 10% for grades 8–11. This continues further into the management level (grades 12 and above) where at the moment there are only two women. Women are clearly under-represented at the higher echelons, presumably corresponding to positions with a higher scientific and technical profile. It should be noted that the current Director General and one division head are women. By total numbers, ESO has more than doubled the number of women in grades 8 to 11 (from 16 to 34), but the relative increase remains rather small (only 4%).

b) The ESO Faculty, Fellows and Students

The ESO Astronomer Charter defines the roles of astronomers and their membership in the ESO Faculty. As of 2006, there are 17 women in the Faculty (to be compared to 74 men), and their fraction has increased fairly steadily over the past decade.

However, we note that the highest fraction of female Faculty members is currently at the Assistant Astronomer level, the entry level for junior staff. The Scientist level (astronomers with reduced research time), also have a higher fraction of women, as can be seen from Figure 2. The global average, including all levels (Full, Associate, Assistant and Scientist) is 18.7% of women.

Complete statistics for ESO fellows and students are available from the year 2000 onwards for both ESO sites, including the gender distribution among the applicants and the gender distribution in the Fellowship and Studentship Selection Committees (FSSC). Table 1 shows the total number and percentages of all ESO Fellows and Students during the last seven years.

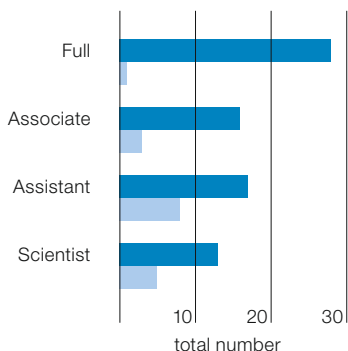


Figure 2: Gender distribution (by total number) of the three categories of ESO Faculty members, and Scientist, in the year 2006 (dark blue: male, light blue: female).

	Female	Male	Students
	Fellows		
Garching	10   34		22   29
Chile	15   36		11   17
All	25   70		33   46
Garching (%)	22.7   77.3		43.1   56.9
Chile (%)	29.4   70.6		39.3   60.7
All (%)	26.3   73.7		41.8   58.2

Table 1: Total number and percentages of ESO fellows and students (2000–2006).

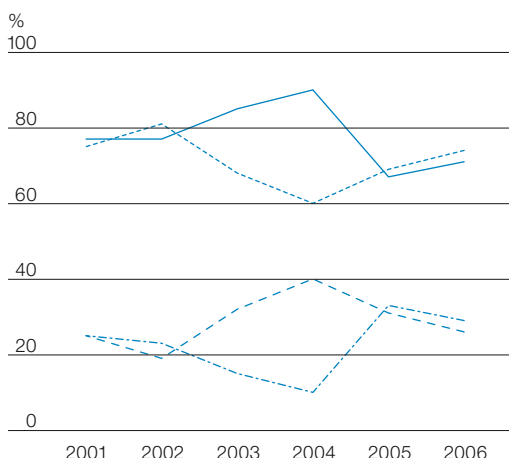


Figure 3: Yearly gender distribution among the selected ESO fellows and applicants to the ESO Fellowship, over the period 2000–2006 (for both Garching and Santiago).

The percentage of females among the selected fellows has been between 10 and 40% over the past few years. The comparison with the distribution among the applicants (Figure 3) shows that the gender balance is reasonably maintained, i.e. there is no obvious discrimination against female candidates.

However, the years 2003 and 2004 show that this is not universally true. In 2004, for instance, only one female fellow was selected out of 34 female applicants! Also, it should be noted that the fraction of female fellows is significantly higher than for female members in the Faculty. Compared to the Assistant Astronomer level in the Faculty, the gender distribution is nearly the same. However, despite the increased number of Fellowships offered in Chile for Paranal, we have observed a steady decrease in the number of female applicants over the last few

years, which has stopped only in the past year. The comparison of the gender distribution between Garching and Chile is shown in Figure 4. The fraction of female fellows has decreased dramatically in Chile – by almost a factor of two since 1999, while the distribution in Garching has been between 25 and 40% over the recorded period. Admittedly, very few applications for ESO Fellowships in Chile were received from female candidates in 2003 and 2004, nevertheless the trends show that constant vigilance is required.

The situation with the students is more positive. While there still appears to be a majority of male applicants, the selection has consistently created a more balanced distribution so that ESO has a fairly high fraction of female students (see Figure 5), which is consistently above 30% and often above 40%. The fluctuations are due to the short-term nature of student

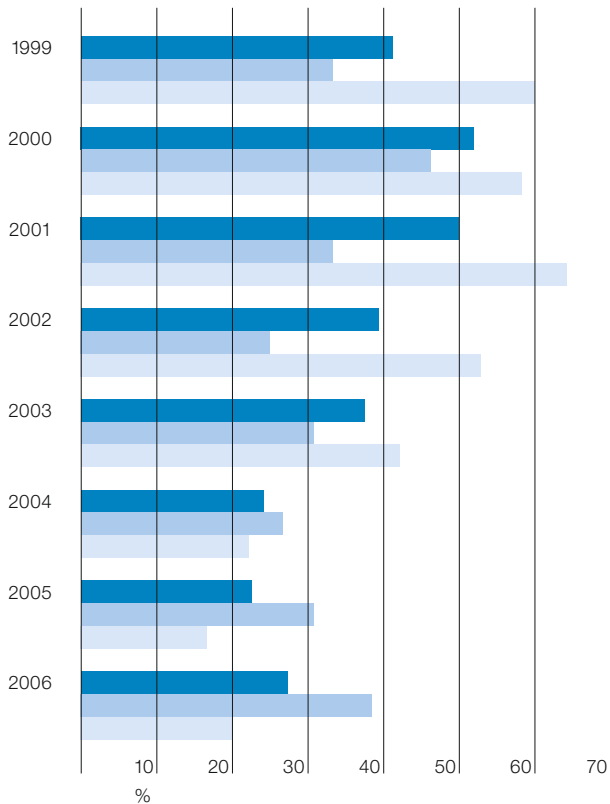


Figure 4: Percentage of female fellows in Garching, in Chile, and as a whole.

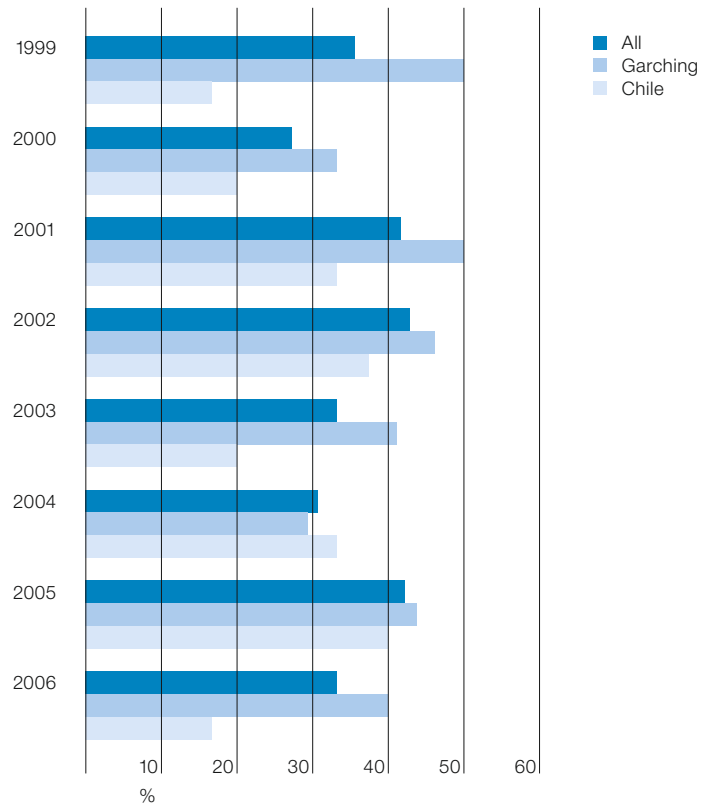


Figure 5: Percentage of female students in Garching, in Chile, and as a whole.

contracts (two years in almost all cases, with the International Max-Planck Research School (IMPRS) contracts running for three years – currently there are six such positions at ESO Garching). The distribution between Garching and Chile is fairly balanced, with the large fluctuations for Chile due to the small number of students (ten positions).

Overall, the situation with young researchers at ESO has improved over the past few years. With the exception of 2003, the ratio of female students has been consistently above 30%. The number of applications from female students is also steadily increasing.

We further investigated the composition of the selection committees for the fellows and the students. In Chile, during the past few years not a single woman has been nominated to this committee,

whereas in Garching, a realistic balance of women on the committee has been achieved. The fraction of women on this committee is higher than the average of the Faculty astronomers.

#### c) ESO Governing Bodies and External Committees

ESO has one main governing body (Council) and several specialised committees that have the task of making decisions and/or recommendations on specific matters. Since membership to these committees is selected in different ways (not only among different committees, but even among different countries for the same committee), the numbers we have gathered on this category are more complex to interpret.

We noted that the more technically-oriented committees show a very low percentage of female representatives, whereas other committees (e.g. Finance Committee and the Users Committee) have reached a very balanced gender distribution. However, every committee shows a positive trend, and the female representation is increasing, though at a slow pace.

#### d) ESO Visitors

The ESO Scientific Visitor Programme aims to promote the scientific interaction between ESO and its community and to enhance ESO's role as an astronomical centre of excellence. The programme is under the responsibility of the Head of the Office for Science, who appoints the members of the two Visitor Selection Committees (VSC, one in Garching and

one in Vitacura) and their respective chairs. Applications to the ESO Scientific Visitor Programme can be submitted by any scientist with an interest in ESO activities and/or collaboration with ESO staff members. ESO can also make formal invitations to scientists with a high scientific profile. On average, ESO Garching is able to support between four and five visitors per month.

From the data we have been able to collect, i.e. the gender distribution of the applicants, as well as of the approved and invited visitors over the past eight years (1999–2006) at ESO Garching, there is clearly no discrimination in the approval of the applications – ESO Garching is usually able to approve almost all applications. Nevertheless, we note that despite the fact that the ESO visitor programme is open to everybody, the number of female applicants represents a very small percentage; the reason for which is not easy to uncover. One possibility is that for female astronomers with family commitments, it is notoriously difficult to take leave of absence from their home institute. However, there is clearly room for improvement, especially for the targeted high-profile astronomers: here, the numbers are extremely small (only three women in the last few years), and ESO should make a special effort to attract senior women for extended visits.

We note that the composition of the VSC-Santiago at the beginning of this year included one female and seven male astronomers, which is identical to the 2006 situation of the VSC-Garching.

e) Invited speakers to Joint Astronomy Colloquia and ESO seminars

ESO is a very lively scientific environment, where many scientific talks are organised on a weekly basis, both in Garching and in Santiago. ESO-Garching has its own Lunch Talk (LT) series, organised by an appointed team of ESO-Garching staff (usually two to three members, who change every two to three years). This committee has the task of running a full schedule of weekly talks, by inviting speakers who cover a broad range of scientific activities and interests. Invitations

are also made based on suggestions provided by other ESO staff members.

Together with MPA, MPE and the LMU-Sternwarte, ESO-Garching also co-organises the Joint Astronomy Colloquia (JAC) series, also held on a weekly basis. The JAC committee includes representatives from all involved institutes. This is recognised as the main scientific colloquium of the week.

Table 2 shows that gender distribution in the Lunch Talk (LT) series is clearly more balanced than the one among JAC speakers, but there is clearly room for improvement here as well. The numbers in the table are yet another reflection of the fact that there are more junior than senior female astronomers. Considering the higher relevance of the JAC series, the very low number of female speakers is discouraging. The JAC committee is currently chaired by a woman and it will be worthwhile to monitor the selection of speakers in the coming years.

### Present and future

All the numbers collected so far and discussed in this report have been taken at face value, i.e. they represent snapshot views of the gender distribution among ESO staff and various ESO governing bodies and committees, during the last few years. No attempt has yet been made to compare these numbers to, for instance, the number of applicants and eventually short-listed candidates for any given staff position. This type of comparison was readily available for the Fellows and Students only, as discussed above. Due to this incompleteness, it is difficult to properly interpret these numbers and draw firm conclusions. In what follows, we attempt to flag the most important outcomes of this pilot project and possible future actions that ESO is considering.

1. Concerning ESO Staff, we have established that the gender distribution is not very balanced (18 % female *versus* 82 % male). The balance is far from being satisfactory, especially in the more technically-oriented divisions, where very few women are employed. It is disappointing that this distribution has remained con-

	Female   Male	JAC
	LT	
1999	3   49	1   32
2000	4   37	5   28
2001	10   29	2   29
2002	5   29	4   26
2003	11   28	1   27
2004	6   19	5   30
2005	5   23	4   33

Table 2: Gender distribution among the invited speakers to Lunch Talks (LT) and the Joint Astronomy Colloquium (JAC).

stant for the past eight years. The women employed at ESO are preferentially in lower grades with very few women in senior positions. In other words, the significant increase in the number of newly-hired staff members required by the start of VLT operations has not resulted in a corresponding increased fraction of female staff (at any level).

2. The conspicuous lack of senior female astronomers is striking. The fraction of women in the Assistant and Associate levels is encouraging, although not yet satisfactory, and it reflects the recent employment history. The Assistant Astronomer level is the entry level for Faculty astronomers at ESO and these are the junior members. It seems important to assess what support is required to have these women succeed both in their research and at ESO, as well as to increase their number further and ensure that the fraction does not decline with increasing seniority. In a few years these numbers should be critically assessed and the reasons for possible changes examined.

3. The gender distribution among the ESO Fellows and Students is in general higher than for the staff and the Faculty. The selection of the Fellows and Students does not show clear discrimination, but constant awareness in the selection process is still required. The low female selection rates in 2003 and 2004 are a warning not to neglect this issue.

4. For the Scientific Visitor Programme, it would probably be helpful to assemble a list of high-profile female scientists to become the target of official invitations to visit ESO. If no improvement is seen over a given amount of time, then one should try to understand the main reasons that

make women decline the invitations (family organisational issues, busy professional schedules, etc.).

5. For the Lunch Talks, but especially for the JAC series, a similar list of high-profile female scientists could be useful in order to significantly increase the number of female speakers. It is well known that the percentage of female invited speakers at any scientific conference remains low. The International Astronomical Union, for instance, is now checking, for each symposium they sponsor, the gender and national distribution of the scientific organising committee and of the invited speakers, requiring the organisers to propose alternative names if the gender balance is not satisfactory. ESO might want to follow a similar philosophy for its own series of symposia and workshops.

The importance of this study is that it provides a baseline for future comparison and should be used as a reference for future studies regarding the status of women at ESO. Once ALMA will have started early operations and ESO may be involved in the development of its next large facility, it may make sense to repeat this study.

Equal career opportunities require working conditions that make it possible to reconcile family needs and career development. Being an international organisation adds extra responsibility to the employer: it is usually more difficult for expatriates to fall back on childcare facilities or rely on family help in the country of employment other than the home country. ESO

has adopted, and will continue to adopt a series of measures that aim to contribute towards an effective personnel policy. Some changes to the regulations to further help women and family members working at ESO have recently been implemented (e.g. on-site daycare, more flexibility on maternity leave, as well as part-time solutions) and discussions of several more are under way with the appropriate committees.

Independently of these important improvements, and despite the fact that the current situation at ESO closely follows the numbers of the other EIROforum<sup>1</sup> institutes (CERN, ESA, ILL, EMBL, ESFR, EFDA), ESO needs to better understand why the number of female staff has not increased over the past few years. Is ESO not attractive enough for female astronomers and engineers? Are the ESO working conditions not suitable for female staff to simultaneously cope with professional career and family commitments? Constant monitoring and increasing awareness will hopefully lead to improvements.

#### Acknowledgements

The investigating team would like to warmly thank the following people for their invaluable help and

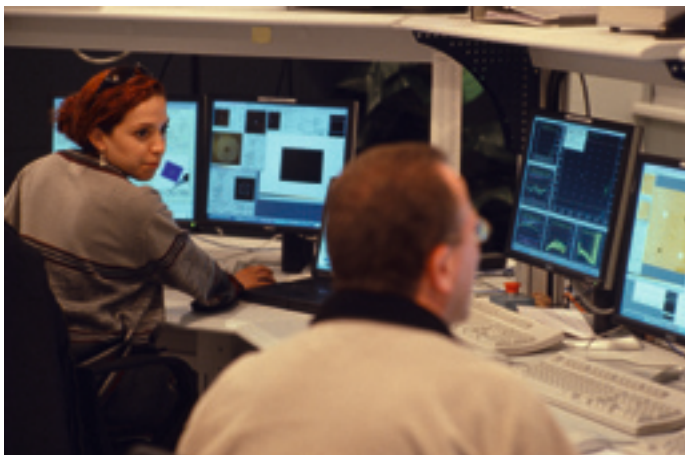
<sup>1</sup> EIROforum is a partnership of Europe's seven largest intergovernmental research organisations, which includes: the European Organization for Nuclear Research (CERN); the European Fusion Development Agreement (EFDA); the European Molecular Biology Laboratory (EMBL); the European Space Agency (ESA); the European Synchrotron Radiation Facility (ESFR); the Institute Laue Langevin (ILL); and ESO.

prompt support in gathering some of the numbers presented in this document: Francky Rombout, Christina Stoffer, Pamela Bristow, Karin Hansen, Sandro D'Odorico, Fernando Comerón, Andreas Kaufer and Markus Kissler-Patig.

#### References

The following list of publications includes recent results from studies similar to ours (some of which were mentioned in the text) as well as some suggestions for further reading. These references can be found in the form of articles or web sites. The list does not intend to be exhaustive, rather a starting point for the interested reader.

- The Baltimore Charter for Women in Astronomy (<http://www.stsci.edu/stsci/meetings/WiA/BaltoCharter.html>)
- The Pasadena Recommendations ([http://www.aas.org/~cswa/Equity\\_Now\\_Pasadena.pdf](http://www.aas.org/~cswa/Equity_Now_Pasadena.pdf))
- The European Commission reviews on Gender Equality ([http://ec.europa.eu/employment\\_social/gender\\_equality/index\\_en.html](http://ec.europa.eu/employment_social/gender_equality/index_en.html)) and their publications, including the most recent (2007) report ([http://ec.europa.eu/employment\\_social/emplweb/gender\\_equality/publications\\_en.cfm](http://ec.europa.eu/employment_social/emplweb/gender_equality/publications_en.cfm))
- A Study on the Status of Women Faculty in Science at MIT (1999 and its 2002 update) (<http://web.mit.edu/faculty/reports/pdf/sos.pdf>)
- Review of the Status of Women at STScI (2002) (<http://www.aura-astronomy.org/nv/womensReport.pdf>) and the AURA (Association of Universities for Research in Astronomy) response to the report (<http://www.aura-astronomy.org/nv/response.pdf>)
- The AIP (American Institute of Physics) Report on "Women in Physics and Astronomy, 2005" (<http://www.aip.org/statistics/trends/reports/women05.pdf>)
- The IAU (International Astronomical Union) Working Group of Women in Astronomy (<http://astronomy.swin.edu.au/IAU-WIAWG/>)
- The AAS (American Astronomical Society) Committee on the Status of Women in Astronomy (<http://www.aas.org/~cswa/>)
- The IUPAP (International Union of Pure and Applied Physics) Working Group on Women in Physics (<http://www.iupap.org/wg/wip/index.html>)



At the control station of Melipal (UT3).

Report on the International Workshop on

# Observing Planetary Systems

held at ESO, Vitacura, Chile, 5–8 March 2007

Michael Sterzik, Christophe Dumas  
(ESO)

## Motivation

Nowadays, the ESO premises in Vitacura host more than 80 PhD students, fellows and astronomers, and represent the research centre for the scientific staff deployed at the different observatory sites in Chile. Several topical working groups help locally to actively promote and foster joint research initiatives among ESO scientists. One example is the “Planetary Sciences Research Group” at ESO Chile (<http://www.sc.eso.org/santiago/science/PlanetaryGroup>), which seeks to understand the formation of planetary systems at large and the place occupied by our own Solar System. Group members are actively involved in observation-oriented programmes making use of ESO facilities to carry out front-line research ranging from discoveries of new brown dwarfs and exoplanets, to the study of primitive Solar System bodies.

Encouraged by the fruitful interdisciplinary research approach of our own group, we proposed to gather both communities of Solar System and extra-planetary system scientists and organise the international workshop “Observing Planetary Systems”. The main idea was to explore the synergy between these two communities and confront them with four key topics: *from Discs to Planets*; *Search for Planets*; *Planetary Chemistry*; *Towards other Earths*. In order to establish such meetings as part of our research culture, we selected the venue to be in our refurbished, large, conference room in Vitacura, equipped with state-of-the-art audio-visual facilities.

The response from the community was overwhelming. While our original plans were to limit attendance to 60–80 participants, nearly 120 scientists participated in the workshop, many of them worldwide recognised leaders in their field: about half of the participants were from European countries, 20% from the USA, 20% from Chile, 5% from other South American countries, and a few researchers joined us from Japan and Australia. A healthy number of students (~ 30% of the participants) demonstrated the attractive-

ness of the field for the next generation of researchers. Each of the four sessions was organised around three presentations by invited speakers, each of 45 min, all contributing to the discussion from a complementary perspective of Solar System and extraplanetary sciences. The addition of contributed talks and a large number of posters deepened our understanding of each subject. All available time-slots were intensively used for lively and open discussions and some poster pop-up sessions were organised at the end of each day.

## Scientific highlights

A few subjectively selected highlights may demonstrate the scientific ideas and prospects presented during this workshop.

The physical, chemical, and morphological evolution of circumstellar discs from gas-dominated rotating optically thick structures towards thin planetesimal discs is a key to understand the formation of planetary systems in general, and our own Solar System in particular. Disc models can be best constrained by applying a combination of modern observing techniques, utilising the highest spatial resolution imaging in the optical and NIR in scattered light, polarimetry and SED determination. Dust settling, i.e. the vertical segregation of particles with different masses and sizes can now be directly probed (Menard). The dynamical history of our own Solar System, as reconstructed by sophisticated numerical N-body integration, teaches us characteristic differences and/or similarities with known extrasolar systems, such as why does our Solar System not have a hot Jupiter? The most likely reason is the resonant hierarchical configuration of our four gas giants. Late heavy bombardment, a cataclysmic episode of planetesimal infall on terrestrial planets, requires a large reservoir of planetesimals and appears therefore compatible with the dust excesses observed in debris discs (Morbidelli). Accuracy limits of radial velocity searches for exoplanets are continuously improving, and the physical limits have still not been reached (contrary to what was thought ten years ago). Precision RV studies will continue to be

of highest relevance for the massive follow-up of planetary transit candidates (Queloz).

Direct imaging of extrasolar planets is a key science driver for many future ground- and space-based instrument developments. A few extrasolar giant planets (EGPs) around nearby young stars are already in reach of current adaptive-optics assisted NIR companion search programmes, and a leap of the astrophysical understanding of EGPs is expected with the next-generation high contrast imagers, like SPHERE (Mouillet). Astrochemistry provides another important link from our own Solar System to other planetary systems. Deuterium-to-hydrogen ratios appear remarkably similar in comets and in the interstellar medium (Kamp). Comets, as messengers from the early Solar System, may reveal the answer to questions like, why is the Earth wet and alive? (Mumma). Transiting (eclipsing) planets play a key role in understanding their physics and chemistry. Atmospheres of hot Jupiters can be studied in detail by transmission spectroscopy, while mass-radius-composition relations allow the interior of super-earth planets to be probed: the era of comparative exoplanetology has just started (Charbonneau)!

The search for signatures of life on exoplanets by the detection of atmospheric and surface biomarkers is a far-reaching goal of future, ambitious, space-based missions. Both ESA and NASA are actively promoting missions not only to detect, but also to characterise, the physical conditions of terrestrial planets (Fridlund, Lawson). Today, Earth is still the only known planet that hosts life, and it can serve as a template to discuss potential biosignatures in other habitable worlds. The search for life beyond our Solar System may soon become a reality – exciting times are ahead (Kaltenegger)!

Contributed talks and posters presented the latest results from ground-based and space-based (e.g. Spitzer) observatories in the search for exoplanets and the study of planetary-system formation, including our own. The prospects for future ground-based interferometric, radial-velocity and high-contrast imaging instruments in the field of exoplanet search

Participants at the workshop on "Observing Stellar Systems" photographed in the garden at ESO Vitacura.



were presented, while several contributions highlighted the importance of combining *in situ* spacecraft missions of the planets and small bodies of our Solar System with ground-based supporting observations (Cassini/Titan, Rosetta/Churyumov-Gerasimenko, Mars space missions). Although we are still lacking evidence for the presence of life outside the Earth, the discussions generated during this four-day workshop deepened our belief that the search for signatures of life in our own Solar System will provide strong guidance to the future exploration of exoplanetary systems.

### Summary

On purpose we opted not to publish printed proceedings of this workshop. In-

stead, all contributions, both oral and poster, were made available for download immediately after the workshop from the conference website (<http://www.sc.eso.org/santiago/science/OPSWorkshop>) – given the consent of the authors. This decision was based on our belief that providing instant access to the research highlights presented during this meeting was more useful than waiting for printed proceedings in a competitive field like this one, where results are rapidly evolving and will be published in refereed journals. The idea to provide near-instantaneous access to the material discussed in this workshop was developed even further by providing, experimentally, a live-stream webcast during the conference (video-streams are also available for download on the conference website). We also believe that the costs saved have been

well invested in making an attractive programme, and supporting some participants to enable their visit in Chile. In total about 40% of the participants received some financial aid; half were students, half researchers, and all students had their registration fees waived.

We would like to thank ESO for allocating the financial support for this workshop, and the Pontificia Universidad Católica de Chile its co-sponsoring. Also, we would like to thank all people who made this workshop possible, in particular Maria-Eugenia Gomez, our librarian who acted as workshop secretary, the ESO-Chile administration for the logistical support received, and the students from the Universidad Católica de Chile, who helped during the four days of this workshop, notably at the time of the registration. The flawless local organisation, the highly praised coffee breaks (including delicious appetisers), joint cocktails and conference dinner all contributed to a warm and friendly atmosphere during the workshop, remembered by all participants.

While meetings of this quality and size take place naturally in many research institutes in Europe and North America, ESO Vitacura largely lacks this experience and we are looking forward to future workshops of this kind organised within our premises.

---

## The Re-launch of the ESO Web

Rein Warmels, Gabriele Zech (ESO)

Recently, the ESO Web went through a major revision and was re-launched with a new Look and Feel and new navigation tools. This article gives an overview of why and how the ESO Web has changed.

The ESO Web plays an integral and indispensable role in the process of doing science with ESO's observing and archive facilities. It provides an effective and adaptive medium for exchanging information, documents and images between scientists, engineers, the media and the general public. Furthermore, it provides various services to the community of users of ESO's observing facilities

and is critical for coordination and dissemination of information, both internal and external to ESO, in particular in the area of science and archive operations.

The ESO Web started its service in 1994. Since then it has expanded rapidly, both in the amount of information and services that are provided as well as in terms of access rates. Currently, the statistics

show that on average 100 000 pages are viewed per month, representing a data transfer volume of the order of 20 Gbytes.

In spite of the information and services that have been added to the ESO Web continuously over the past years, its structure has not been adapted; the 'Look and Feel' still reflected the predominantly science-oriented approach and usage of the ESO Web in the mid-nineties. Since then ESO's observing facilities have been greatly enlarged: Paranal has become fully operational, the concept of service observing was introduced to maximise the operational efficiency and scientific productivity, and the ESO/ECF Science Archive and Virtual Observatory archival research facilities are being offered. In addition, over the past years a large number of science collaborations and projects, and public outreach programmes, were initiated.

New information and services were added arbitrarily to the old structure and could not easily be integrated into the existing navigation. Consequently, the ESO Web became increasingly complex, barely maintainable and it became increasingly difficult to store new information and services that would be easy to find and use.

In particular, the start of science operations of the VLT and its scientific results triggered a substantial increase in the awareness of ESO amongst the public and the media and, consequently, a noticeable change of user profile of the ESO Web. Meanwhile, nearly every private citizen has Internet access and expects that information can be found easily. To support this new aspect of Internet usage, which includes the requirement to present ESO's activities to the general public, ESO's Web presence had clearly to be revised and improved.

During the past months ESO's Public Affairs Department (PAD) has been working on a new ESO Web. This work was done in collaboration with the IT Department. It was guided by the conclusions and recommendations of an internal working group, taking into account that over time the overall user profile has changed significantly. In this sense ESO is following other organisations, such as CERN, in

adapting to the fact that the large majority of web users are from the public domain. Other objectives for making a new ESO web included:

- improve the appearance, i.e. give the ESO Web a more modern 'Look and Feel';
- improve the navigation and provide more functionality;
- improve page content, in particular make sure that the content is up-to-date. Remove old and outdated pages and information;
- restructure the site to serve the different user groups more efficiently;
- find and assign responsible persons for well-defined areas.

The new ESO Web has three major user areas:

1. Public. This area is intended for the general public, press and media, (potential) industrial partners and people interested in working at ESO. The area is completely new, partially based on existing information, but also with new content.
2. Science Users. The area is intended for professional astronomers who are doing, or are planning to do, research using ESO facilities.
3. Intranet. This area is for ESO Staff only.

The new Look and Feel has been implemented throughout the whole Public area (ESO for the Public – see Figure 1) and includes information of general interest. Examples are descriptions of ESO's

observing facilities and the astronomy programmes using these facilities, contact and travel information, ESO's public affairs' activities (including information for press and media), the new ESO Public Image Archive (Figure 2), as well as information for ESO's industrial partners and about current vacancies.

The Science area (Science Users Information) provides information and services for professional astronomers covering ESO's observing and archive facilities. Examples are instrument information, Phase I proposal submission, policies and procedures, service observing and data processing. Also information about science activities, science meetings, the library, and publications can be found here. In the Science area pages at the top navigation levels have been implemented with the new Look and Feel. Lower level pages that are still in the old format will be converted later.

Most of the information in the Intranet area is still in the old layout. It is intended that also in this area the new Look and Feel will be implemented.

The new structure of the ESO Web is reflected in the navigation bar to the left and the breadcrumb navigation at the top of each page. The main areas of Public, Science, and Intranet can be accessed via separate buttons. Each area has its own navigation menu that helps the user to easily find the information or service of interest.

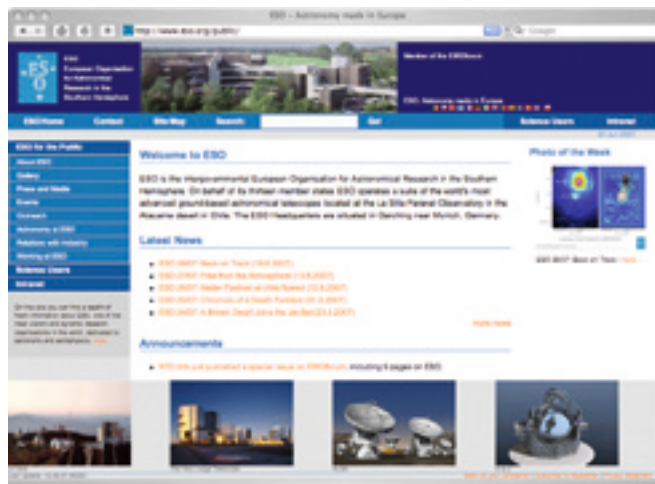


Figure 1: The new ESO home page (Public Area).

The new ESO Web can be reached via ESO's standard URL: <http://www.eso.org/>, which brings the user to the Public portal. The Science Users and Intranet navigation buttons bring users to the Science and Intranet portals respectively; these pages can also be bookmarked as start pages for the ESO Web.

In the current implementation the ESO Web still consists of many single web pages that use a common style and navigation. In the near future it is planned to move to a database-based Content Management System. This will substantially improve maintainability of the site and will serve all web users with the most current information and a common Look and Feel.

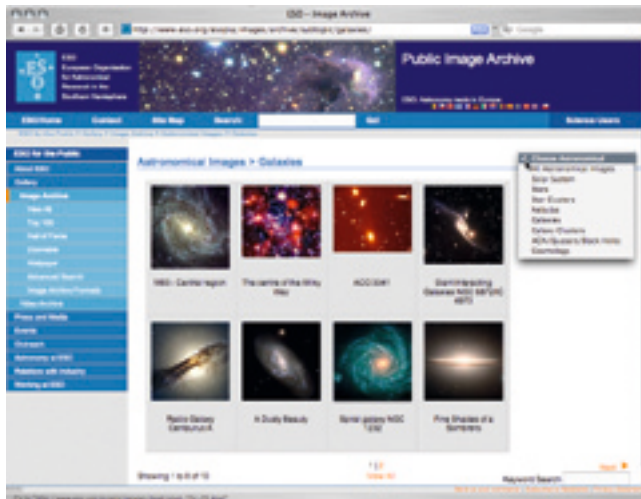


Figure 2: The new ESO Public Image Archive. The page shows the overview of galaxy images currently available.

## Fellows at ESO

### Maria Messineo

I have been an ESO fellow since September 2004. I am interested in studying the morphology and evolution of the Milky Way. Although it is well established that our Galaxy is a barred spiral galaxy, the properties of each Galactic component – Disc, Halo, Bulge, central Bar – are still poorly constrained. It is difficult to properly map the large-scale morphology of the Milky Way, mainly because we observe it from inside the Disc and because light absorption from interstellar dust strongly hampers an unbiased view of its stellar content.

Like Archimedes, I grew up on the ancient and wonderful island of Sicily. I started to study astronomy at the University of Bologna where I graduated in the spring of the 1997 with a Master's Thesis on Galactic globular stellar clusters. I did my Ph.D. research in Leiden studying the distribution of stars in the inner regions of our Galaxy as a direct probe of the gravitational potential.



Maria Messineo

During my Ph.D. I went observing with the IRAM 30-m telescope in Spain several times as well as with the Heinrich Hertz Telescope in Arizona, with the ESO 3.6-m and the CTIO 4-m telescopes in Chile. I always enjoyed my time at the telescopes very much, and so it was obvious that when I joined ESO I would perform my functional work as a sup-

port astronomer on Paranal. At Paranal I mostly work with the UT4-Yepun telescope and operate both of the infrared detectors: NACO and SINFONI. I really enjoy observing and supporting visiting astronomers during their runs, and each time I learn a lot, both scientifically and technically, and receive valuable feedback concerning my research.

Currently I am investigating the spatial distribution of young stellar clusters in the Milky Way using SINFONI data. The aim of this project is to better understand the current star formation in our Galaxy, as well as the locations of spiral arms. From next July I will continue to work on this topic at the Rochester Institute of Technology (USA): more science to carry out and a new world to discover!

### Laura Parker

I arrived at ESO in late 2005 after completing my Ph.D. work at the University of Waterloo in Canada. I am generally interested in all questions related to the formation and evolution of galaxies, as well as understanding the fundamental cosmological parameters which govern the evolution of the Universe. My research focusses on the link between luminous galaxies and the dark-matter halos in which they reside. I study the amount and distribution of dark matter using weak gravitational lensing, and to date my work has focussed mainly on galaxy and galaxy group sized structures.

Since arriving in Garching I have continued my work in weak lensing – which is a leading technique for understanding both

galaxy evolution and fundamental cosmology. I am enjoying working in such a stimulating scientific atmosphere, particularly the many seminars and the lively discussions at morning coffee. The diversity of research carried out by ESO researchers is something hard to match anywhere else. For my functional work I joined the ESO survey team which oversees the planning and execution of public surveys (for the VST and VISTA). My research makes use of large imaging surveys so this project is a perfect fit to my interests.

I will be sad to leave Garching (and the Biergartens) behind but I am excited about moving onto the next chapter in my career. I will join the faculty at McMaster University as an assistant professor in late 2007.



Laura Parker

## Personnel Movements

### Arrivals (1 April–30 June 2007)

Europe	
Arbogast, Dina (F)	Secretary/Assistant
Austin-May, Samantha (GB)	Assistant Head of Personnel Department
Cikic, Zoran (F)	Senior Contract Officer
Clare, Richard (GB)	Physicist
Guerlet, Thibaut (F)	Student
Haimerl, Andreas (D)	Electronics Technician
Hussain, Gaitee (GB)	Astronomer
Laaksonen, Milla (FIN)	Administrative Assistant
Lombardi, Gianluca (I)	Student
Mazzoleni, Ruben (I)	Applied Scientist
Ngoumou Yewondo, Judith Savina (D)	Student
Penker, Thomas (D)	Assistant Facility Management
Tanaka, Masayuki (J)	Fellow
Testi, Leonardo (I)	ALMA European Project Scientist
Chile	
Ederoclite, Alessandro (I)	Operations Astronomer
Elliott, David (GB)	Student
Haguenauer, Pierre (F)	VLTI System Engineer

### Departures (1 April–30 June 2007)

Europe	
Bedin, Luigi (I)	Fellow
Foellmi, Cedric (CH)	Fellow
Huster, Gotthard (D)	Mechanical Engineer
Sadibekova, Tatyana (UZ)	Student
Vasisht, Gautam (IND)	Software Engineer
Chile	
Aguilera, Hugo Freddy (RCH)	Accounting Officer
Eschwey, Jörg (D)	Civil Engineer
Fischman, Nicolas (RCH)	Head of Contract and Procurement
Francois, Patrick (RCH)	Operations Astronomer
Garcia, Enrique (RCH)	Electronics Technician
Hartung, Markus (A)	Fellow
Jehin, Emmanuel (B)	Operations Astronomer
Mella, Juan Alberto (RCH)	Safety Engineer
Shen, Tzu Chiang (CN)	Software Engineer
Soto, Ruben (RCH)	Software Engineer
Vannier, Martin (F)	Fellow
Zagal, Juan (RCH)	Software Engineer



ESO

European Organisation  
for Astronomical  
Research in the  
Southern Hemisphere



## ESO Fellowship Programme 2007/2008

The European Organisation for Astronomical Research in the Southern Hemisphere awards several postdoctoral fellowships each year. The goal of these fellowships is to offer young scientists opportunities and facilities to enhance their research programmes by facilitating close contact between young astronomers and the activities and staff at one of the world's foremost observatories.

With ALMA becoming operational in a few years, ESO offers ALMA Fellowships to complement its regular fellowship programme. Applications by young astronomers with expertise in mm/sub-mm astronomy are encouraged.

In *Garching*, the fellowships start with an initial contract of one year followed by a two-year extension (three years total). The fellows spend up to 25 % of their time on support or development activities in the area of instrumentation, operations support, archive/virtual observatory, VLTi, ALMA, ELT, public affairs or science operations at the Observatory in Chile. In *Chile*, the fellowships are granted for one year initially with an extension of three additional years (four years total). During the first three years, the fellows are assigned to one of the operation groups on Paranal, La Silla or APEX/ALMA. Fellows contribute to the operations at a level of 80 nights per year at the Observatory and 35 days per year at the Santiago Office. During the fourth year there is no functional work and several options are provided. The fellow may be hosted by a Chilean institution (and will thus have access to all telescopes in Chile via the Chilean observing time). Alternatively, she/he may choose to spend the fourth year either at ESO's Astronomy Centre in Santiago, or at the ESO Headquarters in Garching, or at any institute of astronomy/astrophysics in an ESO member state.

All fellows have ample opportunities for scientific collaboration within ESO, both in Garching and Santiago. For more information about ESO's astronomical research activities please consult <http://www.eso.org/sci>. A list of current ESO staff and fellows and their research interests can be found at <http://www.eso.org/sci/activities/personnel>. Additionally, the ESO Headquarters in Munich, Germany hosts the Space Telescope – European Coordinating Facility, and is situated in the immediate neighbourhood of the Max-Planck Institutes for Astrophysics and for Extraterrestrial Physics and only a few kilometres away from the Observatory of the Ludwig-Maximilian University. In Chile, fellows have the opportunity to collaborate with the rapidly expanding Chilean astronomical community in a growing partnership.

We offer an attractive remuneration package including a competitive salary (tax-free), comprehensive social benefits, and provide financial support for relocating families. Furthermore, an expatriation allowance as well as some other allowances may be added. The outline of the terms of service for Fellows (<http://www.eso.org/gen-fac/adm/pers/fellows.html>) provides some more details on employment conditions/benefits.

Candidates will be notified of the results of the selection process between December 2007 and February 2008. Fellowships begin between April and October of the year in which they are awarded. Selected fellows can join ESO only after having completed their doctorate.

**The closing date for applications is 15 October 2007.**

Please apply by filling the web form available at: <https://jobs.eso.org> You can provide the following information by uploading the files directly through the web application form:

- your Curriculum Vitae including a (refereed) publication list
- your proposed research plan (maximum two pages)
- a brief outline of your technical/observational experience (maximum one page)

In addition three letters of reference from persons familiar with your scientific work should be sent to ESO electronically ([vacancy@eso.org](mailto:vacancy@eso.org)) before the application deadline. Preferred format for submissions is pdf.

Please also read our list of FAQs at [http://www.eso.org/~mrejku/fellows\\_FAQ.html](http://www.eso.org/~mrejku/fellows_FAQ.html) regarding fellowship applications.

Questions not answered by the above FAQ page can be sent to: Marina Rejkuba, Tel +49 89 320 06-4 53, Fax +49 89 320 06-4 80, e-mail: [mrejku@eso.org](mailto:mrejku@eso.org)

Although recruitment preference will be given to nationals of ESO member states (members are: Belgium, Denmark, Finland, France, Germany, Italy, the Netherlands, Portugal, Spain, Sweden, Switzerland, the Czech Republic and United Kingdom) no nationality is in principle excluded.

The post is equally open to suitably qualified male and female applicants.

ESO. Astronomy made in Europe



Announcement of

## ALMA Community Meeting

3–4 September 2007, Garching, Germany

Now ALMA has entered its main construction phase, ESO and RadioNet are organising two back-to-back meetings in Garching, aimed at the European astronomical community.

The ALMA Community Meeting will start at 14:00 on Monday 3 September 2007 and end in the late afternoon of Tuesday 4 September. The aim of this one-and-a-half day meeting is to keep the European astronomical community informed about ALMA progress since the last ALMA Community Day in September 2004. The meeting will provide information about the project status, and additional reports on other ALMA activities such as the status of software. The definition of the ALMA Operations Plan and the organisation of the European ALMA Regional Centre (ARC) has considerably advanced during the last year. Plans for ALMA operation and for the organisation of the ARC network in Europe will be presented and discussed at the Community Meeting, with the aim of obtaining feedback

from future ALMA users. Also, a sample of exciting recent scientific results, relevant to ALMA and the opportunities afforded by ALMA in its Early Science phase, will be presented.

The “Surveys for ALMA” workshop will directly follow the Community Meeting, starting on Wednesday 5 September, and end at lunchtime on Thursday 6 September. The rationale behind this meeting is as follows. While ALMA is being constructed in Chile, several ground-based millimetre and submillimetre observatories worldwide are being upgraded and are now coming online. The excellent wide-field survey capabilities of large bolometer arrays such as LABOCA and SCUBA-2 on single-dish sub-millimetre telescopes such as APEX and the JCMT, and the upgraded (sub-)millimetre arrays, such as IRAM, allow prospective ALMA users to develop ambitious science projects and prepare for the use of ALMA. During the first years of operation of ALMA, the Herschel Space Observatory

## Surveys for ALMA Workshop

5–6 September 2007, Garching, Germany

and the Planck mission will also be operational, and provide unprecedented far-infrared survey capabilities. The progress in wide-field near-IR detectors on dedicated telescopes such as VISTA will also provide a major new data set for ALMA follow-up observations. The aim of this one-and-a-half day meeting is to coordinate the planning of these preparatory surveys for ALMA, and to solicit feedback from the community in the planning of the early science follow-up with ALMA from these surveys. The potential for deep legacy type surveys with the completed ALMA array in 2012 will also be briefly discussed.

If you would like to register for one or both of these meetings, or would like to obtain further information, please visit <http://www.eso.org/projects/alma/science/meetings/gar-sep07/>

The registration deadline is 13 July 2007.

Announcement of the MPA/ESO/MPE/USM 2007 Joint Astronomy Conference on

## Gas Accretion and Star Formation in Galaxies

10–14 September 2007, Garching, Germany

This meeting will focus on the following question: how does gas get into galaxies and what are the processes that regulate the rate at which the gas then turns into stars? The conference will bring together both theoreticians and observational astronomers working at different wavelengths, using different techniques, both at low and at high redshifts. The topics to be addressed in the conference are:

1. H<sub>I</sub> observations of gas in and around nearby galaxies
2. The relation between atomic and molecular gas
3. Insights into the gas-star cycle in galaxies from new panchromatic data sets

4. Theoretical models and empirical constraints on the global efficiency with which gas is converted into stars in galaxies
5. Gas inflow mechanisms
6. Feedback processes in galaxies
7. The nature of the Warm/Hot Intergalactic Medium (WHIM). Does gas cool from the hot phase? Insights from XMM/Chandra
8. Physical constraints on gas in the vicinity of galaxies from quasar absorption lines
9. Star formation in high-redshift galaxies

Scientific Advisory Committee: Jacqueline Bergeron (IAP), Andi Burkert (MPIA), Chris Carilli (NRAO), Françoise Combes (ObsPM), Andy Fabian (IoA), Reinhard Genzel (MPE), Ortwin Gerhard (MPE), Tim Heckman (JHU), Guinevere Kauffmann (MPA), Rob Kennicutt (IoA), Eliot Quataert (University of California, Berkeley), Piero Rosati (ESO), Renzo Sancisi (INAF), Ken Sembach (STScI), Mike Shull (University of Colorado, Boulder), Ian Smail (Durham), Jonathan Tan (ETH, Zurich)

Further information can be found at <http://www.mpa-garching.mpg.de/~gassf07/>



A field of 'White Penitents'  
– ice sculpted by solar radiation –  
at the high altitude of the  
ALMA site at Llano de Chajnantor.

ESO is the European Organisation for Astronomical Research in the Southern Hemisphere. Whilst the Headquarters (comprising the scientific, technical and administrative centre of the organisation) are located in Garching near Munich, Germany, ESO operates three observational sites in the Chilean Atacama desert. The Very Large Telescope (VLT), is located on Paranal, a 2 600 m high mountain south of Antofagasta. At La Silla, 600 km north of Santiago de Chile at 2 400 m altitude, ESO operates several medium-sized optical telescopes. The third site is the 5 000 m high Llano de Chajnantor, near San Pedro de Atacama. Here a new submillimetre telescope (APEX) is in operation, and a giant array of 12-m submillimetre antennas (ALMA) is under development. Over 1600 proposals are made each year for the use of the ESO telescopes.

The ESO Messenger is published four times a year: normally in March, June, September and December. ESO also publishes Conference Proceedings and other material connected to its activities. Press Releases inform the media about particular events. For further information, contact the ESO Public Affairs Department at the following address:

ESO Headquarters  
Karl-Schwarzschild-Straße 2  
85748 Garching bei München  
Germany  
Phone +49 89 320 06-0  
Fax +49 89 320 23 62  
information@eso.org  
www.eso.org

The ESO Messenger:  
Editor: Jeremy R. Walsh  
Technical editor: Jutta Boxheimer  
Technical assistant: Mafalda Martins  
www.eso.org/messenger/

Printed by  
Pesckhe Druck  
Schatzbogen 35  
81805 München  
Germany

© ESO 2007  
ISSN 0722-6691

## Contents

### The Organisation

C. Cesarsky – The Czech Republic Joins ESO	2
J. Palouš, P. Hadrava – Astronomy in the Czech Republic	3

### Telescopes and Instrumentation

T. Szeifert et al. – FORS1 is getting Blue: New Blue Optimised Detectors and High Throughput Filters	9
W. Freudling et al. – Towards Precision Photometry with FORS: A Status Report	13
R. Siebenmorgen et al. – Exploring the Near-Infrared at High Spatial and Spectral Resolution: First Results from CRIRES Science Verification	17
F. Gonté et al. – The First Active Segmented Mirror at ESO	23
C. Haupt, H. Rykaczewski – Progress of the ALMA Project	25
T. Wilson – ALMA European Project Scientist Appointed	31

### Astronomical Science

J.-P. Beaulieu et al. – Hunting for Frozen Super-Earths via Microlensing	33
P. E. Nissen et al. – Sulphur Abundances in Metal-Poor Stars – First Result from CRIRES Science Verification	38
R. Scarpa et al. – Using Globular Clusters to Test Gravity in the Weak Acceleration Regime	41
J. Zuther et al. – Dissecting the Nuclear Environment of Mrk 609 with SINFONI – the Starburst-AGN Connection	44
S. Savaglio et al. – GHostS – Gamma-Ray Burst Host Studies	47
C. Tapken et al. – The Puzzle of the Ly $\alpha$ Galaxies: New Results from the VLT	51

### Astronomical News

M. Grenon – Nature Around the ALMA Site – Part 2	57
U. Grothkopf et al. – Using the <i>h</i> -index to Explore the Scientific Impact of the VLT	62
F. Primas – Status of Women at ESO: a Pilot Study on ESO Staff Gender Distribution	67
M. Sterzik, C. Dumas – Report on the International Workshop on Observing Planetary Systems	72
R. Warmels, G. Zech – The Re-launch of the ESO Web	73
Fellows at ESO – M. Messineo, L. Parker	75
Personnel Movements	76
ESO Fellowship Programme 2007/2008	77
Announcement of ALMA Community Meeting and Surveys for ALMA Workshop	78
Announcement of the MPA/ESO/MPE/USM 2007 Joint Astronomy Conference on Gas Accretion and Star Formation in Galaxies	78

Front Cover Picture: The three types of ALMA antenna at the ALMA Test Facility at Socorro, New Mexico are shown, from left to right: US (Vertex RSI); European (AEC Consortium); Japanese (Mitsubishi). Since this photograph, the Japanese antenna has been removed and the US and European antennas have been linked interferometrically (see ESO PR 10/07). Photograph by Hans Hermann Heyer (ESO).